Anharmonic Phonons in Graphene from First Principles

Mordechai Kornbluth

Submitted in partial fulfillment of the
requirements for the degree of
Doctor of Philosophy
in the Graduate School of Arts and Sciences

COLUMBIA UNIVERSITY

2017

ABSTRACT

Anharmonic Phonons in Graphene from First Principles

Mordechai Kornbluth

In this work, we develop a new flexible formalism to calculate anharmonic interatomic interactions from first principles at arbitrary order. Using the recently-developed slave-mode basis, we Taylor-expand the potential with a minimal number of independent coefficients. The anharmonic dynamical tensor, a higher-order generalization of the dynamical matrix in strain+reciprocal space, is calculated via a generalized frozen phonon methodology. We perform high-throughput calculations, emphasizing efficiency with multidimensional finite differences and Hellman-Feynman forces. Applying the methodology to graphene, we show convergence through fifth order terms. Our calculated force constants produce stress-strain curves, bond-length relaxations, and phonon spectra that agree well with those expected within DFT. We show that to fully capture anharmonic effects, long-range interactions must be included.

Contents

List of Figures

List of Tables

Acknowledgements

I would like to acknowledge the assistance of all those who helped me reach where I am today. Homiletically, a doctoral examination is a measurement of my current state, and therefore collapses my wavefunction to the observed eigenstate. It is therefore appropriate to undergo a self-examination as well (*cheshbon ha-nefesh*), and acknowledge those who brought me to this milestone. It is impossible to live without support from friends, family, and colleagues, as per Ecclesiastes 4:9-12 and Talmud Bavli Ta'anis 23a.

First I acknowledge the nurturing care and support of God and my parents, who raised me despite my antics. On a related note, of Akiva and Yael, whose antics I am getting back. And of course Aviva, for unconditional support and partnership.

The support of my colleagues in the Marianetti group, current and former: Pierre, Hyowon, Yue, Jia, Dalal, and Alex, your positions as postdocs help bring our group up to the top of our field. Eric, Xinyuan, Chanul, Zhengqian, and Lyuwen, as a fellow student I share the ups and downs of the graduate experience, and I am glad it was more up than down.

The support of my committee: Professor Latha Venkataraman and Professor Aron Pinczuk, thank you for your excellent class lectures, participation in my oral exam, and agreeing to be on my committee. Professor Jeffrey Kysar and Professor James Hone, thank you for joining my committee and I hope you enjoy the graphene angle of the work. And of course Professor Chris Marianetti, thank you for five years of mentorship, teaching, research, and more. I couldn't have asked for a better advisor.

This research used resources of the National Energy Research Scientific Computing Center, a DOE Office of Science User Facility supported by the Office of Science of the U.S.

Department of Energy under Contract No. DE-AC02-05CH11231. This research was partially supported by a DARPA Young Faculty Award, Grant No. D13AP00051 and by the National Science Foundation (Grant No. CMMI-1150795).

Dedication

I dedicate this dissertation to my children, Akiva and Yael. May God bless you with the intellectual and moral strength to excel and fulfill your potentials to the fullest, and the enjoyment of His beautiful universe. As Koheles says in Ecclesiastes, life is a path function, not a state function.

Chapter 1

Introduction

With the explosion of computing power over the past few decades, new realms of computation become available. Computation is often cheaper and faster than experiment, allowing rapid screening of materials, methods, and physical effects. Molecular dynamics has become increasingly popular, with applications for drug design, materials synthesis, and device engineering. In material science and physics, computational resources have led to the accelerating materials-by-design intiative [1]. Here we focus on phonon scattering, which is most frequently used for calculating phonon lifetimes, thermal conductivity, and temperature-dependent effects [2, 3]. When the atoms in a material approximately move in a force field generated by the electronic interactions (the Born-Oppenheimer approximation), they can be modeled using a classical potential, also known as a force field.

The most common force fields are empirical potentials, where the parameterized interaction parameters are fitted to experimental data. However, these provide limited predictive capability; the model's quality is limited by the parameters used. More recently, first-principles quantum-mechanical calculations are used to compute interactions. These have significantly greater predictive capability, including discovery of new physics, as long as the methods and assumptions of the calculations hold.

This work describes a new methodology to calculate all interatomic interactions from first principles at arbitrary order and range, using efficient high-throughput computations. We apply the methodology to the anharmonic interactions in graphene up to fifth order, which are necessary to capture the behavior of the phonons under strain. We also publish our computed parameters in a slave-mode notation, which can be easily used in future

computations or simulations.

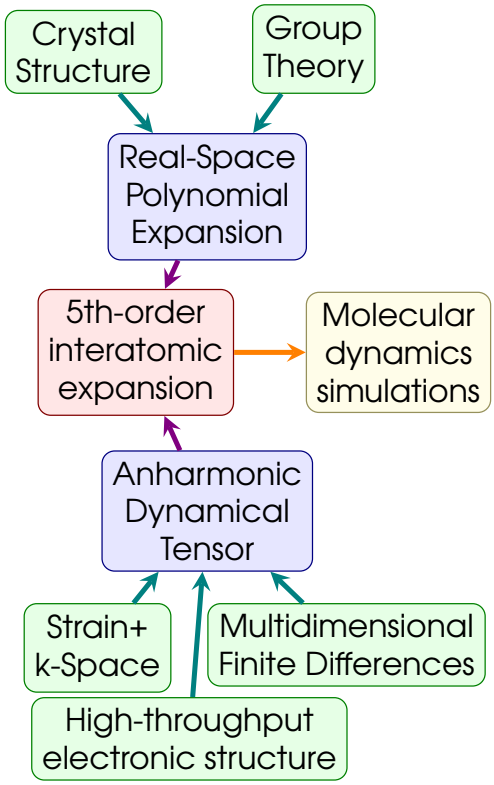

Figure 1.1: Overview of our methodology

As depicted in Figure 1.1, we divide the methodology into three steps, required for constructing any set of interatomic interaction parameters. First, in Chapter 2, we define our energy function and its parameters, using a symmetrized Taylor expansion around a high-symmetry state at a fixed range. We use the crystal structure and group theory to define a real-space polynomial expansion. In Chapter 3, we take some computational measurements that let us determine our parameters. We use density-functional theory to compute the anharmonic dynamical tensor along a non-uniform grid. Using multidimensional finite differences in high-throughput electronic-structure calculations, we find the derivatives of the energy in strain+reciprocal space. Finally, in Chapter 4, we convert our measurements to the parameters sought. We use Fourier transforms, least-squares fitting, and cross-validation to determine our symmetrically independent parameters. This provides us with a 5th-order interatomic expansion, which can be used for molecular dynamics simulations. Chapter 5

applies this methodology to graphene, showing quantitative agreement with the expected observables.

Chapter 2

Polynomial Construction

The first step to building interatomic interactions is to determine the form of the Hamiltonian. A continuum-elasticity model [4–8] describes interactions in only an averaged way [9]. A local-anharmonic approximation [10] treates only the pairwise interactions, omitting multiatom terms. When performing a Fourier interpolation on a uniform mesh, all interactions within a fixed range are determined, where the range is determined by the coarseness of the reciprocal-space mesh [11–15]. Although our mesh is nonuniform, the maximum range of our model is analogously limited by our sampling in reciprocal space. We form a Taylor expansion [16–19] within a fixed range. The polynomial expansion of order λ describing all interactions within N atoms and d dimensions has the form

$$V_\lambda = \sum_{\vec{j}}^{N_j} c_{\vec{j}} \prod_{a=1}^{\lambda} x_{j_a} \tag{2.1}$$

where $c_{\vec{j}}$ is a force constant for a particular monomial $\vec{j}$. The total number of monomials can be described by combinations-with-replacement notation as $N_j = \left(\binom{Nd}{\lambda}\right) = \frac{(Nd+\lambda)!}{(Nd+\lambda-\lambda!-1)\lambda!}$. An expansion around equilibrium allows $V_{\lambda=1}$ to be zero, but the other terms are combinatorically numerous.

The energetics of the material in question must converge with respect to the range N, which is nontrivial. However, there is evidence that some anharmonic effects are primarily short-range [10, 20], which leads us to expect relatively quick convergence. Nonanalytic effects cannot be captured in a real-space polynomial, and must be treated explicitly in k-space via a perturbative Hamiltonian [21, 22].

Next, we must treat the symmetry of the problem, to avoid a combinatorically large number of terms in our expansion. Past work has used explicit constraining equations [23, 24], which creates a complicated parameter space. Other work uses homogeneity of free space with respect to rotation to create constraining equations [25–28]. This correlates terms of different orders, which negates a major advantage of the Taylor expansion, that of separating the contributions of each order. (See also Chapter 2.3 for details.) Here we use the slave-mode basis that successfully explained the anharmonic phonons in PbTe [20, 29], related to the collective-cluster-deformation (CCD) method [18].

Next we detail the formalism and implementation; detailed examples appear in Chapter 2.3.

2.1 Point Group Symmetrization

We seek to construct a polynomial expansion describing all interactions of a cluster of N atoms in d dimensions. If we do not include symmetry, the polynomial is combinatorically large. However, symmetry provides a relationship between many of them.

The expansion is written as the linear combination of N_i polynomials:

$$V_\lambda = \sum_i^{N_i} c_i \cdot \Gamma_i(\vec{r}_1 \dots \vec{r}_N) \tag{2.2}$$

where we define Γ_i to be symmetry-independent polynomial functions, meaning that each must transform as the symmetric irreducible representation of the point group. They are defined up to a rank-preserving linear transformation, and may be chosen to be orthonormal. This assures that c_i are defined by physical interactions, while Γ_i are defined purely by the symmetries of the system. To describe the symmetries, we use group theory and representation theory, approaches that excel in describing complex physics of a crystal, including dynamical crystals [30], alloys and disorder [31, 32], and carbon nanotubes [33].

We define Γ_i via a basis formed of the slave modes of our cluster of N atoms. The slave

modes $\vec{\phi}$ are symmetrized and orthogonalized according to the point group of the cluster:

$$\vec{\phi} = Q\vec{r} \qquad \phi_k = \sum_a Q_{ka} r_a \tag{2.3}$$

where k indexes over the normalized modes, each orthonormal row of Q transforms like a single irreducible representation (or row thereof) of the point group, and a indexes over the degrees of freedom of the cluster. Because we have not yet applied the translation group, our clusters may overlap, so the slave modes may overdescribe the degrees of freedom of the crystal (hence the name). We will handle this overdescription later.

A uniform translation cannot affect the energy of the cluster (homogeneity of free space with respect to uniform translation), so we can remove the rows associated with uniform translation (i.e. set any associated c_i to zero). However, it is nontrivial to apply homogeneity of free space with respect to free rotation. At second order, we can set the rotation mode to zero, but higher-order effects couple the polynomials of different orders, which removes our ability to calculate our terms order-by-order and prevent sloshing between orders. (See Chapter 2.3 for an example.) We therefore do not explicitly impose rotational invariance; accurate computation of the coefficients will ensure the results are accurate nonetheless.

Thus our symmetry-independent polynomial functions are:

$$\Gamma_i = \sum_j S_{ij} \prod_k \phi_k^{p_{ijk}} \tag{2.4}$$

where we use those polynomials whose symmetric direct product has one or more elements that transform like the symmetric irreducible representation. S_{ij} are the Clebsch-Gordon coefficients associated with the products of irreducible representations; for one-dimensional irreducible representations, j takes only one value and $S_i = 1$. We thus have constructed a polynomial as per Equation (2.2) that obeys all point-group symmetry for any value of c_i.

Equivalent to the above, we can define the potential energy of the cluster in the Cartesian

basis as:

$$V_\lambda = \vec{c} \cdot \hat{\Gamma} \cdot \vec{x}^{(\lambda)} \tag{2.5}$$

where $\vec{c}$ are the symmetry-independent coefficients, $\vec{x}^{(\lambda)}$ are the set of all Cartesian monomials of order λ, and $\hat{\Gamma}$ is a full-rank matrix where each row is invariant under both arbitrary translation and any operation of the point group, i.e. $\hat{\Gamma}_i \cdot \vec{x}^{(\lambda)} = \hat{\Gamma}_i \cdot \hat{R}\vec{x}^{(\lambda)}$ where $\hat{R}$ can be either a uniform translation or any operation in the point group.

There are two gauge transformations that can be performed to this equation:

$$\vec{\phi}^{(\lambda)} = Q^{(\lambda)}\vec{x}^{(\lambda)} \qquad \hat{\Gamma}^{(\phi)} = \hat{\Gamma}Q^{-1} \tag{2.6}$$

$$\vec{c'} = \vec{c}\,U^{-1} \qquad \hat{\Gamma}' = U\,\hat{\Gamma} \tag{2.7}$$

The former is equivalent to the symmetrization of modes discussed earlier, using a unitary transformation $Q^{(\lambda)}$. The latter, which we take to be a full-rank transformation U, takes linear combinations of Γ_i while renormalizing the associated coefficients, and will be important when we apply the symmetries of the translation group.

2.2 Translation Group Symmetrization

The above suffices for a molecular cluster, but for a periodic crystal we must add translational symmetry. This may result in an overcomplete description of the system, where our N_i terms are not actually independent, which is why they are called slave modes. We thus must project each symmetrically independent term Γ_i onto the symmetric irreducible representation of the translation group. We define $\hat{T}^{(\lambda)}$ as this projection operator operating on $\vec{x}^{(\lambda)}$, which can be calculated as

$$\hat{T}^{(\lambda)} = \sum_{\vec{R}} \hat{T}^{(\lambda)}_{\vec{R}} \tag{2.8}$$

which is the sum of all translation operations. When we sum the total energy over all overlapping clusters, we get

$$U_\lambda = \sum_{\vec{R}} V_{\vec{R}}^{(\lambda)} = \vec{c} \cdot \hat{\nu} \cdot \vec{x}^{(\lambda)} \tag{2.9}$$

where $\hat{\nu} = \hat{\Gamma}\hat{T}^{(\lambda)}$. Although Γ is in general full-rank, ν may be rank deficient, such that there are only $\mathrm{rnk}(\nu)$ physically independent coefficients.

Let us assume that we can compute real-space interatomic force constants $\Omega_j = \partial^\lambda U_\lambda / \partial x_j^{(\lambda)}$; we will return later to the mechanisms of these computations. We can take derivatives of Equation 2.9 to find $\Omega_j = \vec{c} \cdot \hat{\nu}$, which lets us solve for our coefficients $\vec{c}$:

$$\vec{c} = \vec{\Omega}\hat{\nu}^+ \tag{2.10}$$

where $\hat{\nu}^+$ is the Moore-Penrose pseudoinverse of $\hat{\nu}$. If our computation of Ω has no noise or error, this is exact; if it includes error, it provides the best fit in a least-squares sense.

How does this pseudoinverse procedure change with a change of basis? From the gauge relation of Equation (2.7), we can show:

$$\vec{c} = \vec{c'}U = \vec{\Omega}(U\hat{\nu})^+ U \tag{2.11}$$

If $\hat{\nu}$ is full rank, then the properties of the Moore-Penrose pseudoinverse give $(U\hat{\nu})^+ = \hat{\nu}^+ U^{-1}$, retrieving Equation (2.10). Otherwise, the values of c associated with $\ker(\nu'^T)$ are set to zero, an effect that depends on the choice of U. This will not affect any observables but may affect the reported calculated parameters. Therefore, in the presence of a rank-deficient $\hat{\nu}$, any reported values of $\vec{c}$ are defined up to arbitrary values of $\ker(\nu^T)$. Detailed illustrations appear in the examples of Chapter 2.3.

2.3 Group Theory Examples

Some simple examples with the two-dimensional dimer and square have been worked out in Ref. 29. Here we present some further examples to illustrate the gauge freedom of our system in the case of rank-deficient $\hat{\nu}$.

Four-Atom Linear Chain

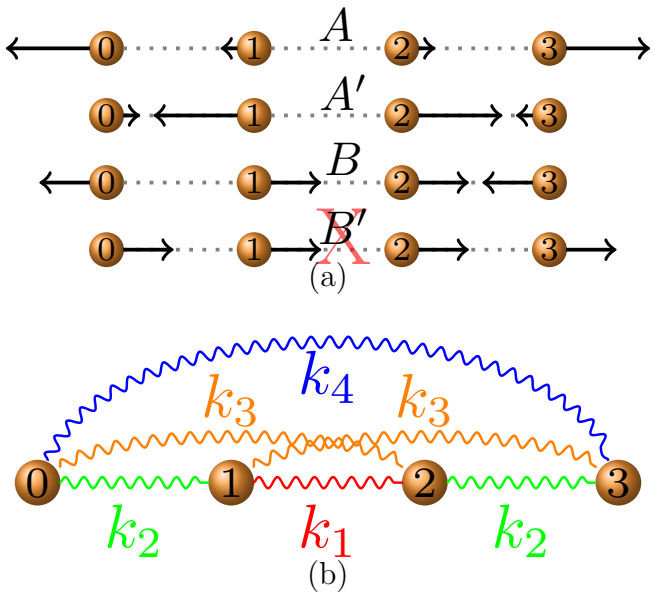

Figure 2.1: The four-atom linear chain, in one dimension. (a) The symmetrized modes of the molecular cluster, including the B' translation mode that can be removed from the Hamiltonian due to homogeneity of free space with respect to translation. (b) Springs connecting the atoms in the cluster, up to the third-nearest-neighbor spring constant. When the translation group is ignored (i.e. the molecular cluster), k_1 and k_2 need not be equivalent.

Treatment of the one-dimensional four-atom chain is particularly illustrative for the translation group and gauge freedom. Here the point group is C_2; as shown in Figure 2.1(a), the symmetrized normal modes can be chosen as (before normalization):

$$\begin{pmatrix} \phi_A \\ \phi'_A \\ \phi_B \\ \phi'_B \end{pmatrix} = \begin{pmatrix} -3 & -1 & 1 & 3 \\ 1 & -3 & 3 & -1 \\ -1 & 1 & 1 & -1 \\ 1 & 1 & 1 & 1 \end{pmatrix} \begin{pmatrix} x_0 \\ x_1 \\ x_2 \\ x_3 \end{pmatrix} \tag{2.12}$$

We remove the uniform translation ϕ'_B and find the second-order contributions to the energy are only:

$$V_2 = c_1\phi_A^2 + c_2\phi_A'^2 + c_3\phi_A\phi'_A + c_4\phi_B^2 \tag{2.13}$$

noting that the two modes that transform as A can couple to each other.

When we apply the translation group to the one-dimensional four-atom chain, we find a rank-deficient $\hat{\nu}$. The translation projector at second order is:

$$\hat{T}^{(2)}\vec{x}^{(2)} = \begin{pmatrix} 1&1&1&1&0&0&0&0&0&0\\ 1&1&1&1&0&0&0&0&0&0\\ 1&1&1&1&0&0&0&0&0&0\\ 1&1&1&1&0&0&0&0&0&0\\ 0&0&0&0&1&1&1&0&0&0\\ 0&0&0&0&1&1&1&0&0&0\\ 0&0&0&0&1&1&1&0&0&0\\ 0&0&0&0&0&0&0&1&1&0\\ 0&0&0&0&0&0&0&1&1&0\\ 0&0&0&0&0&0&0&0&0&1 \end{pmatrix} \begin{pmatrix} x_0^2\\ x_1^2\\ x_2^2\\ x_3^2\\ x_0x_1\\ x_1x_2\\ x_2x_3\\ x_0x_2\\ x_1x_3\\ x_0x_3 \end{pmatrix} \tag{2.14}$$

Leading to a $\hat{\nu}$ (unnormalized) of:

$$\hat{\nu} = \hat{\Gamma}\hat{T}^{(2)} = \begin{pmatrix} 10&10&10&10&5&5&5&-6&-6&-9\\ 10&10&10&10&-15&-15&-15&6&6&-1\\ 0&0&0&0&5&5&5&-8&-8&3\\ 2&2&2&2&-1&-1&-1&-2&-2&1 \end{pmatrix} \tag{2.15}$$

with the rows of $\hat{\nu}$ corresponding to $\phi_A^2, \phi_A'^2, \phi_A\phi'_A, \phi_B^2$, respectively. The rank of this matrix is only 3. By examining $\ker(\nu^T)$, we can see that $c_2 + 2c_3 - 5c_3$ is a gauge freedom, and can take any value without changing any observable. This necessarily cannot include c_1, which, being associated with the ϕ_{A_1} strain mode, is the elastic modulus of the crystal; this can be directly measured.

This was using the slave-mode gauge; now we turn to a spring gauge. Figure 2.1 shows the four springs of our cluster, which we can express as $\vec{c'} = (k_1\ k_2\ k_3\ k_4)^T$. Now we apply

this as a unitary transformation via Equation (2.7):

$$U = \frac{1}{100}\begin{pmatrix} 1 & 9 & 6 & 0 \\ 2 & 8 & -8 & 50 \\ 8 & 2 & 8 & 50 \\ 9 & 1 & -6 & 0 \end{pmatrix} \tag{2.16}$$

$$\hat{\nu}' = \begin{pmatrix} 0 & 1 & 1 & 0 & 0 & -2 & 0 & 0 & 0 & 0 \\ 1 & 1 & 1 & 1 & -2 & 0 & -2 & 0 & 0 & 0 \\ 1 & 1 & 1 & 1 & 0 & 0 & 0 & -2 & -2 & 0 \\ 1 & 0 & 0 & 1 & 0 & 0 & 0 & 0 & 0 & -2 \end{pmatrix} \tag{2.17}$$

In this basis, the gauge freedom ($\ker(\nu'^T)$) is $2k_1 - k_2$, which can take any value. Physically, this means that because each nearest-neighbor spring appears once as k_1 and twice as k_2, when summed over the entire lattice, any effect of $2k_1 - k_2$ will be zero. We can choose to set $k_1 = k_2$ due to translational symmetry, but any observable (i.e. after summation over the entire lattice) will be correct even without that choice.

Two-Dimensional Hexagon

The symmetrized normal modes for the hexagon (point group C_{6v}) are, before normalization:

$$\begin{pmatrix} \phi_{A_1} \\ \phi_{A_2} \\ \phi_{E_{200}} \\ \phi_{E_{201}} \\ \phi_{E_{210}} \\ \phi_{E_{211}} \\ \phi_{B_1} \\ \phi_{B_2} \\ \phi_{E_{100}} \\ \phi_{E_{101}} \\ \phi_{E_{110}} \\ \phi_{E_{111}} \end{pmatrix} = \begin{pmatrix} 2 & 0 & 1 & \sqrt{3} & -1 & \sqrt{3} & -2 & 0 & -1 & -\sqrt{3} & 1 & -\sqrt{3} \\ 0 & 2 & -\sqrt{3} & 1 & -\sqrt{3} & -1 & 0 & -2 & \sqrt{3} & -1 & \sqrt{3} & 1 \\ 0 & 4 & \sqrt{3} & -1 & \sqrt{3} & 1 & 0 & -4 & -\sqrt{3} & 1 & -\sqrt{3} & -1 \\ 0 & 0 & 3 & -\sqrt{3} & -3 & -\sqrt{3} & 0 & 0 & -3 & \sqrt{3} & 3 & \sqrt{3} \\ 0 & 0 & \sqrt{3} & 3 & \sqrt{3} & -3 & 0 & 0 & -\sqrt{3} & -3 & -\sqrt{3} & 3 \\ 4 & 0 & -1 & -\sqrt{3} & 1 & -\sqrt{3} & -4 & 0 & 1 & \sqrt{3} & -1 & \sqrt{3} \\ 0 & 2 & \sqrt{3} & -1 & -\sqrt{3} & -1 & 0 & 2 & \sqrt{3} & -1 & -\sqrt{3} & -1 \\ 2 & 0 & -1 & -\sqrt{3} & -1 & \sqrt{3} & 2 & 0 & -1 & -\sqrt{3} & -1 & \sqrt{3} \\ 2 & 0 & -1 & \sqrt{3} & -1 & -\sqrt{3} & 2 & 0 & -1 & \sqrt{3} & -1 & -\sqrt{3} \\ 0 & -2 & \sqrt{3} & 1 & -\sqrt{3} & 1 & 0 & -2 & \sqrt{3} & 1 & -\sqrt{3} & 1 \\ 1 & 0 & 1 & 0 & 1 & 0 & 1 & 0 & 1 & 0 & 1 & 0 \\ 0 & 1 & 0 & 1 & 0 & 1 & 0 & 1 & 0 & 1 & 0 & 1 \end{pmatrix} \begin{pmatrix} x_1 \\ y_1 \\ x_2 \\ y_2 \\ x_3 \\ y_3 \\ x_4 \\ y_4 \\ x_5 \\ y_5 \\ x_6 \\ y_6 \end{pmatrix} \tag{2.18}$$

as shown in Figure 2.2. Once more, we can remove the last two modes as pure translation modes. We are thus left with ten slave modes. The Clebsch-Gordon coefficients ensure that the force constants associated with the two rows of a given E representation are the same; therefore, there are only eight second-order force constants in the cluster. We can bring

this to seven by setting $c_{A_2} = 0$ due to homogeneity of free space with respect to rotation. (Although Ref. 34 uses six, one is complex; the imaginary part of δ adjusts the phonon spectrum.)

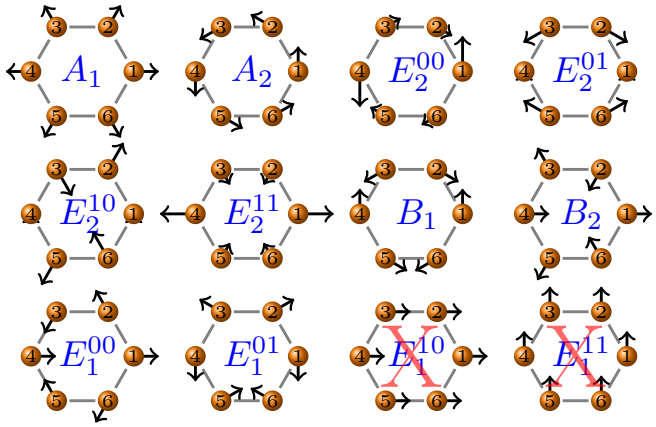

Figure 2.2: Symmetrized modes of the two-dimensional hexagon. The first superscript numbers the instance of the given irreducible representation; the second numbers the row of the mode within that irreducible representation. The pure-translation modes are removed thanks to homogeneity of free space with respect to uniform translation.

Chapter 4.1 details the methodology of taking the derivatives of slave-modes with respect to strain. Here we detail the corresponding calculations for the two-dimensional hexagon. In the point group C_{6v}, the two-dimensional strain decomposes as $A_1 + E_2$, with A_1 being biaxial strain and E_2 being asymmetric and shear strains; see Chapter 3.5 for further details and conventions. We will apply this to the strain derivatives of Equation (4.1) to calculate Θ, which are the transformations of the symmetrized modes by strains:

$$\Theta_{biax} \propto \mathbb{1} \tag{2.19}$$

$$\Theta_{asym} \propto \begin{pmatrix} 0 & 0 & 0 & 1 & 0 & 1 & 0 & 0 & 0 & 0 \\ 0 & 0 & -1 & 0 & -1 & 0 & 0 & 0 & 0 & 0 \\ 0 & -1 & \frac{-1}{\sqrt{2}} & 0 & \frac{1}{\sqrt{2}} & 0 & 0 & 0 & 0 & 0 \\ 1 & 0 & 0 & \frac{1}{\sqrt{2}} & 0 & \frac{-1}{\sqrt{2}} & 0 & 0 & 0 & 0 \\ 0 & -1 & \frac{1}{\sqrt{2}} & 0 & \frac{-1}{\sqrt{2}} & 0 & 0 & 0 & 0 & 0 \\ 1 & 0 & 0 & \frac{-1}{\sqrt{2}} & 0 & \frac{1}{\sqrt{2}} & 0 & 0 & 0 & 0 \\ 0 & 0 & 0 & 0 & 0 & 0 & 0 & 0 & 0 & \sqrt{2} \\ 0 & 0 & 0 & 0 & 0 & 0 & 0 & 0 & \sqrt{2} & 0 \\ 0 & 0 & 0 & 0 & 0 & 0 & 0 & \sqrt{2} & 0 & 0 \\ 0 & 0 & 0 & 0 & 0 & 0 & \sqrt{2} & 0 & 0 & 0 \end{pmatrix} \tag{2.20}$$

$$\Theta_{shear} \propto \begin{pmatrix} 0 & 0 & \sqrt{2} & 0 & \sqrt{2} & 0 & 0 & 0 & 0 & 0 \\ 0 & 0 & 0 & \sqrt{2} & 0 & \sqrt{2} & 0 & 0 & 0 & 0 \\ \sqrt{2} & 0 & 0 & -1 & 0 & 1 & 0 & 0 & 0 & 0 \\ 0 & \sqrt{2} & -1 & 0 & 1 & 0 & 0 & 0 & 0 & 0 \\ \sqrt{2} & 0 & 0 & 1 & 0 & -1 & 0 & 0 & 0 & 0 \\ 0 & \sqrt{2} & 1 & 0 & -1 & 0 & 0 & 0 & 0 & 0 \\ 0 & 0 & 0 & 0 & 0 & 0 & 0 & 0 & 2 & 0 \\ 0 & 0 & 0 & 0 & 0 & 0 & 0 & 0 & 0 & -2 \\ 0 & 0 & 0 & 0 & 0 & 0 & 2 & 0 & 0 & 0 \\ 0 & 0 & 0 & 0 & 0 & 0 & 0 & -2 & 0 & 0 \end{pmatrix} \tag{2.21}$$

The first, $\Theta_{A_1} \propto \mathbb{1}$, indicates that biaxial strain will multiply each mode by a constant; e.g. 1% biaxial strain will change a 1 Å distortion in B_2 to a 1.01 Å distortion also in B_2. The others are less trivial, but still obey the multiplication table for C_{6v}, most notably that a non-shear E_2 strain will transform an A_1 distortion into the second row of an E_2 distortion and vice versa, and mutatis mutandis for the shear E_2 strain and the first row. A general formula for computing Θ appears in Chapter 3.5.

Rotation

To understand how rotation couples terms of different orders, consider the simple two-dimensional dimer of diameter 1. As shown in Figure 2.3, this C_{2v} cluster decomposes as a stretch (σ) mode (A_1), a shear (π) mode (A_2), and translation ($B_1 + B_2$). We remove the translation modes due to homogeneity of free space, leaving only A_1 and A_2. By group theory, the only symmetry-independent terms in our Taylor expansion are $A_1^m A_2^n$, where m

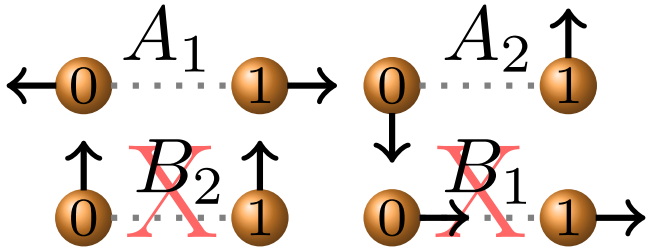

Figure 2.3: Symmetrized modes of the two-dimensional dimer. The pure-translation modes are removed thanks to homogeneity of free space with respect to uniform translation.

and n are nonnegative integers, and n is even.

A continuous rotation of angle θ corresponds to an amplitude of $1-\cos\theta$ on the A_1 mode and of $\sin\theta$ on the A_2 mode. Now let us Taylor-expand an arbitrary potential:

$$V = \sum_{m,n} c_{m,n} A_1^m A_2^n = \sum_{m,n} c_{m,n} (1-\cos\theta)^m \sin^n\theta \tag{2.22}$$

By homogeneity of free space with respect to rotation, we know $\partial^p V/\partial\theta^p = 0\ \forall p$. This gives us a set of constraining equations, one for each p. The first requires $c_{0,2} = 0$, but the others all couple terms of different orders explicitly.

Applying this to the slave modes, the three-dimensional cube (point group O_h) is particularly illustrative. The Cartesian representation of the cube decomposes to tensile strain ($A_{1g} + E_g$), shear strain (T_{2g}), rotation (T_{1g}), translation (T_{1u}), and six degrees of internal motion ($T_{2g} + A_{2u} + E_u + T_{2u}$).

If we blindly apply the formalism described earlier to impose translational symmetry at second order, we create the $\hat{\nu}$ matrix at second order. Its null row space ($\ker(\nu^T)$) gives three gauge freedoms; up to constant factors, they are:

1. $c_{T_{1u}^2} + c_{T_{2g}^{(rot)} \times T_{2g}^{(int)}} + c_{T_{2u}^2}$: Translation, internal degrees of freedom, and coupling between internal degrees of freedom and rotation.
2. $c_{A_{2u}^2} + c_{E_u^2} + c_{T_{1u}^2} + c_{T_{2g}^{(rot)} \times T_{2g}^{(int)}} + c_{T_{2u}^2}$: Also translation, internal degrees of freedom,

and coupling between internal degrees of freedom and rotation.

3. $c_{A_{1g}^2} + c_{E_g^2} + c_{T_{1g}^2} + c_{T_{2g}^{(rot)2}}$: Tensile strain, shear strain, and rotation.

The last one is problematic, because all four constants are directly observable via lattice distortions (whether experimental or computational). So how can their sum be a gauge freedom that can take any value; it can't possibly sum to zero over the whole cluster?! The answer is that this is a fictitious gauge freedom, much like the rotation of the single hexagon (and similar in the 2D square [29]), because rotation has not yet been applied. When we apply rotation, however, this is not a true degree of freedom; the force constant associated with $T_{2g}^{(rot)}$ is zero.

Physically, by neglecting rotational invariance, we are breaking the crystal symmetry; one cannot have point- and space-group symmetry, together with homogeneity of free space with respect to arbitrary translation, without also having homogeneity of free space with respect to arbitrary rotation.

Alternatively, instead of explicitly setting rotational invariance, we can use a Cartesian-monomial basis. This eliminates the slave modes' gauge freedom in the final fitting process, removing the issue. A third option is to include strain derivatives in our dataset; this ensures that our gauge freedom is set to the physically observable value. This is one strong motivation, besides computational efficiency, of computing our force constants in strain+reciprocal space.

Chapter 3

The Anharmonic Dynamical Tensor

After determining the form of our Hamiltonian, we must choose how to determine the physical parameters of the Hamiltonian. The simplest approach is the empirical potential, which fits the parameters to mirror some observed value or effect. Many such potentials have been fabricated, including some specifically for graphene and carbon-based materials [35–46]. However, such models include only the effects they are designed to mimic, and their predictive power for other situations is limited. We will show that the "phonon-optimized" empirical potentials for graphene fail to capture the anharmonic behavior of the phonons. We therefore focus on first-principles methods to compute interatomic interactions.

We will focus on density-functional theory in the local-density approximation, which is well-established and generally captures the physics of graphene [47, 48]. For other materials, in principle one can use beyond-DFT approaches, such as DFT+U, dynamical mean-field theory (DMFT) [49], GW, or others, as long as the total energy can be computed. Furthermore, we will show that computing the forces significantly reduces the computational cost; recent work has shown that forces can be computed via DMFT [50, 51] and GW [52].

The interatomic interactions in crystals are best described in reciprocal space (the irreducible representations of the translation group), where the quanta of excitation are known as phonons. The dynamical matrix contains the derivatives of the energy with respect to phonons. At harmonic order, there are four main ways to calculate the phonon spectrum via density-functional theory:

1. The frozen-phonon method displaces the atoms in a material according to a phonon $u^{\vec{k}}$, and measures the reciprocal-space forces induced thereby on the atoms of the crystal. The

derivative $-\partial F_i^{\vec{k}}/\partial u_j^{\vec{k}}$ gives the dynamical matrix. This is the simplest method, and the one we use here (with some subtleties). The cost of the calculation depends on the wavevector $\vec{k}$, and specifically the size of a cell that contains $\vec{k}$ as one of its reciprocal lattice vectors. A common notation for this condition is that $\vec{k}$ "fits within" the cell.

2. Density-functional perturbation theory (DFPT) [53–56] is an application of second-order perturbation theory that takes derivatives of the wavefunctions (or Kohn-Sham orbitals) to form the dynamical matrix. This allows independent calculations for each phonon wavevector $\vec{k}$. A given calculation might be more expensive than frozen phonon (if $\vec{k}$ fits within a relatively small cell) or not (if it does not).

3. The simple supercell method [48, 57, 58] computes the real-space force constants, which can then be Fourier transformed to the dynamical matrix. A supercell is generated that is large enough that real-space interactions decay between the center and the boundaries of the supercell. Then an atom is perturbed by x_i to create forces F_j on the other atoms; the force constants are $-\partial F_j/\partial x_i$. In addition to being expensive to create such a large supercell, this method requires convergence with respect to supercell size, which is generally difficult.

4. The k+supercell method [59], implemented in the Phonopy code [60], performs the same calculation as the simple supercell method, but is essentially a Fourier interpolation. It ensures that any wavevector $\vec{k}$ that is a reciprocal lattice vector gets its dynamical matrix from the calculated forces, which prevents any range issues from affecting it. However, due to the nonlinear scaling of density-functional theory, this is significantly more expensive than performing DFPT or frozen-phonon computations for each wavevector in the supercell reciprocal lattice and performing a direct Fourier transform.

5. Molecular dynamics can be performed in an *ab-initio* calculation. Each point along the trajectory contains a set of atomic positions and forces. These can be fit to real-space force constants where $F_i = -\sum_j \Phi_{ij} x_j$.

Extending this to the anharmonic interactions can be done in a few ways:

1. One can perform a small correction to the harmonic terms to account for anharmonic

perturbations. This method is popular for temperature-dependent effects, where the anharmonic contributions are assumed to be relatively small. A related approach is to expand the Hamiltonian to second order around a point that is not the ground state, providing phonon-like quasiparticles around that point. Examples, of various degrees of sophistication, include the quasiharmonic approximation (QHA), self-consistent phonon theory (SCPH) [61, 62] or self-consistent harmonic approximation (SCHA) [63, 64], and a temperature-dependent effective potential (TDEP) [65–68]. However, when calculations are performed at a fixed temperature, it is temptingly misleading to extend the results to an entirely different temperature.

2. Alternatively, the harmonic methods described above can be extended to anharmonic force constants, simply by changing the numerical order of the derivative. However, great care must be taken to ensure numerical convergence with higher-order derivatives, which is generally difficult. This is the approach we take.

Here we describe a rapid, efficient, and high-throughput approach to calculate the interatomic interactions using a generalization of the frozen-phonon method. We calculate the derivatives of energy in a strain+phonon basis, which we later use to determine the coefficients for our polynomial expansion.

3.1 Derivation of the Anharmonic Dynamical Tensor

The formal treatment of interatomic interactions in a periodic crystal is to transform the force constants to reciprocal space, which is equivalent to symmetrization in terms of irreducible representations of the translation group. At harmonic order in real space, we consider the interatomic force constants $\Phi_{\vec{R}}^{\alpha\beta}$, a matrix containing the force constants between each degree of freedom (α) of the primitive cell at $\vec{0}$ and a degree of freedom (β) of the primitive cell at location $\vec{R}$. A Fourier transform of Φ gives the dynamical matrix $\mathcal{D}_{\vec{k}}^{\alpha\beta}$, which describes the forces that a phonon u_α with periodicity $\vec{k}$ exerts on another phonon u_β with periodicity $-\vec{k}$.

The anharmonic extensions are the anharmonic interatomic force constants

$$\Phi^{\alpha,\beta,\dots}_{\vec{0},\vec{R}_1,\dots} \equiv \frac{\partial^\lambda U}{\partial x^\alpha_{\vec{0}} \partial x^\beta_{\vec{R}_1} \dots} \tag{3.1}$$

and the anharmonic dynamical tensor (ADT)

$$\mathfrak{D}^{\alpha,\beta,\dots}_{\vec{k}_1,\vec{k}_2,\dots} \equiv \frac{\partial^\lambda U}{\partial u^\alpha_{\vec{k}_1} \partial u^\beta_{\vec{k}_2} \dots} \tag{3.2}$$

The Fourier transform is performed by the relationship

$$x_{\vec{R}} = \sum_{\vec{k}} e^{i\vec{k}\vec{R}} u_{\vec{k}} \tag{3.3}$$

to ensure that $\sum_{\vec{R}} x_{\vec{R}} = \sum_{\vec{k}} u_{\vec{k}}$. Hence if we examine a single term of the Taylor expansion of order λ,

$$\sum_{\vec{R}} \left(\Phi^{\alpha_0,\alpha_1,\dots}_{\vec{R},\vec{R}_1+\vec{R},\dots} \prod_{l=0}^{\lambda} x^{\alpha_l}_{\vec{R}_l+\vec{R}} \right) = \sum_{\vec{k}_0,\vec{k}_1,\dots} \left(\sum_{\vec{R}} e^{i\vec{R}\sum_l \vec{k}_l} \right) \mathfrak{D}^{\alpha_0,\alpha_1,\dots}_{\vec{k}_0,\vec{k}_1,\dots} \prod_{l=0}^{\lambda} u^{\alpha_l}_{\vec{k}_l} e^{i\vec{k}_l\vec{R}_l} \tag{3.4}$$

This demonstrates two important features of the ADT: First, the ADT is the Fourier transform of the anharmonic interatomic force constants. Second, by the parentheses in Equation (3.4), phonons couple to each other if and only if they sum to a reciprocal lattice vector. This is also known as conservation of crystal momentum, and is equivalent to ensuring the ADT transforms like the fully symmetric irreducible representation of the translation group ($\sum_l \vec{k}_l$ is a reciprocal lattice vector). If they sum to a reciprocal lattice vector other than Γ, the process is known as umklapp scattering, which is the main mechanism of the atomic contribution to thermal transport. (At second order, only $-\vec{k}$ couples to $\vec{k}$, which is equivalent to $u_{\vec{k}}$ coupling to $u^*_{\vec{k}}$, which retrieves the usual $U = \langle u_{\vec{k}} | \mathcal{D}_{\vec{k}} | u_{\vec{k}} \rangle$.)

3.2 Incorporating Strain

The Fourier transform works well for an infinite crystal, using e.g. Born-von Karman boundary conditions. However, we can gather high-precision force constants using a mixed strain-phonon basis. This is possible because it is simple and inexpensive to compute strain via first-principles calculations, as it amounts to merely adjusting the lattice parameters. Although it is physically impossible to distort a nonrelativistic infinite crystal, we can describe the effect of strain on a bulk material by computing the properties of a distortion of space on an infinite crystal. We will return to the application to slave modes in Chapter 4.1.

3.3 Computation of the Anharmonic Dynamical Tensor

As described above, multiple methods can be used to compute the anharmonic dynamical tensor. In principle DFPT can be used, but it is difficult to converge higher-order derivatives of the electronic orbitals, and has not yet been demonstrated even at fourth order. We elect to use the method of frozen phonons, where we impose a phonon on a cell via direct perturbation of atoms, and directly calculate the energy and forces. The computational expense depends on the phonon wavelength, and specifically the size of cell necessary for the wavevector to be a reciprocal lattice vector.

We add to this the method of finite differences and quadratic error tails described in Chapter 3.4, combined with high-throughput high-precision DFT calculations, to converge the ADT entries. Unlike a polynomial fit, a finite-difference approach will ensure there is no sloshing between orders, and give us ADT entries that are converged term-by-term and order-by-order. We also get one derivative from Hellman-Feynman forces, so a fifth-order contribution requires only a fourth-order stencil; details are presented in Chapter 3.5.

3.4 Finite Differences of Arbitrary Order and Dimension

The method of finite differences is well-known, but much of the treatment emphasizes one-variable functions. The work on multivariable functions rarely exceeds quadratic order. For background and introductory references, see Refs. 69–71. Here we present derivation for a uniform grid to find a derivative of arbitrary order and arbitrary number of variables. We can thus use the quadratic error tail to ensure a converged result.

The key to numerical differentiation is the stencil. Here we restrict ourselves to a uniformly-meshed symmetric (central) stencil of spacing δ that provides a well-defined error tail. Suppose we want to find the derivative of a multivariable function $f(x_1, x_2, \ldots)$ by taking measurements of f along a stencil of spacing δ. We can take linear combinations of these measurements to compute the derivative:

$$\partial^{\vec{k}} f \equiv \frac{\partial^{\lambda} f}{\partial x_1, x_2, \ldots} = \sum_m a_m f_m + \mathcal{O}(\delta^2) \tag{3.5}$$

where m indexes points on our stencil. We measure these values within $\delta_{min} \leq \delta \leq \delta_{max}$, where δ_{min} is the computational boundary where small denominators create numerical error, and δ_{max} is the function-dependent boundary where contributions of $\mathcal{O}(\delta^4)$ become significant. Thus we can fit our finite-difference data to a quadratic curve, $q(\delta) = q(0)+\alpha\delta^2+\mathcal{O}(\delta^4)$, and compute the converged derivative $\partial^{\vec{k}} f = q(0)$.

The derivation of the one-dimensional symmetric stencil is well-known; we will shortly generalize to multiple dimensions. For one dimension, we expand our function as a Taylor series:

$$f_m = f(x + m\delta) = \sum_{n=0}^{\infty} \frac{m^n}{n!} \delta^n f^{(n)}(x) \tag{3.6}$$

We take a linear combination of Equation (3.6), multiplying each measurement f_m by a value

a_m, and separate out the derivatives:

$$\sum_n b_n \delta^n f^{(n)} = \sum_{m=-M}^{M} a_m f_m - \sum_{m=-M}^{M} a_m f_0 \tag{3.7}$$

for some values of a_m and b_n. Rearranging to isolate a particular derivative of order k,

$$b_k f^{(k)} = \delta^{-k} \left(\sum_{m=-M}^{M} a_m f_m - \sum_{m=-M}^{M} a_m f_0 \right) - \sum_{n \neq k} b_n \delta^{n-k} f^{(n)} \tag{3.8}$$

We wish to solve this where b_n is zero for as many terms as possible, thus isolating $f^{(k)}$ as dependent only on the stencil observations f_m:

$$b_n \equiv \sum_{m=-M}^{M} \frac{m^n}{n!} a_m = \begin{cases} 1 & n = k \\ 0 & n \neq k \ \& \ 1 \leq n \leq n_{max} \end{cases} \tag{3.9}$$

It can be shown that $n_{max} = 2M$. We thus have $2M$ linear equations where $b_n = \delta_{nk}$ and wish to solve for a_m; this amounts to solving a matrix whose entries are $m^n/n!$. We can thus account for all terms up to $\mathcal{O}(\delta^{n_{max}-k})$. Our error tail is $\mathcal{O}(\delta^p)$, where if k is odd (so $a_m = -a_{-m}$) then $p = 1 + 2M - k$, and if k is even (so $a_m = a_{-m}$) then $p = 2 + 2M - k$. Choosing the appropriate value of M will ensure the quadratic error tail ($p = 2$).

Now we extend this to a function of L variables. The Taylor expansion of f is:

$$f_{\vec{m}} = f_{\vec{0}} + \sum_{\vec{n} \in \mathbb{Z}^L_{\geq 0}} \delta^{|n|_1} \prod_{l}^{L} \frac{m_l^{n_l}}{n_l!} \partial^{\vec{n}} f \tag{3.10}$$

where the values of our derivatives ($\vec{n}$) are restricted to the first quadrant, octant, etc. (i.e. all n_l are nonnegative) and $|k|_1$ is the one-norm defined as $\sum_{l=1}^{L} |k_l|$. A linear combination

of these equations and rearrangement of terms gives:

$$b_{\vec{k}}\partial^{\vec{k}}f = \frac{1}{\delta^{|k|_1}}\left(\sum_{\vec{m}} a_{\vec{m}} f_{\vec{m}} - \sum_{\vec{m}} a_{\vec{m}} f_0\right) - \sum_{\vec{n}\neq\vec{k}} b_{\vec{n}}\delta^{|n|_1-|k|_1}\partial^{\vec{n}}f \tag{3.11}$$

where $\vec{m}$ iterates over all points in our stencil, with entry l of the vector iterating from $-M_l$ to M_l (for our symmetric central stencil). Just as for the one-dimensional case, we calculate $b_{\vec{n}}$ as

$$b_{\vec{n}} \equiv \sum_{\vec{m}}\prod_{l}^{L}\frac{m_l^{n_l}}{n_l!}a_{\vec{m}} = \begin{cases} 1 & \vec{n}=\vec{k} \\ 0 & \vec{n}\neq\vec{k}\ \&\ 1\leq|n|_1\leq n_{max} \end{cases} \tag{3.12}$$

and again solve for a_m by inverting the matrix with entries $\prod_l^L \frac{m_l^{n_l}}{n_l!}$. The error tail is $\mathcal{O}(\delta^{|p|_1})$, where if k_l is even then $p_l = 1+2M_l-k$ and if k_l is odd then $p_l = 2+2M_l-k$. This can be shown by noting that if $b_{\vec{k}}=1$, all values of $b_{\vec{n}}$ are zero unless, for all l, n_l and k_l are either both even or both odd.[1]

It is notable that even with δ being constant for all values of l (a stencil size that is constant across all variables), the error tail due to the finite-difference method can still be chosen to be $\mathcal{O}(\delta^2)$. However, we still must ensure that the sampled range is within $\delta_{min}\leq\delta\leq\delta_{max}$ defined earlier, which is not guaranteed to be the same for all variables.

3.5 Hellman-Feynman Derivatives

Once density-functional theory computes the Kohn-Sham orbitals, we can find the forces via Hellman-Feynman forces, giving us one derivative without any extra computational cost. Although the VASP code gives real-space forces on each atom, a Fourier transform gives us the forces in k-space, i.e. the force on a particular phonon $\partial E/\partial u_{\vec{k}}$, and we can similarly calculate the stress to find the derivative in strain. This reduces the order of the finite-

[1]Equivalently, let $\hat{S}_l$ be an operator that flips the sign on the l-th element of a vector; then if k_l is even then $a_{\vec{m}} = a_{\hat{S}_l\vec{m}}$, and if k_l is odd then $a_{\vec{m}} = -a_{\hat{S}_l\vec{m}}$.

difference calculation, and thus in general the size of the stencil required to compute as well. However, there are a number of subtleties to this approach, for which care must be taken. We detail some of these subtleties here.

Real Displacements

Unfortunately, the universe is not designed to allow atomic displacements of an imaginary distance. Therefore, we cannot compute a phonon $u_{\vec{k}} = \sum_{\vec{k}} e^{i\vec{k}\vec{r}} x_{\vec{r}}$ directly. Instead, we impose a cosine or sine displacement $v_{\pm\vec{k}} = (u_{\vec{k}} \pm u_{-\vec{k}})/\sqrt{2}$ (using the fact that $u_k = u^*_{-k}$). Hence those derivatives that are calculated via a finite-difference derivative will actually compute

$$\frac{\partial E}{\partial v_{\pm\vec{k}}} = \frac{\partial E}{\partial u_{\vec{k}}} \pm \frac{\partial E}{\partial u_{-\vec{k}}} \tag{3.13}$$

while those that are computed via Hellman-Feynman forces will compute $\partial E/\partial u_{\vec{k}}$.

Example: At second order, the real (imaginary) part of the dynamical matrix can be considered the coupling between a cosine wave of a particular wavevector with the cosine (sine) wave of the same wavevector. Using only cosine displacements will not allow computation of the imaginary part of the dynamical matrix from energy derivatives. However, when we use Hellman-Feynman forces, we can measure directly when a cosine displacement causes a cosine (sine) force, which yields the real (imaginary) part of the dynamical matrix.

A finite-difference stencil is much more efficient if we can reduce the number of axes required. Therefore we use only cosine displacements, and retrieve Hellman-Feynman forces that include all sinusoidal couplings.

Strain Conventions

In two dimensions, we define the strain tensor as

$$\begin{pmatrix} x' \\ y' \end{pmatrix} = \begin{pmatrix} 1+\varepsilon_{xx} & \varepsilon_{xy}/2 \\ \varepsilon_{xy}/2 & 1+\varepsilon_{yy} \end{pmatrix} \begin{pmatrix} x \\ y \end{pmatrix} \tag{3.14}$$

and define the symmetric and asymmetric strains as:

$$\varepsilon_{biax} = \frac{\varepsilon_{xx} + \varepsilon_{yy}}{\sqrt{2}} \qquad \varepsilon_{asym} = \frac{\varepsilon_{xx} - \varepsilon_{yy}}{\sqrt{2}} \tag{3.15}$$

In the C_{6v} point group, ε_{biax} transforms as A_1,while ε_{asym} and ε_{xy} transform as the two rows of E_2.

In three dimensions, the strain tensor is

$$\begin{pmatrix} x' \\ y' \\ z' \end{pmatrix} = \begin{pmatrix} \varepsilon_{xx} & \frac{\varepsilon_{xy}}{2} & \frac{\varepsilon_{xz}}{2} \\ \frac{\varepsilon_{xy}}{2} & \varepsilon_{yy} & \frac{\varepsilon_{yz}}{2} \\ \frac{\varepsilon_{xz}}{2} & \frac{\varepsilon_{yz}}{2} & \varepsilon_{zz} \end{pmatrix} \begin{pmatrix} x \\ y \\ z \end{pmatrix} \tag{3.16}$$

and we can decompose the strains into:

$$\varepsilon_{+} = \frac{\varepsilon_{xx} + \varepsilon_{yy} + \varepsilon_{zz}}{\sqrt{3}} \quad \varepsilon_{-1} = \frac{\varepsilon_{xx} - \varepsilon_{yy}}{\sqrt{2}} \quad \varepsilon_{-2} = \frac{-\varepsilon_{xx} - \varepsilon_{yy} + 2\varepsilon_{zz}}{\sqrt{6}} \tag{3.17}$$

True Stress

When we calculate stresses from first principles, we must take care with respect to true and engineering stress. The stress computed from Hellman-Feynman forces is the true stress, whereas the strain derivatives we will compute (using Θ of Equation 4.1) use engineering strains. In the following derivations, Greek letters (σ, ε) refer to engineering stresses and strains, while Latin letters (S, e) refer to true stresses and strains.

By definition, engineering strain is taken relative to the initial length, while true strain is relative to its current length:

$$\varepsilon = \frac{L_f - L_i}{L_i} \qquad e = \int_{L_i}^{L_f} \frac{dL}{L} = \ln(1 + \varepsilon) \tag{3.18}$$

and thus the stresses, i.e. derivatives of energies, are related as:

$$S = -\frac{dE}{de} = -\frac{dE}{d\varepsilon}\frac{d\varepsilon}{de} = \sigma(1+\varepsilon) \tag{3.19}$$

This works for tensile strain. However, once we add shear strain, the calculations are non-trivial to solve; now the integral $e_{xx} = \int dx/x$ turns into an integral in both dx and dy.

The simplest solution is to rotate the system to its principal axes, where there is no shear strain, to decouple the axial strains, from which the usual formulae apply.

Example: 2D Suppose ϵ and e are the engineering and true strain in the Cartesian basis, and η and h are the engineering and true strains in the diagonalized (principal) basis. The transformation is simply $H^{-1} = \text{eigvec}(\hat{\varepsilon})^T$, with normalized eigenvectors.

$$\begin{pmatrix} x \\ y \end{pmatrix} = \hat{\varepsilon}\begin{pmatrix} x_0 \\ y_0 \end{pmatrix} = \begin{pmatrix} 1+\varepsilon_{xx} & \varepsilon_{xy}/2 \\ \varepsilon_{xy}/2 & 1+\varepsilon_{yy} \end{pmatrix}\begin{pmatrix} x_0 \\ y_0 \end{pmatrix} \tag{3.20}$$

$$H^{-1} \equiv \text{eigvec}(\hat{\varepsilon})^T \tag{3.21}$$

$$\eta = H\varepsilon H^{-1} \qquad h = \ln(\eta) \qquad e = H^{-1}hH \tag{3.22}$$

$$e_{ik} = \sum_j H_{ij}^{-1} \ln\left(\sum_{ml} H_{jm}\varepsilon_{ml}H_{lj}^{-1}\right) H_{jk} \tag{3.23}$$

$$-S_a = \frac{\partial V}{\partial \varepsilon_a} = \sum_b \frac{\partial e_b}{\partial \varepsilon_a}\frac{\partial V}{\partial e_b} = -D_{ab}\sigma_b \tag{3.24}$$

Normalization

When we perform a DFT calculation, we want to measure the energy, stress, and forces at a given point on the stencil, using the smallest possible cell. We must therefore normalize our phonons such that energy, stress, and forces can be normalized per-atom, to allow comparison between different cells with a quadratic error tail.

Example: Suppose we want to compute ΓMM scattering. This requires a two-axis stencil, one for Γ and one for M. This generally requires a 2-cell supercell, but those points of the stencil that are on the Γ axis (so $M = 0$) require only one unit cell. Therefore we

need to compare the energies and forces of one unit cell with those of two unit cells.

We seek to fix our independent variables, ε (strain) and $\delta_{\vec{k}} u_{\vec{k}}$ (phonon amplitude) to be intensive properties, while E (energy) $S = \partial E/\partial\varepsilon$ (stress), and $f_{\vec{k}} = \partial E/\partial u_{\vec{k}}$ (phonon force) are extensive properties that scale with cell size; then we can divide those by cell size to retrieve per-cell quantities.

It is almost never worth it to use an unnormalized basis. The phonon is normalized when summed over each $\vec{t}$ of our N unit cells in the supercell:

$$\sum_{\vec{t}}^{N} |\langle x_{\vec{t}}|u_{\vec{k}}\rangle|^2 = 1 \Rightarrow \langle x_{\vec{t}}|u_{\vec{k}}\rangle = e^{i\vec{k}\vec{t}}/\sqrt{N} \tag{3.25}$$

We impose a distortion on atom j of cell $\vec{t}$ that does not depend upon N:

$$|d_{\vec{t},j}\rangle = \delta_0 \cos(\vec{k}\vec{t})|x_{\vec{t},j}\rangle \tag{3.26}$$

Then the total phonon amplitude is:

$$\langle u_{\vec{k}}|d\rangle = \frac{\delta_0}{\sqrt{N}} \sum_{\vec{t},j} e^{-i\vec{k}\vec{t}} \cos(\vec{k}\vec{t}) \propto \sqrt{N} \tag{3.27}$$

which causes an energy and force

$$E = \frac{1}{2}\mathcal{D}\langle u_{\vec{k}}|d\rangle^2 \propto N \quad \langle u_{\vec{k}}|F\rangle = -\mathcal{D}\langle u_{\vec{k}}|d\rangle \propto \sqrt{N} \tag{3.28}$$

The energy is extensive already. The force must first be multiplied by $\sqrt{N}$ to get an extensive quantity. Therefore, our finite-difference calculations will use the dependent quantity of $\langle u_{\vec{k}}|F\rangle\sqrt{N}$.

Stress also requires normalization, for a different reason. As discussed in Chapter 3.4, although we are assured of a quadratic error tail from the finite differences, we are not assured that the limit of numerical accuracy (δ_{min}) or quartic contributions (δ_{max}) are the

same for each axis of our stencil. We therefore need to scale our strain to some length scale for accurate comparison with phonons.

Under strain tensor $\hat{\varepsilon}$, a lattice vector $\vec{V}$ is adjusted by length $|(\hat{\varepsilon} - \mathbb{1})\vec{V}|$; this quantity, averaged over all vectors, should be equal to the scaling δ of the phonons.

Orthogonalization

Orthogonalization of strain axes to each other, or phonon axes to each other, is simple. However, orthogonalizing strains to phonons is not, because they are noncommutative operations. To wit, straining a cell by $\hat{\varepsilon}$ followed by a phonon $\delta_{\vec{k}}$ differs from first creating the phonon $\delta_{\vec{k}}$ and then straining by $\hat{\varepsilon}$, because the strain distorts the phonon. Equivalently, if we impose the strain first, then constant values of $\delta_{\vec{k}}$ have the same displacement in Cartesian coordinates. If we impose the phonon first, then constant values of $\delta_{\vec{k}}$ have the same displacement in lattice coordinates, but not in Cartesian coordinates.

The mathematics described in Chapter 3.2 and Chapter 4.1 use a strain-first approach, so we use that convention. However, the partial derivatives from Hellman-Feynman forces must be scaled appropriately.

Let δ refer to a distortion (phonon) of constant Cartesian amplitude, and λ refer to a distortion of constant amplitude in lattice coordinates, where the lattice vectors are V. A strain tensor $\hat{\varepsilon}$ transforms our variables as follows:

$$V' = \hat{\varepsilon}V \quad \lambda' = \lambda \quad \delta' = \hat{\varepsilon}\delta = \hat{\varepsilon}V\lambda \tag{3.29}$$

The derivatives we seek for finite differences are:

$$F = -\left(\frac{\partial E}{\partial \delta}\right)_{\varepsilon} \quad \sigma_c = -\left(\frac{\partial E}{\partial \varepsilon}\right)_{\delta} \tag{3.30}$$

The force F is a Fourier transform of the Hellman-Feynman atomic forces, with some normalization. The stress is not as simple, however. The Hellman-Feynman forces at a particular

point of the stencil give the true stress:

$$S = -\left(\frac{\partial E}{\partial e}\right)_{\lambda} \tag{3.31}$$

where e is the true strain. This can be converted to σ_c with multivariable calculus.

Chapter 4

Determining the Parameters

We built the polynomial expansion as described in Chapter 2, and can calculate the ADT in strain+phonon space as described in Chapter 3. Now we bring the two together, to determine the independent coefficients in our polynomial expansion.

The polynomial expansion is in real space, while the ADT is provided in reciprocal space. The simplest approach is a straightforward uniform Fourier transform, also known as Fourier interpolation, to calculate the ADT at arbitrary wavevectors from a uniform mesh of measurments in reciprocal space [13]. However, this approach has two major disdvantages. First, it does not incorporate the information from strain derivatives, which is a relatively easy calculation. Second, especially at anharmonic orders, it requires significantly more computation than a nonuniform mesh. When calculating the coupling of phonons of different wavevectors, one must use a cell where all such wavevectors fit within the cell (i.e. are reciprocal lattice vectors). Different wavevectors along a 3x3 mesh may take a 9-cell calculation, whereas a nonuniform mesh can measure points along finer meshes (e.g. 4x4) that require smaller computations (e.g. only a 4-cell calculation, depending on the wavevector).

We therefore sample a large number of ADT entries along a nonuniform mesh, taking care to pick the points that are efficient to compute. Below we show the linear relationship between the ADT entries and the sought polynomial-expansion coefficients, allowing us to use standard statistical tools for this linear problem.

4.1 Strain and Phonon Derivatives

We return to the symmetrized modes described earlier. The derivative of a mode ϕ_k with respect to strain ε_α is

$$\frac{\partial \phi_k}{\partial \varepsilon_\alpha} = \sum_{k'} \Theta_{\alpha k k'} \phi_{k'0} \tag{4.1}$$

where Θ is a symmetry-obedient linear transformation between modes. An example for the hexagonal lattice appears in Chapter 2.3. Detailed symmetrized-strain conventions are provided in Chapter 3.5.

When we apply this to our polynomial expansion of Equation (2.4), as an expansion around $\vec{\phi}^0$ (the equilibrium or high-symmetry structure), we can find:

$$\frac{\partial \Gamma_i}{\partial \varepsilon_\alpha} = \frac{\partial}{\partial \varepsilon_\alpha} S_{ij} \prod_k (\phi_k - \phi_k^0)^{p_{ijk}} = S_{ij} \left(\sum_{k'} \Theta_{\alpha k k'} \phi_{k'}^0 \right) p_{ijk} \prod_{k''} (\phi_{k''} - \phi_{k''}^0)^{p_{ijk''} - \delta_{kk''}} \tag{4.2}$$

Then we can transform $\vec{\phi}$ to Cartesian coordinates via Equation (2.3), and then to k-space phonons via Equation (3.3). This gives us an equation relating the k-space phonons to the $\vec{n}$th derivative of Γ_i with respect to strain:

$$\partial_{\varepsilon}^{\vec{n}} \Gamma_i = f(\vec{u}_{\vec{k}_0}^{\alpha_0}, \vec{u}_{\vec{k}_1}^{\alpha_1}, \dots) \tag{4.3}$$

Now we can compute the derivatives in k-space, obtaining $\hat{M}$, the linear relationship between derivatives and symmetry-independent terms:

$$\frac{\partial^\lambda U}{\partial \epsilon_{\alpha_0}, \dots \partial u_{\vec{k}_1}^{\alpha_1}, \dots} = \sum_i c_i M_i^{\alpha_0, \dots \vec{k}_1, \alpha_1, \dots} \tag{4.4}$$

One can apply a similar methodology to treat the Jahn-Teller effect, emphasizing the cooperative effects produced by strain+$\vec{k} = 0$ distortions [72].

4.2 Fitting Procedure

We thus accumulate a set of calculated ADT parameters, the left-hand side of Equation (4.4), and their linear relationships to the sought coefficients c_i, given by the matrix M on the right-hand side of Equation (4.4). Furthermore, terms of different orders do not couple; to wit, the M matrix links ADT entries and polynomial terms of strictly the same order. We can therefore compute the terms order-by-order without any sloshing between orders. This is notably different from the popular polynomial fit, which fits all orders simultaneously, allowing the possibilities of sloshing between orders.

We perform a least-squares fitting technique to eliminate noise from our data. This noise can emerge from a few different sources. First, our quadratic error tails may not be perfectly converged when we extrapolate from finite-difference stencil-spacing δ to zero. The Taylor expansion assumes well-defined derivatives; a phase transition in a material may break that assumption. Finally, the range of the interactions may not be fully captured by the polynomial expansion. This could be fixed by increasing the range, or it could be a nonanalytic effect that cannot be captured by any finite set of real-space interactions (such as polarization [22, 55] or a Kohn anomaly [73]).

Our algorithm is described in Chapter 4.3; we use a weighted least-squares fit with leave-one-out cross-validation [18] to increase predictive power. Previous researchers have calculated interatomic force constants with various machine-learning techniques, such as neural networks [74–76], Bayesian optimization [77], compressive sensing [78–80], and the least-absolute-shrinkage selection operator (LASSO) [61]. The last two are notable in their assumptions; compressive sensing assumes a basis in which terms are sparse, while LASSO assumes a basis in which terms have small magnitudes. In fact, we have shown that the choice of basis and gauge has no small amount of freedom. Although a basis can be chosen that has either sparse or small-magnitude terms, there is little reason to *a priori* assume that a particular basis has one or the other [10, 20].

4.3 Weighted Least-Squares Fitting with Cross-Validation

We create, as described, a linear relationship between our symmetrized coefficients $\vec{c}$ and the measured energy-derivatives (ADT entries) in strain+k-space $\vec{\Omega}$:

$$\vec{\Omega} = M\vec{c} \tag{4.5}$$

Because we have determined each value of $\vec{\Omega}$ via a fitted extrapolation of a quadratic curve to $\delta = 0$, as described in Chapter 3.4, we can compute an estimated standard error $\vec{\sigma}$ for each measured value of $\vec{\Omega}$ as the standard error of the quadratic fit. To reduce error, we oversample $\vec{\Omega}$ and choose only those points with a converged quadratic fit $|\sigma/\Omega| < \alpha$. We described some of the variety of machine-learning algorithms to solve this linear equation; we use only weighted least-squares and iterative leave-one-out cross-validation.

Some of our measurements $\vec{\Omega}$ have more error ($\vec{\sigma}$) than others. We consider this a weighted least-squares problem, which can be formed into an ordinary least-squares problem by the following renormalization: $\vec{M}' = \sqrt{W} \cdot M$ and $\vec{\Omega}' = \sqrt{W} \cdot \vec{\Omega}$, where W is a weighting matrix consisting of $1/\sigma^2$ on its diagonals. This ensures that the measurements with smaller uncertainties contribute more significantly to the fitting.

A least-squares fit is defined as the solution x to the equation $b = Ax + r$, for fixed A and b, where $\langle r|r\rangle$ is minimized. The covariance matrix is $S = (A^T A)^{-1}$, and the so-called hat matrix $H = ASA^T$. The least-squares solution is $x = SA^T b$, giving residuals of $(\mathbb{1} - H)b$. The standard variance of x is given by the diagonal entries of S multiplied by the mean-squared error $\langle r|r\rangle/M$; the standard error is merely the square root of the variance.

We measure the predictive power of the fit via the leave-one-out cross-validation score (LOOCV), which can be found via the prediction residual error sum of squares (PRESS). This provides the average error of each point if we leave that point as the test-set and all

the remaining points as the training set. Averaging such a value over all datapoints yields the cross-validation (CV) score:

$$\varsigma_{CV}^2 = \frac{1}{M}\sum_m \left(\frac{r_m}{1-H_{mm}}\right)^2 = \frac{1}{M}\sum_m \left(\frac{b_m - H_m \cdot \vec{b}}{1-H_{mm}}\right)^2 \tag{4.6}$$

The question, then, is which combination of symmetry-independent terms will minimize the CV score. We implement the following algorithm: Looping through each Cartesian monomial, we either set it to zero (labeling this monomial as part of the noise), or set it to the least-squares nonzero value, whichever will lower the CV score. After a few loops (usually no more than five), the algorithm converges to a fixed dataset where removing or adding any single term will not enhance the predictive capability of the fit, as measured by the CV score. Unlike compressive sensing [78–80], which assumes a sparse parameter space, our procedure finds a parameter space of the appropriate sparseness to balance the noise present in our data with the predictive power of the fit.

Chapter 5

Application to Graphene

We now apply the above methodology to graphene. We focus on graphene due to the great interest it has attracted, mostly due to its physical and electronic properties [81–83]. Of particular interest is its strength and behavior under strain [84–87] and its negative thermal expansion [88–91], both of which are properties of the anharmonic phonons and have need of efficient computations with first-principles accuracy.

Graphene's strength under biaxial strain remains anomalous, because density-functional theory predicts a Kekule-like distortion that leads to mechanical failure, as is found in many other two-dimensional materials, but experiment does not find such a failure at the predicted strain [92–94]. Some suggestions have been proposed, including empirical simulations [95–97], but further progress requires a highly-accurate first-principles potential.

The harmonic phonons, have been studied in graphene, both in experiment [98, 99] and first principles calculations [48, 58]. Anharmonic phonon scattering and thermal properties have also been studied [13–15, 90, 91, 100–103], but no first-principles parameters have been published. Various empirical approaches have been implemented as well [42, 104, 105], as well as continuum-elasticity models [4–7] and first-principles molecular dynamics simulations [106–109]. Here we present first-principles computation of anharmonic parameters that can be used in any classical computation.

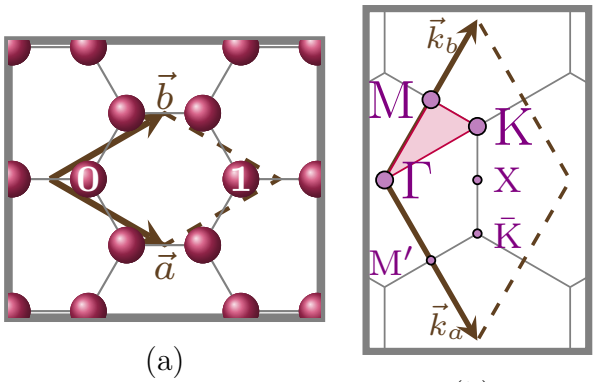

(a) (b)

Figure 5.1: Diagrams of the primitive real-space and reciprocal lattice in graphene. In the reciprocal lattice, the irreducible Brillouin zone is shaded.

5.1 Methods and Conventions

For the group theory, we use the conventions of Ref. 110, Appendix C. We use graphene primitive and reciprocal lattices shown in Figure 5.1, with the armchair direction in real space along x. For empirical potentials, we use the Tersoff and Brenner potentials with the parameters that have been optimized for phonon calculations [38].

For electronic-structure calculations, we use density functional theory as implemented in the Vienna Ab-initio Simulation Package (VASP) [111–114] using the local density approximation (LDA) functional, and PAW- (projector augmented wave) based pseudopotentials [115]. The convergence of quadratic error tails depends on high-precision calculations. Our results converged with a plane-wave cutoff energy of 625 eV and electronic k-point meshes of 40x40x1 in the primitive unit cell, with supercells' meshes adjusted proportionally to the reciprocal-lattice vectors' length. The k-point integration is performed with a Gaussian smearing of 0.2 eV. These provide the quadratic error tails found in Figure 5.2. This selection of phonon-scattering error tails shows clear convergence with respect to stencil size δ.

To build our dataset, we compute entries in the anharmonic dynamical tensor that can be computed with 12 or fewer atoms. We select those derivatives (entries in the ADT)

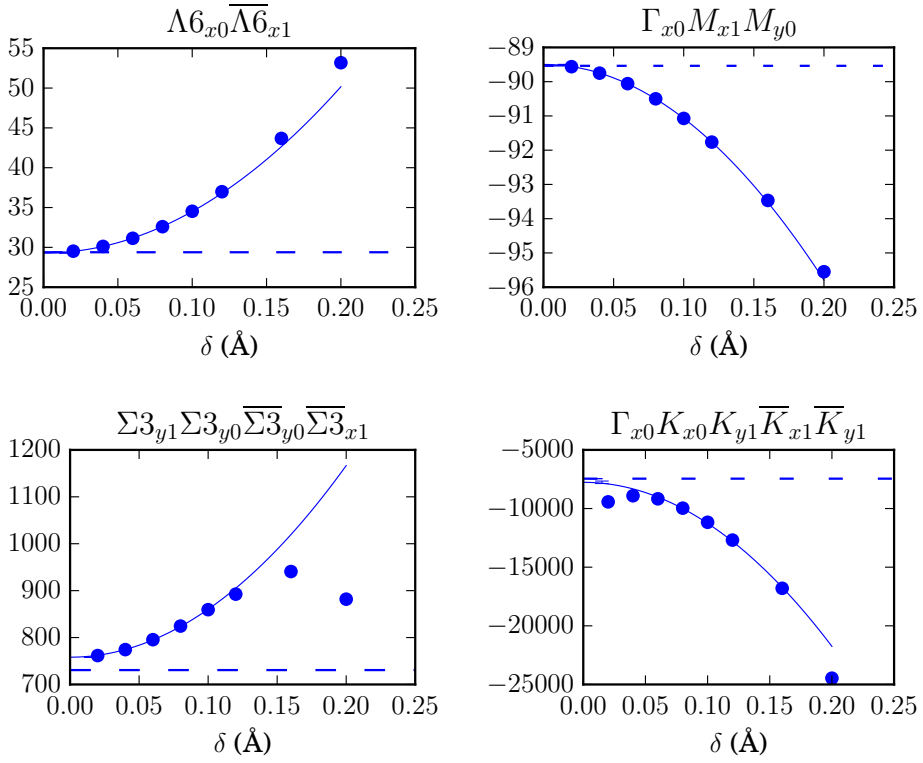

Figure 5.2: Selection of finite-difference plots for ADT entries. The solid line shows the quadratic fit, while the dashed line shows the value of the least-squares fit.

whose convergence is the best, as defined by the errors in the quadratic fit. Figure 5.3 shows the quality of the least-squares fit, by comparing the DFT-calculated values with the value consistent with the least-squares fit. The agreement is good, with minor noise that is consistent with the sources described in Chapter 4.

We have listed the calculated parameters in Chapter 7; a plot of the Cartesian monomials as a function of interaction range appears in Figure 5.4. As expected, the term magnitudes generally decay with distance. The symmetrized-mode decompositions for the hexagon are given in Chapter 2.3.

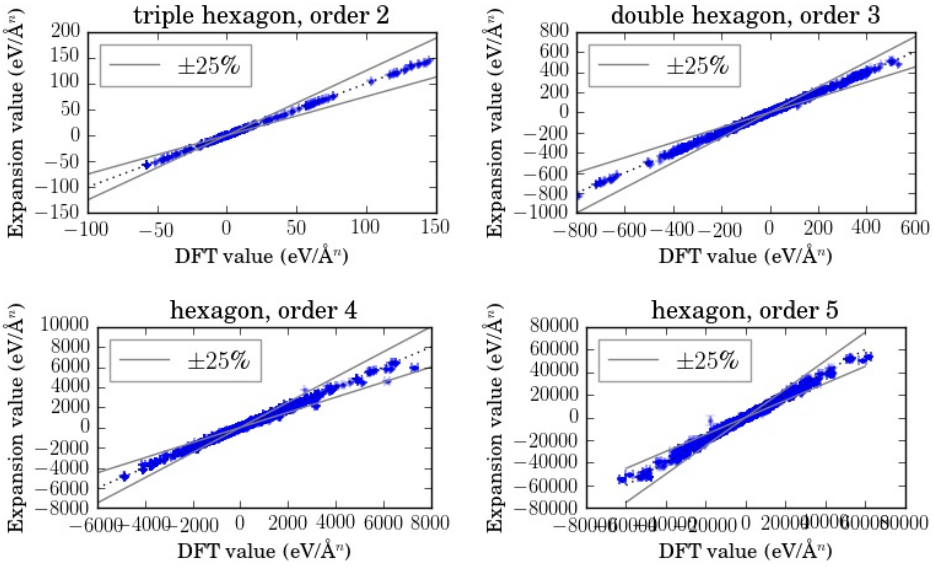

Figure 5.3: Validation of least-squares fits by comparing the DFT-calculated values in the ADT to those of the expansion (least-squares fit). Lines at 25% error show the quality of the fit. See text regarding noisiness of the data.

5.2 Calculated quantities

To validate the quantitative effects of our coefficients, we compare the parameters with DFT calculations in this section. However, it must be noted that there is some evidence that the local-density approximation (LDA) does not capture all of the phonon qualities, especially the electron-phonon coupling such as the Kohn anomaly at the Γ and K points [21, 47, 48, 73, 116–118]. Further precision is possible, either by computing the anharmonic dynamical tensor with more precise (and costly) methods, or by adding a nonanalytic term similar to that done for polarization [22, 55].

The simplest computation is the second-order force constants in k-space, which are the phonon spectra. Figure 5.5 shows the convergence with respect to interaction range. At harmonic order, the short-ranged empirical potentials fail to capture the phonon spectrum, and even the single hexagon does not capture the full spectrum. However, the double and triple hexagon appear to adequately capture the interactions. It should be noted that the

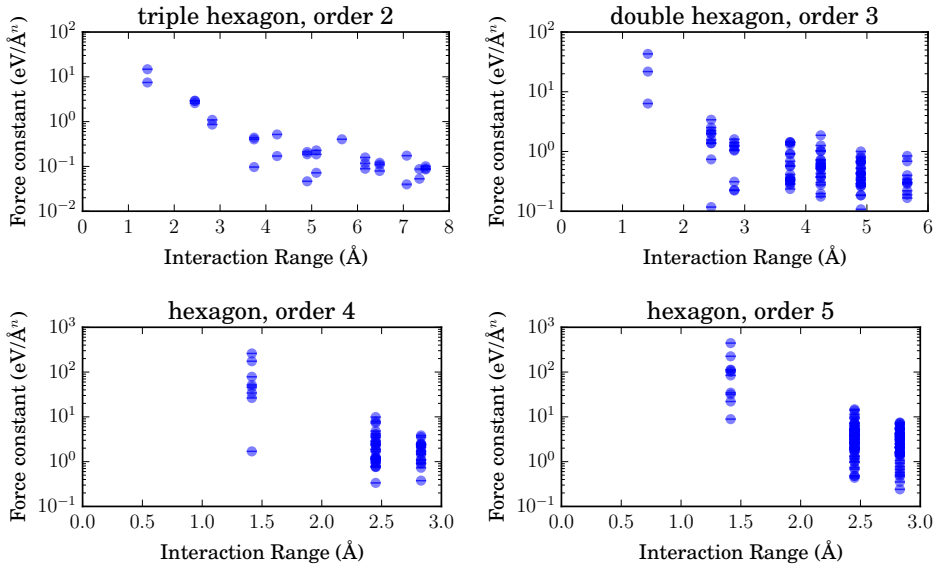

Figure 5.4: Force constants as a function of distance, with logarithmic scaling; data appears in Chapter 7.

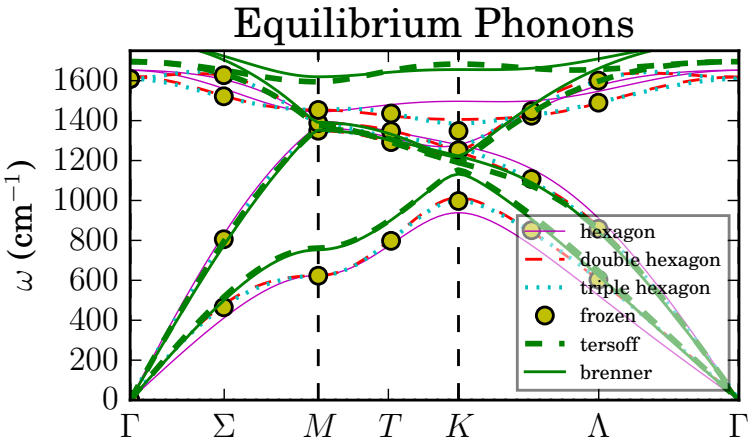

Figure 5.5: Phonon dispersions for different ranges of 2nd-order interactions.

double hexagon is greatly inferior to the triple hexagon if one does not implement cross-validation.

We can also plot the phonon frequencies as a function of strain, as in Figure 5.6. We choose to plot the frequency squared, to more clearly display the activation of each order as the strain increases. The quadratic term is constant, cubic linear, etc.

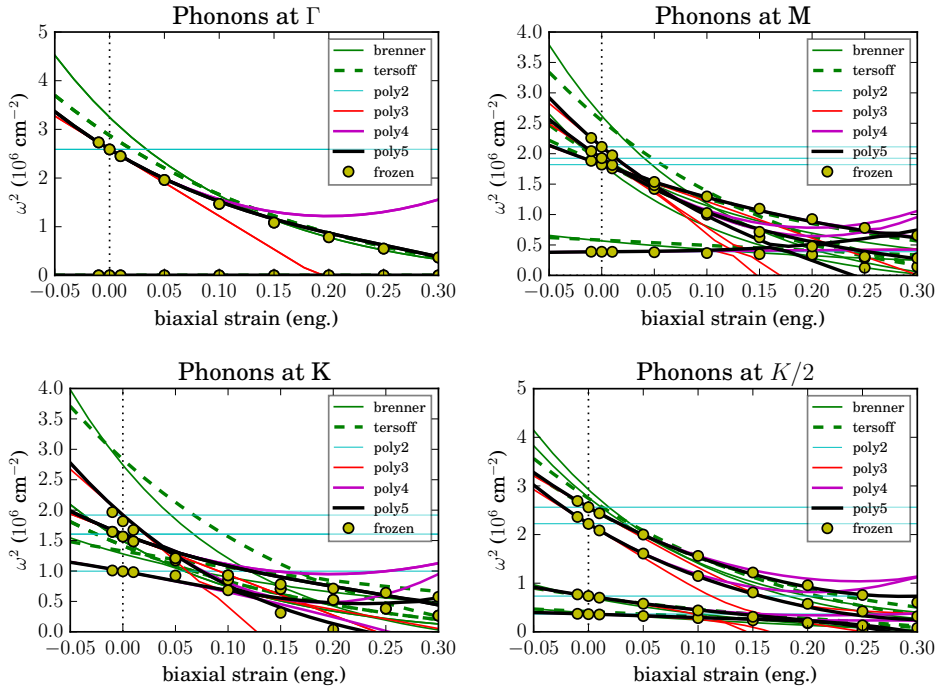

Figure 5.6: Phonon eigenvalues (frequency squared) as a function of biaxial strain.

In Figure 5.7, we plot the stress-strain curves as a function of biaxial, armchair, zigzag, and shear strains. The primitive cells are fully relaxed, making this a validation of the A_1 and E_2 terms of our expansion. It is seen that the polynomial expansion agrees with the frozen-phonon calculations for both compressive and expansive strain, up until the elastic breaking, whereas the empirical potentials are not as reliable.

In Figure 5.8, we plot the atomic relaxation as a function of armchair, zigzag, and shear strains. Biaxial strain causes no spontaneous symmetry breaking in the primitive cell, so it is linear. The nearest-neighbor bond length, relative to the equilibrium bond length and normalized to the cube root of the volume, is plotted. This presents another validation of the A_1 and E_2 terms of our expansion, where the plotted data is only very distantly related to the inputs of our parameter calculation. The polynomials follow the frozen-phonon calculations up until the elastic breaking, whereas the empirical potentials are not as reliable.

Figure 5.9 shows the full phonon spectrum at 10% strain in different directions. These

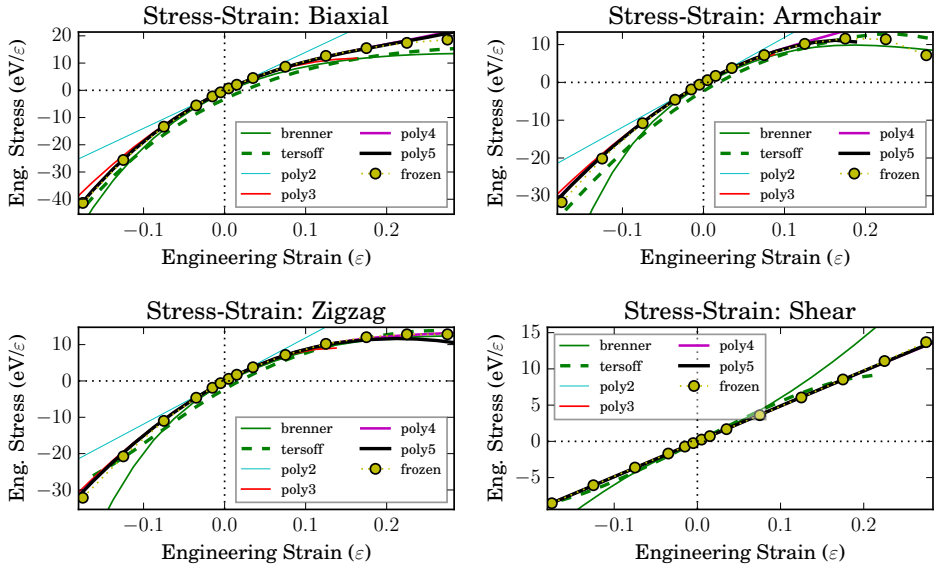

Figure 5.7: Stress-strain curves for biaxial, armchair, zigzag, and shear strains.

validate the terms that couple phonons to strain. At 10% strain, the fourth-order polynomials successfully capture the physics. However, Figure 5.10 shows the phonons at 23.5% biaxial strain. There we can see that the qualitative K-softening is correct, but quantitative predictions do not match the DFT frozen-phonon calculations, including a spurious M-point softening. This might be caused by long-range effects, problems in the fitting procedure, or higher-order contributions. It would be surprising, however, if sixth-order contributions softened the phonons more, because usually odd-order contributions soften the phonons while even-order contributions stabilize them.

Figure 5.11 shows the Gruneisen parameters across the phonon spectrum. They are defined as the logarithmic derivative of the phonon frequencies with respect to change in volume; for graphene, that is proportional to the logarithmic derivative with respect to biaxial strain. These serve as validation of the third-order terms that include at least one A_1 (strain) term. Although three branches agree well with DFT, the lower acoustical branch does not. This indicates that our third-order terms are of insufficient range, despite using the double hexagon.

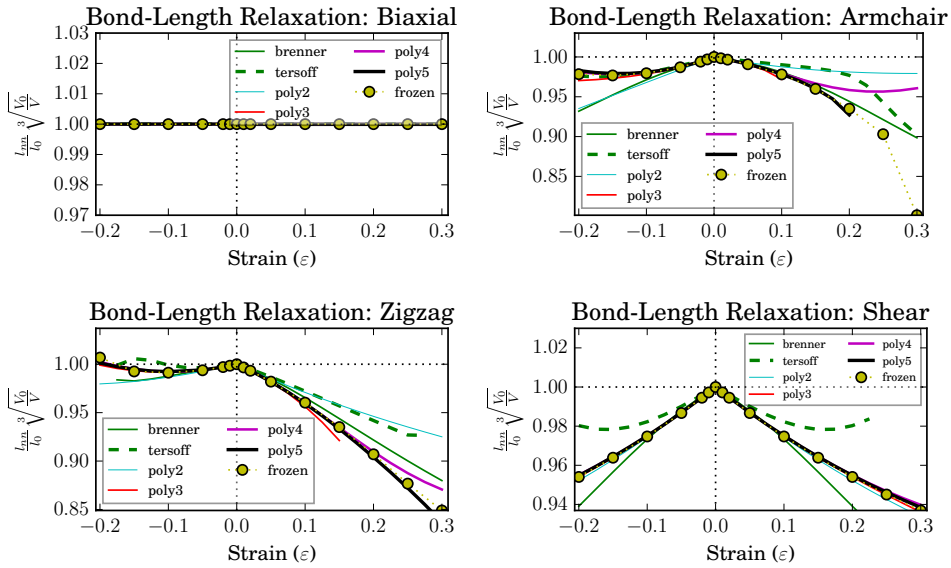

Figure 5.8: Atomic relaxation under biaxial, armchair, zigzag, and shear strains. Values are normalized to nearest-neighbor length in equilibrium (l_0) and the cube root of volume expansion (V/V_0).

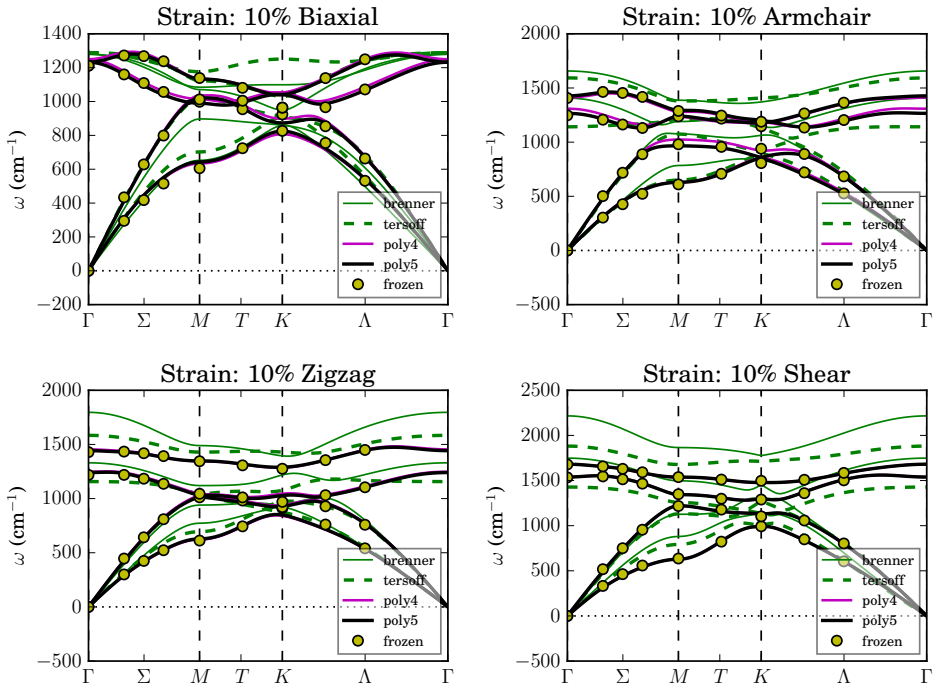

Figure 5.9: Phonon dispersion curves at 10% strain, for biaxial, armchair, zigzag, and shear strains.

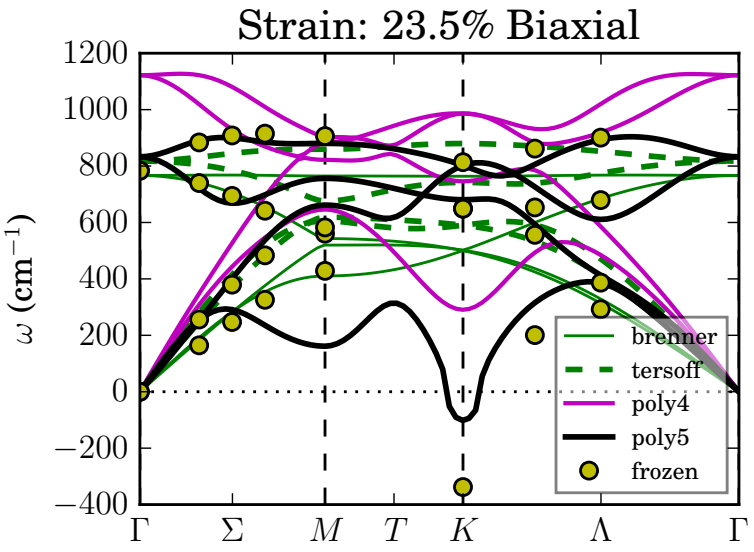

Figure 5.10: Phonon dispersions under 23.5% biaxial strain. See text.

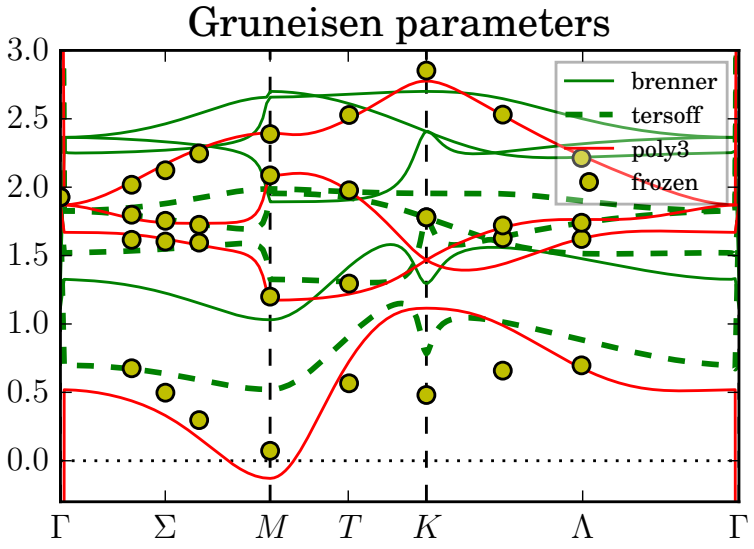

Figure 5.11: Gruneisen parameters, the logarithmic derivative of phonon frequencies with respect to volume change, as a function of wavevector. Once more the empirical potentials are sigificantly inferior; see text.

Chapter 6

Conclusions and Outlook

In this work, we have described and implemented a methodology to compute interatomic interactions from first principles up to arbitrary order. We implement group theory to minimize the number of free coefficients allowed in our expansion. The anharmonic dynamical tensor is sampled on a nonuniform grid up to arbitrary order using multidimensional finite differences and high-throughput electronic-structure calculations. This gives us the polynomial coefficients via a least-squares fitting procedure, which fits our data order-by-order.

Our application to graphene revealed that the interactions are long range even at third order, as even the double hexagon does not capture the third-order Gruneisen parameters properly. However, our fourth- and fifth-order terms appear correct, capturing the stress-strain curves, phonon behavior under strain, and atomic relaxation under non-biaxial (symmetry-breaking) strain.

Each part of our methodology has potential for future development. The potential can be separated into a short-range and long-range component, of which the long-range component might be treated in reciprocal space, while the short-range component is expected to converge faster in real space. Similar "mixed-basis" methodologies have had success describing polarization [22, 55] and the cluster expansion [119, 120]. The anharmonic dynamical tensor can be sampled on different uniform and nonuniform grids (to optimize the trade-off between computation expense and dataset size) or with different electronic-structure methods beyond DFT-LDA. The transformation or fitting procedure can benefit from recently-developed machine-learning methods to enhance the predictive power of the data. Finally, the entire approach can be applied to new materials, both hypothetical and actual materials,

to discover their anharmonic properties.

Chapter 7

Parameter Values

Here we report the parameter values with standard errors.

We report the Cartesian force constants (monomial coefficients), which are given by an irreducible set of Cartesian interactions. Each variable is given by its Cartesian direction (x or y), atom of the primitive cell (0 or 1), and translation vector ($t_a t_b$), as per the conventions of Figure 5.1. Point- and space-group symmetry operations can be used to generate all interactions in the cluster. Each interaction has a defined range between atoms, which are reported scaled to the nearest-neighbor distance l_{nn}. This data also appears in Figure 5.4.

We then report the force constants of the slave-mode notation, which are significantly more concise and require no further symmetry operations to use.

Coord.	Coord.	Range/l_{nn}	Value (eV/Å^2)
$x_0(00)$	$x_1(\bar{1}0)$	1	-14.7593 ± 0.0003
$x_0(00)$	$y_1(\bar{1}0)$	1	-7.4776 ± 0.0003
$x_0(00)$	$x_0(01)$	$\sqrt{3}$	-2.9108 ± 0.0003
$x_0(00)$	$y_0(01)$	$\sqrt{3}$	-2.9162 ± 0.0027
$x_0(00)$	$x_0(1\bar{1})$	$\sqrt{3}$	2.585 ± 0.0003
$x_0(00)$	$x_1(00)$	2	0.8599 ± 0.0009
$x_0(00)$	$x_1(0\bar{2})$	2	-1.0945 ± 0.0008
$x_0(00)$	$x_1(\bar{1}1)$	$\sqrt{7}$	-0.4015 ± 0.0005
$x_0(00)$	$y_1(\bar{1}1)$	$\sqrt{7}$	0.4384 ± 0.0004
$x_0(00)$	$x_1(1\bar{2})$	$\sqrt{7}$	-0.0967 ± 0.0007
$x_0(00)$	$x_0(11)$	3	-0.5164 ± 0.0006
$x_0(00)$	$x_0(2\bar{1})$	3	-0.1703 ± 0.0004
$x_0(00)$	$x_0(02)$	$\sqrt{12}$	-0.0465 ± 0.0002
$x_0(00)$	$y_0(02)$	$\sqrt{12}$	-0.1869 ± 0.0017
$x_0(00)$	$x_0(2\bar{2})$	$\sqrt{12}$	0.21 ± 0.0003
$x_0(00)$	$x_1(01)$	$\sqrt{13}$	0.0719 ± 0.0004
$x_0(00)$	$y_1(01)$	$\sqrt{13}$	0.1856 ± 0.0008
$x_0(00)$	$x_1(1\bar{3})$	$\sqrt{13}$	-0.2279 ± 0.0007
$x_0(00)$	$x_1(2\bar{2})$	4	0.0 ± 0.0

Coord.	Coord.	Range/l_{nn}	Value (eV/Å^2)
$x_0(00)$	$y_1(2\bar{2})$	4	-0.403 ± 0.0003
$x_0(00)$	$x_1(2\bar{1})$	$\sqrt{19}$	0.1584 ± 0.0005
$x_0(00)$	$y_1(2\bar{1})$	$\sqrt{19}$	0.0886 ± 0.0003
$x_0(00)$	$x_1(2\bar{3})$	$\sqrt{19}$	0.1173 ± 0.0007
$x_0(00)$	$x_0(12)$	$\sqrt{21}$	-0.1088 ± 0.0002
$x_0(00)$	$y_0(12)$	$\sqrt{21}$	0.1203 ± 0.0038
$x_0(00)$	$x_0(3\bar{1})$	$\sqrt{21}$	-0.0791 ± 0.0002
$x_0(00)$	$x_0(3\bar{2})$	$\sqrt{21}$	0.0 ± 0.0
$x_0(00)$	$x_1(11)$	5	0.1737 ± 0.0014
$x_0(00)$	$x_1(1\bar{4})$	5	0.0397 ± 0.0009
$x_0(00)$	$x_0(30)$	$\sqrt{27}$	0.0 ± 0.0
$x_0(00)$	$y_0(30)$	$\sqrt{27}$	0.087 ± 0.0027
$x_0(00)$	$x_0(3\bar{3})$	$\sqrt{27}$	0.053 ± 0.0002
$x_0(00)$	$x_1(20)$	$\sqrt{28}$	-0.1005 ± 0.0008
$x_0(00)$	$y_1(20)$	$\sqrt{28}$	-0.0856 ± 0.0003
$x_0(00)$	$x_1(2\bar{4})$	$\sqrt{28}$	-0.0894 ± 0.0008

Table 7.1: Second-order Cartesian coefficients for the triple hexagon. All other interatomic force constants can be derived from these by symmetry.

Coord.	Coord.	Coord.	Range/l_{nn}	Value (eV/Å^3)
$x_0(00)$	$x_0(00)$	$x_1(0\bar{1})$	1	-6.3499 ± 0.0007
$x_0(00)$	$x_0(00)$	$y_1(0\bar{1})$	1	21.7708 ± 0.0005
$x_0(00)$	$y_1(0\bar{1})$	$y_1(0\bar{1})$	1	42.9821 ± 0.0006
$x_0(00)$	$x_0(10)$	$x_1(0\bar{1})$	$\sqrt{3}$	-1.3696 ± 0.0007
$x_0(00)$	$x_0(10)$	$y_1(0\bar{1})$	$\sqrt{3}$	-2.0133 ± 0.0007
$x_0(00)$	$x_0(00)$	$y_0(10)$	$\sqrt{3}$	2.5159 ± 0.0003
$x_0(00)$	$x_0(10)$	$x_0(10)$	$\sqrt{3}$	3.3975 ± 0.0003
$x_0(00)$	$x_0(00)$	$x_0(10)$	$\sqrt{3}$	-1.9699 ± 0.0003
$x_0(00)$	$y_0(1\bar{1})$	$x_1(0\bar{1})$	$\sqrt{3}$	-2.226 ± 0.0009
$x_0(00)$	$y_0(1\bar{1})$	$y_0(1\bar{1})$	$\sqrt{3}$	0.0 ± 0.0
$x_0(00)$	$x_0(00)$	$x_0(1\bar{1})$	$\sqrt{3}$	-0.7372 ± 0.0003
$x_0(00)$	$x_0(10)$	$y_0(1\bar{1})$	$\sqrt{3}$	1.5649 ± 0.0006
$x_0(00)$	$x_0(1\bar{1})$	$x_1(0\bar{1})$	$\sqrt{3}$	0.0 ± 0.0
$x_0(00)$	$x_0(1\bar{1})$	$x_0(10)$	$\sqrt{3}$	0.1172 ± 0.0006
$x_0(00)$	$x_0(00)$	$y_0(1\bar{1})$	$\sqrt{3}$	-1.3819 ± 0.0005
$x_0(00)$	$x_0(00)$	$x_1(00)$	2	-0.222 ± 0.0008
$x_0(00)$	$x_0(10)$	$y_1(00)$	2	0.0 ± 0.0
$x_0(00)$	$y_0(10)$	$y_1(00)$	2	-0.3116 ± 0.001
$x_0(00)$	$y_0(10)$	$x_1(00)$	2	1.064 ± 0.0007
$x_0(00)$	$x_0(10)$	$x_1(00)$	2	-1.222 ± 0.0006
$x_0(00)$	$x_0(1\bar{1})$	$x_1(0\bar{2})$	2	1.2643 ± 0.0006
$x_0(00)$	$y_0(1\bar{1})$	$x_1(0\bar{2})$	2	-1.6025 ± 0.0009
$x_0(00)$	$y_0(1\bar{1})$	$y_1(0\bar{2})$	2	-0.2261 ± 0.0006
$x_0(00)$	$x_0(1\bar{1})$	$y_1(0\bar{2})$	2	1.0337 ± 0.0007
$x_0(00)$	$x_0(00)$	$x_1(0\bar{2})$	2	0.0 ± 0.0

Coord.	Coord.	Coord.	Range/l_{nn}	Value (eV/Å^3)
$x_0(00)$	$x_0(00)$	$y_1(0\bar{2})$	2	-1.406 ± 0.0005
$x_0(00)$	$x_0(10)$	$y_1(0\bar{2})$	$\sqrt{7}$	0.0 ± 0.0
$x_0(00)$	$x_0(10)$	$x_1(0\bar{2})$	$\sqrt{7}$	0.0 ± 0.0
$x_0(00)$	$y_0(1\bar{1})$	$x_1(00)$	$\sqrt{7}$	0.2352 ± 0.0009
$x_0(00)$	$x_0(1\bar{1})$	$x_1(00)$	$\sqrt{7}$	-0.3378 ± 0.0005
$x_0(00)$	$y_0(10)$	$y_1(1\bar{1})$	$\sqrt{7}$	0.4117 ± 0.0005
$x_0(00)$	$x_0(00)$	$x_1(1\bar{1})$	$\sqrt{7}$	-0.2853 ± 0.0005
$x_0(00)$	$x_0(00)$	$y_1(1\bar{1})$	$\sqrt{7}$	0.5744 ± 0.0007
$x_0(00)$	$y_0(10)$	$x_1(1\bar{1})$	$\sqrt{7}$	-0.686 ± 0.0008
$x_0(00)$	$y_1(1\bar{1})$	$y_1(1\bar{1})$	$\sqrt{7}$	0.0 ± 0.0
$x_0(00)$	$x_0(10)$	$x_1(1\bar{1})$	$\sqrt{7}$	-1.3858 ± 0.0007
$x_0(00)$	$y_0(1\bar{1})$	$y_1(00)$	$\sqrt{7}$	-0.5662 ± 0.0007
$x_0(00)$	$x_0(10)$	$y_1(1\bar{1})$	$\sqrt{7}$	0.3149 ± 0.0005
$x_0(00)$	$x_0(1\bar{1})$	$y_1(00)$	$\sqrt{7}$	-1.432 ± 0.0006
$x_0(00)$	$y_0(1\bar{1})$	$y_1(1\bar{2})$	$\sqrt{7}$	0.0 ± 0.0
$x_0(00)$	$x_0(10)$	$x_1(1\bar{2})$	$\sqrt{7}$	-0.3441 ± 0.0008
$x_0(00)$	$x_0(10)$	$y_1(1\bar{2})$	$\sqrt{7}$	0.0 ± 0.0
$x_0(00)$	$x_0(1\bar{1})$	$y_1(1\bar{2})$	$\sqrt{7}$	-1.2977 ± 0.0008
$x_0(00)$	$y_0(1\bar{1})$	$x_1(1\bar{2})$	$\sqrt{7}$	0.9007 ± 0.0006
$x_0(00)$	$x_1(1\bar{2})$	$x_1(1\bar{1})$	$\sqrt{7}$	-0.3281 ± 0.0006
$x_0(00)$	$x_0(1\bar{1})$	$x_1(1\bar{2})$	$\sqrt{7}$	1.4382 ± 0.0007
$x_0(00)$	$x_0(00)$	$x_1(1\bar{2})$	$\sqrt{7}$	-0.926 ± 0.0007
$x_0(00)$	$x_0(00)$	$y_1(1\bar{2})$	$\sqrt{7}$	0.3644 ± 0.0005
$x_0(00)$	$y_1(1\bar{2})$	$y_1(1\bar{2})$	$\sqrt{7}$	-0.2856 ± 0.0006
$x_0(00)$	$x_0(11)$	$x_0(11)$	3	0.0 ± 0.0
$x_0(00)$	$x_0(00)$	$x_0(11)$	3	1.0281 ± 0.0004
$x_0(00)$	$x_0(2\bar{1})$	$y_0(10)$	3	0.0 ± 0.0
$x_0(00)$	$x_0(2\bar{1})$	$x_1(0\bar{2})$	3	0.0 ± 0.0
$x_0(00)$	$x_0(2\bar{1})$	$x_1(0\bar{1})$	3	0.5185 ± 0.0005
$x_0(00)$	$x_0(2\bar{1})$	$x_1(00)$	3	0.0 ± 0.0
$x_0(00)$	$x_0(2\bar{1})$	$x_1(1\bar{2})$	3	-0.3696 ± 0.0006
$x_0(00)$	$x_0(2\bar{1})$	$x_1(1\bar{1})$	3	0.0 ± 0.0
$x_0(00)$	$x_0(2\bar{1})$	$y_1(0\bar{2})$	3	0.0 ± 0.0
$x_0(00)$	$x_0(2\bar{1})$	$y_1(0\bar{1})$	3	0.0 ± 0.0
$x_0(00)$	$x_0(2\bar{1})$	$y_1(00)$	3	0.1968 ± 0.0003
$x_0(00)$	$x_0(2\bar{1})$	$y_1(1\bar{2})$	3	-0.6467 ± 0.0003
$x_0(00)$	$x_0(2\bar{1})$	$y_1(1\bar{1})$	3	-0.6084 ± 0.0003
$x_0(00)$	$y_0(1\bar{1})$	$y_0(2\bar{1})$	3	-0.3018 ± 0.0005
$x_0(00)$	$y_0(10)$	$y_0(2\bar{1})$	3	-0.5595 ± 0.0004
$x_0(00)$	$y_0(2\bar{1})$	$x_1(0\bar{2})$	3	1.8658 ± 0.0006
$x_0(00)$	$y_0(2\bar{1})$	$x_1(0\bar{1})$	3	0.0 ± 0.0
$x_0(00)$	$y_0(2\bar{1})$	$x_1(00)$	3	-0.1751 ± 0.0007
$x_0(00)$	$y_0(2\bar{1})$	$x_1(1\bar{2})$	3	0.5473 ± 0.0006
$x_0(00)$	$y_0(2\bar{1})$	$x_1(1\bar{1})$	3	0.7274 ± 0.0008
$x_0(00)$	$x_0(10)$	$y_0(2\bar{1})$	3	-0.5907 ± 0.0004
$x_0(00)$	$x_0(10)$	$x_0(2\bar{1})$	3	0.0 ± 0.0
$x_0(00)$	$x_0(2\bar{1})$	$y_0(1\bar{1})$	3	0.0 ± 0.0

Coord.	Coord.	Coord.	Range/l_{nn}	Value (eV/Å^3)
$x_0(00)$	$x_0(1\bar{1})$	$x_0(2\bar{1})$	3	-1.2587 ± 0.0004
$x_0(00)$	$y_0(2\bar{1})$	$y_0(2\bar{1})$	3	-0.4278 ± 0.0004
$x_0(00)$	$y_0(2\bar{1})$	$y_1(0\bar{2})$	3	-1.0136 ± 0.0009
$x_0(00)$	$x_0(2\bar{1})$	$x_0(2\bar{1})$	3	-0.2762 ± 0.0004
$x_0(00)$	$x_0(00)$	$x_0(2\bar{1})$	3	0.3769 ± 0.0003
$x_0(00)$	$x_0(00)$	$y_0(2\bar{1})$	3	-0.7072 ± 0.0004
$x_0(00)$	$x_0(1\bar{1})$	$y_0(2\bar{1})$	3	-0.5162 ± 0.0005
$x_0(00)$	$x_0(00)$	$x_0(20)$	$\sqrt{12}$	-0.4348 ± 0.0003
$x_0(00)$	$x_0(20)$	$x_1(0\bar{1})$	$\sqrt{12}$	-0.1847 ± 0.0006
$x_0(00)$	$x_0(20)$	$x_1(00)$	$\sqrt{12}$	0.0 ± 0.0
$x_0(00)$	$x_0(20)$	$x_1(1\bar{1})$	$\sqrt{12}$	-0.2598 ± 0.0005
$x_0(00)$	$x_0(20)$	$y_1(0\bar{1})$	$\sqrt{12}$	0.0 ± 0.0
$x_0(00)$	$x_0(20)$	$y_1(00)$	$\sqrt{12}$	0.0 ± 0.0
$x_0(00)$	$x_0(20)$	$y_1(1\bar{2})$	$\sqrt{12}$	0.0 ± 0.0
$x_0(00)$	$x_0(20)$	$y_1(1\bar{1})$	$\sqrt{12}$	-0.3414 ± 0.0006
$x_0(00)$	$x_0(20)$	$x_0(20)$	$\sqrt{12}$	0.3664 ± 0.0001
$x_0(00)$	$x_0(20)$	$x_1(1\bar{2})$	$\sqrt{12}$	0.3275 ± 0.0005
$x_0(00)$	$x_0(1\bar{1})$	$x_0(20)$	$\sqrt{12}$	0.2868 ± 0.0003
$x_0(00)$	$x_0(00)$	$y_0(20)$	$\sqrt{12}$	0.0 ± 0.0
$x_0(00)$	$x_0(1\bar{1})$	$y_0(20)$	$\sqrt{12}$	0.0 ± 0.0
$x_0(00)$	$x_0(10)$	$y_0(20)$	$\sqrt{12}$	0.6722 ± 0.0004
$x_0(00)$	$x_0(2\bar{1})$	$x_0(20)$	$\sqrt{12}$	0.1076 ± 0.0003
$x_0(00)$	$x_0(2\bar{1})$	$y_0(20)$	$\sqrt{12}$	0.0 ± 0.0
$x_0(00)$	$x_0(10)$	$x_0(20)$	$\sqrt{12}$	-0.2826 ± 0.0004
$x_0(00)$	$x_0(1\bar{1})$	$y_0(2\bar{2})$	$\sqrt{12}$	0.6917 ± 0.0005
$x_0(00)$	$y_0(2\bar{2})$	$y_1(0\bar{1})$	$\sqrt{12}$	0.0 ± 0.0
$x_0(00)$	$x_0(10)$	$y_0(2\bar{2})$	$\sqrt{12}$	0.4389 ± 0.0004
$x_0(00)$	$y_0(2\bar{2})$	$y_0(2\bar{2})$	$\sqrt{12}$	0.5206 ± 0.0003
$x_0(00)$	$x_0(2\bar{2})$	$x_0(20)$	$\sqrt{12}$	-0.1844 ± 0.0005
$x_0(00)$	$x_0(2\bar{2})$	$y_0(10)$	$\sqrt{12}$	0.6331 ± 0.0005
$x_0(00)$	$x_0(2\bar{2})$	$x_1(0\bar{2})$	$\sqrt{12}$	-1.001 ± 0.0008
$x_0(00)$	$y_0(2\bar{2})$	$x_1(0\bar{1})$	$\sqrt{12}$	-0.8232 ± 0.0007
$x_0(00)$	$x_0(2\bar{2})$	$x_1(0\bar{1})$	$\sqrt{12}$	0.2921 ± 0.0007
$x_0(00)$	$x_0(20)$	$y_0(2\bar{2})$	$\sqrt{12}$	-0.4089 ± 0.0005
$x_0(00)$	$x_0(10)$	$x_0(2\bar{2})$	$\sqrt{12}$	0.5274 ± 0.0004
$x_0(00)$	$x_0(2\bar{2})$	$y_1(0\bar{1})$	$\sqrt{12}$	-0.2651 ± 0.0005
$x_0(00)$	$x_0(00)$	$y_0(2\bar{2})$	$\sqrt{12}$	0.4285 ± 0.0003
$x_0(00)$	$x_0(00)$	$x_0(2\bar{2})$	$\sqrt{12}$	0.0 ± 0.0
$x_0(00)$	$x_0(1\bar{1})$	$x_0(2\bar{2})$	$\sqrt{12}$	0.0 ± 0.0
$x_0(00)$	$x_0(2\bar{1})$	$y_0(2\bar{2})$	$\sqrt{12}$	0.7768 ± 0.0003
$x_0(00)$	$y_0(2\bar{2})$	$x_1(0\bar{2})$	$\sqrt{12}$	-0.675 ± 0.0007
$x_0(00)$	$x_0(20)$	$y_1(0\bar{2})$	4	-0.286 ± 0.0004
$x_0(00)$	$x_0(20)$	$x_1(0\bar{2})$	4	0.6842 ± 0.0004
$x_0(00)$	$y_1(2\bar{2})$	$y_1(2\bar{2})$	4	0.0 ± 0.0
$x_0(00)$	$x_0(1\bar{1})$	$x_1(2\bar{2})$	4	0.0 ± 0.0
$x_0(00)$	$y_0(2\bar{2})$	$y_1(00)$	4	-0.22 ± 0.0006

Coord.	Coord.	Coord.	Range/l_{nn}	Value (eV/Å^3)
$x_0(00)$	$y_0(2\bar{2})$	$x_1(00)$	4	0.0 ± 0.0
$x_0(00)$	$x_0(10)$	$x_1(2\bar{2})$	4	0.3038 ± 0.0005
$x_0(00)$	$y_0(10)$	$x_1(2\bar{2})$	4	0.3412 ± 0.0005
$x_0(00)$	$x_0(00)$	$y_1(2\bar{2})$	4	0.1664 ± 0.0002
$x_0(00)$	$y_0(1\bar{1})$	$y_1(2\bar{2})$	4	0.3005 ± 0.0007
$x_0(00)$	$y_0(1\bar{1})$	$x_1(2\bar{2})$	4	-0.8422 ± 0.0005
$x_0(00)$	$x_0(00)$	$x_1(2\bar{2})$	4	0.0 ± 0.0
$x_0(00)$	$x_0(10)$	$y_1(2\bar{2})$	4	0.0 ± 0.0
$x_0(00)$	$x_0(2\bar{2})$	$x_1(00)$	4	0.0 ± 0.0
$x_0(00)$	$x_0(2\bar{2})$	$y_1(00)$	4	0.0 ± 0.0
$x_0(00)$	$y_0(10)$	$y_1(2\bar{2})$	4	-0.3997 ± 0.0007
$x_0(00)$	$x_0(1\bar{1})$	$y_1(2\bar{2})$	4	-0.1889 ± 0.0004

Table 7.2: Third-order Cartesian coefficients for the double hexagon. All other interatomic force constants can be derived from these by symmetry.

Coord.	Coord.	Coord.	Coord.	Range/l_{nn}	Value (eV/Å^4)
$x_0(00)$	$x_0(00)$	$x_0(00)$	$x_1(\bar{1}\bar{1})$	1	-174.427 ± 0.0018
$x_0(00)$	$x_0(00)$	$x_1(\bar{1}\bar{1})$	$x_1(\bar{1}\bar{1})$	1	260.2172 ± 0.0036
$x_0(00)$	$x_0(00)$	$y_1(\bar{1}\bar{1})$	$y_1(\bar{1}\bar{1})$	1	-45.8903 ± 0.0017
$x_0(00)$	$x_0(00)$	$x_0(00)$	$x_1(\bar{1}0)$	1	26.3887 ± 0.0008
$x_0(00)$	$x_0(00)$	$x_0(00)$	$y_1(\bar{1}0)$	1	-1.6949 ± 0.0012
$x_0(00)$	$y_1(\bar{1}0)$	$y_1(\bar{1}0)$	$y_1(\bar{1}0)$	1	-78.4511 ± 0.0011
$x_0(00)$	$x_0(00)$	$y_1(\bar{1}0)$	$y_1(\bar{1}0)$	1	51.4366 ± 0.0013
$x_0(00)$	$x_0(00)$	$x_1(\bar{1}0)$	$x_1(\bar{1}0)$	1	-34.2011 ± 0.0014
$x_0(00)$	$x_0(00)$	$y_0(0\bar{1})$	$y_0(0\bar{1})$	$\sqrt{3}$	0.0 ± 0.0
$x_0(00)$	$x_0(00)$	$x_0(01)$	$y_0(01)$	$\sqrt{3}$	2.4472 ± 0.0018
$x_0(00)$	$x_0(00)$	$x_0(01)$	$x_1(\bar{1}0)$	$\sqrt{3}$	4.8069 ± 0.0012
$x_0(00)$	$x_0(00)$	$y_0(01)$	$x_1(\bar{1}0)$	$\sqrt{3}$	0.0 ± 0.0
$x_0(00)$	$x_0(01)$	$x_0(01)$	$x_1(\bar{1}0)$	$\sqrt{3}$	7.9109 ± 0.0015
$x_0(00)$	$x_0(01)$	$x_0(01)$	$y_1(\bar{1}0)$	$\sqrt{3}$	-2.8797 ± 0.0015
$x_0(00)$	$x_0(01)$	$x_1(\bar{1}0)$	$x_1(\bar{1}0)$	$\sqrt{3}$	-9.8798 ± 0.0015
$x_0(00)$	$x_0(01)$	$y_1(\bar{1}0)$	$y_1(\bar{1}0)$	$\sqrt{3}$	-1.1759 ± 0.0012
$x_0(00)$	$y_0(01)$	$y_0(01)$	$x_1(\bar{1}0)$	$\sqrt{3}$	4.163 ± 0.0011
$x_0(00)$	$y_0(01)$	$y_0(01)$	$y_1(\bar{1}0)$	$\sqrt{3}$	1.6746 ± 0.001
$x_0(00)$	$y_0(01)$	$x_1(\bar{1}0)$	$x_1(\bar{1}0)$	$\sqrt{3}$	0.0 ± 0.0
$x_0(00)$	$x_0(00)$	$y_0(01)$	$y_1(\bar{1}0)$	$\sqrt{3}$	3.4853 ± 0.0014
$x_0(00)$	$x_0(00)$	$y_0(01)$	$y_0(01)$	$\sqrt{3}$	-1.0912 ± 0.001
$x_0(00)$	$x_0(00)$	$x_0(01)$	$y_1(\bar{1}0)$	$\sqrt{3}$	2.2908 ± 0.0014
$x_0(00)$	$x_0(00)$	$x_0(01)$	$x_0(01)$	$\sqrt{3}$	-2.7851 ± 0.0008
$x_0(00)$	$x_0(00)$	$x_0(00)$	$y_0(0\bar{1})$	$\sqrt{3}$	-1.1367 ± 0.0006
$x_0(00)$	$x_0(00)$	$x_0(00)$	$x_0(01)$	$\sqrt{3}$	0.0 ± 0.0
$x_0(00)$	$x_0(00)$	$x_0(00)$	$y_0(01)$	$\sqrt{3}$	-0.7906 ± 0.0007
$x_0(00)$	$y_0(0\bar{1})$	$y_0(0\bar{1})$	$y_0(0\bar{1})$	$\sqrt{3}$	0.0 ± 0.0
$x_0(00)$	$x_0(01)$	$x_0(01)$	$x_0(01)$	$\sqrt{3}$	-1.0038 ± 0.0009

Coord.	Coord.	Coord.	Coord.	Range/l_{nn}	Value (eV/Å^4)
$x_0(00)$	$y_0(01)$	$y_0(01)$	$y_0(01)$	$\sqrt{3}$	1.1575 ± 0.0007
$x_0(00)$	$x_0(01)$	$x_0(01)$	$y_0(10)$	$\sqrt{3}$	0.9323 ± 0.0013
$x_0(00)$	$x_0(00)$	$x_1(\bar{1}0)$	$y_1(0\bar{1})$	$\sqrt{3}$	0.0 ± 0.0
$x_0(00)$	$x_0(00)$	$x_1(\bar{1}0)$	$x_1(0\bar{1})$	$\sqrt{3}$	-7.2838 ± 0.0016
$x_0(00)$	$x_0(00)$	$x_0(00)$	$y_0(1\bar{1})$	$\sqrt{3}$	1.2434 ± 0.0006
$x_0(00)$	$x_0(00)$	$x_0(00)$	$x_0(1\bar{1})$	$\sqrt{3}$	-1.2778 ± 0.0005
$x_0(00)$	$x_0(01)$	$y_0(10)$	$y_0(10)$	$\sqrt{3}$	-0.3357 ± 0.001
$x_0(00)$	$x_0(00)$	$y_0(01)$	$y_0(10)$	$\sqrt{3}$	0.0 ± 0.0
$x_0(00)$	$x_0(00)$	$y_1(\bar{1}0)$	$y_1(0\bar{1})$	$\sqrt{3}$	-1.8776 ± 0.0018
$x_0(00)$	$x_0(00)$	$x_0(01)$	$y_0(10)$	$\sqrt{3}$	0.0 ± 0.0
$x_0(00)$	$x_0(00)$	$x_0(01)$	$x_0(10)$	$\sqrt{3}$	0.7643 ± 0.0018
$x_0(00)$	$x_0(00)$	$y_0(1\bar{1})$	$y_0(1\bar{1})$	$\sqrt{3}$	-3.7986 ± 0.0008
$x_0(00)$	$x_1(\bar{1}0)$	$y_1(0\bar{1})$	$y_1(0\bar{1})$	$\sqrt{3}$	2.5023 ± 0.0013
$x_0(00)$	$x_0(00)$	$x_0(1\bar{1})$	$x_0(1\bar{1})$	$\sqrt{3}$	0.0 ± 0.0
$x_0(00)$	$x_0(00)$	$x_0(1\bar{1})$	$y_0(0\bar{1})$	$\sqrt{3}$	0.7561 ± 0.0015
$x_0(00)$	$x_0(01)$	$x_0(01)$	$x_0(10)$	$\sqrt{3}$	-1.8463 ± 0.001
$x_0(00)$	$x_0(00)$	$x_0(00)$	$x_1(00)$	2	-0.9353 ± 0.0009
$x_0(00)$	$x_0(01)$	$y_1(00)$	$y_1(00)$	2	0.0 ± 0.0
$x_0(00)$	$x_0(00)$	$x_1(00)$	$x_1(00)$	2	3.8539 ± 0.0015
$x_0(00)$	$x_0(00)$	$x_1(\bar{1}0)$	$y_1(00)$	2	-2.2231 ± 0.0016
$x_0(00)$	$x_0(00)$	$y_1(00)$	$y_1(00)$	2	1.6998 ± 0.0011
$x_0(00)$	$x_0(00)$	$x_1(00)$	$y_1(\bar{1}0)$	2	0.0 ± 0.0
$x_0(00)$	$x_0(00)$	$x_0(1\bar{1})$	$y_1(0\bar{2})$	2	-3.5343 ± 0.0015
$x_0(00)$	$y_1(0\bar{2})$	$y_1(0\bar{2})$	$y_1(0\bar{2})$	2	-0.377 ± 0.0006
$x_0(00)$	$y_0(01)$	$y_1(0\bar{1})$	$y_1(0\bar{1})$	2	-0.8988 ± 0.0012
$x_0(00)$	$y_0(01)$	$x_1(0\bar{1})$	$x_1(0\bar{1})$	2	-1.1121 ± 0.0014
$x_0(00)$	$x_0(00)$	$x_1(0\bar{2})$	$x_1(0\bar{2})$	2	0.0 ± 0.0
$x_0(00)$	$y_0(01)$	$y_0(01)$	$y_1(0\bar{1})$	2	2.5709 ± 0.0016
$x_0(00)$	$x_0(00)$	$y_1(0\bar{2})$	$y_1(0\bar{2})$	2	-1.4471 ± 0.0009
$x_0(00)$	$y_0(01)$	$y_0(01)$	$x_1(0\bar{1})$	2	1.6992 ± 0.0012
$x_0(00)$	$x_0(00)$	$x_0(00)$	$y_1(0\bar{2})$	2	0.0 ± 0.0
$x_0(00)$	$x_0(01)$	$y_1(0\bar{1})$	$y_1(0\bar{1})$	2	2.3996 ± 0.0013
$x_0(00)$	$x_0(01)$	$y_0(10)$	$y_1(\bar{1}0)$	2	0.0 ± 0.0
$x_0(00)$	$x_0(01)$	$x_1(0\bar{1})$	$x_1(0\bar{1})$	2	0.0 ± 0.0
$x_0(00)$	$x_0(00)$	$x_0(01)$	$y_1(0\bar{1})$	2	1.5356 ± 0.0016
$x_0(00)$	$x_0(00)$	$x_0(00)$	$x_1(0\bar{2})$	2	-1.0793 ± 0.0006
$x_0(00)$	$x_0(01)$	$x_0(01)$	$y_1(0\bar{1})$	2	0.0 ± 0.0
$x_0(00)$	$x_0(00)$	$y_0(01)$	$x_1(0\bar{1})$	2	-2.3843 ± 0.002
$x_0(00)$	$x_0(01)$	$x_0(01)$	$x_1(0\bar{1})$	2	2.4094 ± 0.001
$x_0(00)$	$x_0(00)$	$y_0(01)$	$y_1(0\bar{1})$	2	0.73 ± 0.0014
$x_0(00)$	$x_0(00)$	$x_0(01)$	$x_1(0\bar{1})$	2	0.0 ± 0.0
$x_0(00)$	$y_0(01)$	$x_1(\bar{1}0)$	$y_1(0\bar{1})$	2	-2.0848 ± 0.0023

Table 7.3: Fourth-order Cartesian coefficients for the single hexagon. All other interatomic force constants can be derived from these by symmetry.

Coord.	Coord.	Coord.	Coord.	Coord.	Range/l_{nn}	Value (eV/Å^5)
$x_0(00)$	$x_0(00)$	$x_0(00)$	$y_1(\overline{11})$	$y_1(\overline{11})$	1	101.4484 ± 0.0045
$x_0(00)$	$x_0(00)$	$x_0(00)$	$x_1(\overline{11})$	$x_1(\overline{11})$	1	-443.1788 ± 0.0116
$x_0(00)$	$x_0(00)$	$x_0(00)$	$x_0(00)$	$x_1(\overline{11})$	1	224.7275 ± 0.0057
$x_0(00)$	$y_1(\overline{11})$	$y_1(\overline{11})$	$y_1(\overline{11})$	$y_1(\overline{11})$	1	-8.8954 ± 0.0033
$x_0(00)$	$x_0(00)$	$x_0(00)$	$x_0(00)$	$x_1(\overline{1}0)$	1	22.0258 ± 0.0026
$x_0(00)$	$x_0(00)$	$y_1(\overline{1}0)$	$y_1(\overline{1}0)$	$y_1(\overline{1}0)$	1	-111.679 ± 0.0036
$x_0(00)$	$x_0(00)$	$x_0(00)$	$x_1(\overline{1}0)$	$y_1(\overline{1}0)$	1	-112.1413 ± 0.0039
$x_0(00)$	$x_0(00)$	$x_0(00)$	$x_1(\overline{1}0)$	$x_1(\overline{1}0)$	1	-34.6628 ± 0.0053
$x_0(00)$	$x_0(00)$	$x_0(00)$	$y_1(\overline{1}0)$	$y_1(\overline{1}0)$	1	0.0 ± 0.0
$x_0(00)$	$y_1(\overline{1}0)$	$y_1(\overline{1}0)$	$y_1(\overline{1}0)$	$y_1(\overline{1}0)$	1	84.1294 ± 0.0025
$x_0(00)$	$x_0(00)$	$x_0(00)$	$x_0(00)$	$y_1(\overline{1}0)$	1	31.7124 ± 0.002
$x_0(00)$	$x_0(00)$	$y_0(01)$	$x_1(\overline{1}0)$	$x_1(\overline{1}0)$	$\sqrt{3}$	0.6805 ± 0.0037
$x_0(00)$	$x_0(00)$	$x_0(00)$	$x_0(01)$	$x_1(\overline{1}0)$	$\sqrt{3}$	5.5104 ± 0.0037
$x_0(00)$	$x_0(00)$	$x_0(00)$	$x_0(01)$	$y_1(\overline{1}0)$	$\sqrt{3}$	2.0519 ± 0.0047
$x_0(00)$	$x_0(00)$	$x_0(01)$	$x_1(\overline{1}0)$	$y_1(\overline{1}0)$	$\sqrt{3}$	-4.7939 ± 0.0074
$x_0(00)$	$x_0(00)$	$x_0(00)$	$y_0(01)$	$x_1(\overline{1}0)$	$\sqrt{3}$	0.0 ± 0.0
$x_0(00)$	$x_0(00)$	$x_0(00)$	$y_0(01)$	$y_1(\overline{1}0)$	$\sqrt{3}$	4.3303 ± 0.0034
$x_0(00)$	$x_0(01)$	$x_0(01)$	$x_0(01)$	$y_0(00)$	$\sqrt{3}$	0.0 ± 0.0
$x_0(00)$	$x_0(01)$	$x_0(01)$	$x_0(01)$	$x_1(\overline{1}0)$	$\sqrt{3}$	-4.8004 ± 0.0043
$x_0(00)$	$x_0(01)$	$x_0(01)$	$x_0(01)$	$y_1(\overline{1}0)$	$\sqrt{3}$	0.0 ± 0.0
$x_0(00)$	$x_0(01)$	$x_1(\overline{1}0)$	$x_1(\overline{1}0)$	$x_1(\overline{1}0)$	$\sqrt{3}$	6.1681 ± 0.0044
$x_0(00)$	$x_0(00)$	$x_0(01)$	$y_0(01)$	$x_1(\overline{1}0)$	$\sqrt{3}$	0.0 ± 0.0
$x_0(00)$	$y_0(01)$	$y_0(01)$	$y_0(01)$	$x_1(\overline{1}0)$	$\sqrt{3}$	-2.2221 ± 0.0035
$x_0(00)$	$y_0(01)$	$y_0(01)$	$y_0(01)$	$y_1(\overline{1}0)$	$\sqrt{3}$	0.0 ± 0.0
$x_0(00)$	$y_0(01)$	$x_1(\overline{1}0)$	$x_1(\overline{1}0)$	$x_1(\overline{1}0)$	$\sqrt{3}$	0.0 ± 0.0
$x_0(00)$	$x_0(00)$	$y_0(0\overline{1})$	$x_1(\overline{11})$	$x_1(\overline{11})$	$\sqrt{3}$	-14.7671 ± 0.0079
$x_0(00)$	$x_0(00)$	$y_0(01)$	$y_1(\overline{1}0)$	$y_1(\overline{1}0)$	$\sqrt{3}$	-2.7572 ± 0.0051
$x_0(00)$	$y_0(01)$	$y_0(01)$	$x_1(\overline{1}0)$	$x_1(\overline{1}0)$	$\sqrt{3}$	0.0 ± 0.0
$x_0(00)$	$x_0(01)$	$x_0(01)$	$y_1(\overline{1}0)$	$y_1(\overline{1}0)$	$\sqrt{3}$	-1.2981 ± 0.0046
$x_0(00)$	$x_0(01)$	$x_0(01)$	$x_1(\overline{1}0)$	$x_1(\overline{1}0)$	$\sqrt{3}$	0.0 ± 0.0
$x_0(00)$	$x_0(00)$	$x_0(00)$	$y_0(0\overline{1})$	$x_1(\overline{11})$	$\sqrt{3}$	9.8799 ± 0.0053
$x_0(00)$	$x_0(00)$	$x_0(00)$	$y_0(0\overline{1})$	$y_1(\overline{11})$	$\sqrt{3}$	-7.276 ± 0.0043
$x_0(00)$	$x_0(00)$	$y_0(0\overline{1})$	$y_0(0\overline{1})$	$x_1(\overline{11})$	$\sqrt{3}$	-4.1245 ± 0.0049
$x_0(00)$	$x_0(00)$	$x_0(01)$	$x_0(01)$	$x_1(\overline{1}0)$	$\sqrt{3}$	4.5149 ± 0.0045
$x_0(00)$	$x_0(00)$	$x_0(01)$	$x_0(01)$	$y_1(\overline{1}0)$	$\sqrt{3}$	2.0227 ± 0.005
$x_0(00)$	$x_0(00)$	$x_0(01)$	$x_1(\overline{1}0)$	$x_1(\overline{1}0)$	$\sqrt{3}$	-11.299 ± 0.0062
$x_0(00)$	$x_0(00)$	$x_0(01)$	$y_1(\overline{1}0)$	$y_1(\overline{1}0)$	$\sqrt{3}$	4.0809 ± 0.0047
$x_0(00)$	$x_0(00)$	$y_0(01)$	$y_0(01)$	$x_1(\overline{1}0)$	$\sqrt{3}$	-1.902 ± 0.004
$x_0(00)$	$x_0(00)$	$y_0(01)$	$y_0(01)$	$y_1(\overline{1}0)$	$\sqrt{3}$	3.2294 ± 0.0057
$x_0(00)$	$x_0(00)$	$y_0(0\overline{1})$	$y_1(\overline{11})$	$y_1(\overline{11})$	$\sqrt{3}$	0.0 ± 0.0
$x_0(00)$	$x_0(00)$	$x_0(00)$	$x_0(01)$	$y_0(01)$	$\sqrt{3}$	2.4868 ± 0.0027
$x_0(00)$	$x_0(01)$	$y_1(\overline{1}0)$	$y_1(\overline{1}0)$	$y_1(\overline{1}0)$	$\sqrt{3}$	-5.2632 ± 0.0036
$x_0(00)$	$y_0(01)$	$y_0(01)$	$y_1(\overline{1}0)$	$y_1(\overline{1}0)$	$\sqrt{3}$	2.5579 ± 0.0045
$x_0(00)$	$x_0(00)$	$x_0(00)$	$y_0(01)$	$y_0(01)$	$\sqrt{3}$	0.0 ± 0.0
$x_0(00)$	$y_0(01)$	$y_0(01)$	$y_0(01)$	$y_0(01)$	$\sqrt{3}$	-1.1552 ± 0.0014
$x_0(00)$	$x_0(01)$	$x_0(01)$	$x_0(01)$	$x_0(01)$	$\sqrt{3}$	0.4352 ± 0.0019

Coord.	Coord.	Coord.	Coord.	Coord.	Range/l_{nn}	Value (eV/Å^5)
$x_0(00)$	$x_0(00)$	$y_0(01)$	$y_0(01)$	$y_0(01)$	$\sqrt{3}$	0.0 ± 0.0
$x_0(00)$	$y_0(0\bar{1})$	$y_0(0\bar{1})$	$y_0(0\bar{1})$	$y_0(0\bar{1})$	$\sqrt{3}$	0.7364 ± 0.0016
$x_0(00)$	$x_0(00)$	$x_0(00)$	$y_0(0\bar{1})$	$y_0(0\bar{1})$	$\sqrt{3}$	2.5772 ± 0.0025
$y_0(00)$	$y_0(00)$	$y_0(00)$	$y_0(00)$	$y_0(01)$	$\sqrt{3}$	-3.6187 ± 0.0016
$x_0(00)$	$x_0(00)$	$x_0(01)$	$x_0(01)$	$x_0(01)$	$\sqrt{3}$	2.1507 ± 0.0017
$x_0(00)$	$x_0(00)$	$y_0(0\bar{1})$	$y_0(0\bar{1})$	$y_0(0\bar{1})$	$\sqrt{3}$	-3.834 ± 0.0026
$x_0(00)$	$x_0(00)$	$x_0(00)$	$x_0(00)$	$y_0(01)$	$\sqrt{3}$	0.0 ± 0.0
$x_0(00)$	$x_0(00)$	$x_0(00)$	$x_0(01)$	$x_0(01)$	$\sqrt{3}$	-3.8073 ± 0.0018
$x_0(00)$	$x_0(00)$	$x_0(00)$	$x_0(00)$	$x_0(01)$	$\sqrt{3}$	0.0 ± 0.0
$y_0(00)$	$y_0(00)$	$y_0(00)$	$y_0(01)$	$y_0(01)$	$\sqrt{3}$	0.0 ± 0.0
$x_0(00)$	$x_0(00)$	$x_0(00)$	$x_0(00)$	$y_0(0\bar{1})$	$\sqrt{3}$	-2.4361 ± 0.0018
$x_0(00)$	$x_0(00)$	$x_0(00)$	$x_0(01)$	$x_0(10)$	$\sqrt{3}$	-0.9801 ± 0.0036
$x_0(00)$	$x_0(00)$	$x_0(1\bar{1})$	$y_1(0\bar{1})$	$y_1(0\bar{1})$	$\sqrt{3}$	-0.4809 ± 0.0035
$x_0(00)$	$x_0(00)$	$x_0(00)$	$x_0(1\bar{1})$	$y_0(0\bar{1})$	$\sqrt{3}$	-1.8336 ± 0.0053
$x_0(00)$	$x_0(00)$	$x_0(01)$	$x_0(01)$	$x_0(10)$	$\sqrt{3}$	0.0 ± 0.0
$x_0(00)$	$x_0(00)$	$x_0(01)$	$x_0(01)$	$y_0(10)$	$\sqrt{3}$	-1.327 ± 0.0054
$x_0(00)$	$x_0(00)$	$x_0(01)$	$y_0(10)$	$y_0(10)$	$\sqrt{3}$	5.0911 ± 0.0059
$x_0(00)$	$x_0(00)$	$x_0(00)$	$y_0(0\bar{1})$	$y_0(1\bar{1})$	$\sqrt{3}$	3.6272 ± 0.0035
$x_0(00)$	$x_0(00)$	$y_0(01)$	$y_0(01)$	$y_0(10)$	$\sqrt{3}$	-5.1105 ± 0.0072
$x_0(00)$	$x_0(00)$	$x_0(1\bar{1})$	$y_0(0\bar{1})$	$y_0(0\bar{1})$	$\sqrt{3}$	0.0 ± 0.0
$x_0(00)$	$x_0(00)$	$x_0(00)$	$x_0(00)$	$x_0(1\bar{1})$	$\sqrt{3}$	0.0 ± 0.0
$x_0(00)$	$y_1(\bar{1}0)$	$y_1(\bar{1}0)$	$y_1(0\bar{1})$	$y_1(0\bar{1})$	$\sqrt{3}$	3.1348 ± 0.0054
$x_0(00)$	$x_0(00)$	$x_1(\bar{1}0)$	$x_1(\bar{1}0)$	$x_1(0\bar{1})$	$\sqrt{3}$	9.1764 ± 0.0057
$x_0(00)$	$x_0(00)$	$x_1(\bar{1}0)$	$x_1(\bar{1}0)$	$y_1(0\bar{1})$	$\sqrt{3}$	-6.3802 ± 0.0046
$x_0(00)$	$x_0(00)$	$x_1(\bar{1}0)$	$y_1(0\bar{1})$	$y_1(0\bar{1})$	$\sqrt{3}$	5.0274 ± 0.0049
$x_0(00)$	$x_0(00)$	$y_1(\bar{1}0)$	$y_1(\bar{1}0)$	$y_1(0\bar{1})$	$\sqrt{3}$	-3.1627 ± 0.0051
$x_0(00)$	$x_0(01)$	$x_0(01)$	$x_0(10)$	$x_0(10)$	$\sqrt{3}$	2.8597 ± 0.005
$x_0(00)$	$x_0(01)$	$x_0(01)$	$y_0(10)$	$y_0(10)$	$\sqrt{3}$	-3.6722 ± 0.0059
$x_0(00)$	$x_1(\bar{1}0)$	$x_1(\bar{1}0)$	$y_1(0\bar{1})$	$y_1(0\bar{1})$	$\sqrt{3}$	-5.2555 ± 0.0059
$x_0(00)$	$x_1(\bar{1}0)$	$x_1(\bar{1}0)$	$x_1(0\bar{1})$	$x_1(0\bar{1})$	$\sqrt{3}$	-7.0086 ± 0.007
$x_0(00)$	$y_0(01)$	$y_0(01)$	$y_0(10)$	$y_0(10)$	$\sqrt{3}$	-1.7926 ± 0.006
$x_0(00)$	$x_0(00)$	$x_0(00)$	$x_0(00)$	$y_0(1\bar{1})$	$\sqrt{3}$	2.9651 ± 0.0019
$x_0(00)$	$x_1(\bar{1}0)$	$y_1(0\bar{1})$	$y_1(0\bar{1})$	$y_1(0\bar{1})$	$\sqrt{3}$	7.2641 ± 0.004
$x_0(00)$	$x_0(00)$	$x_0(00)$	$x_0(01)$	$y_0(10)$	$\sqrt{3}$	3.2824 ± 0.0035
$x_0(00)$	$y_0(1\bar{1})$	$y_0(1\bar{1})$	$y_0(1\bar{1})$	$y_0(1\bar{1})$	$\sqrt{3}$	-0.9932 ± 0.0017
$x_0(00)$	$x_1(\bar{1}0)$	$x_1(\bar{1}0)$	$x_1(\bar{1}0)$	$y_1(0\bar{1})$	$\sqrt{3}$	0.0 ± 0.0
$x_0(00)$	$x_0(01)$	$x_0(01)$	$x_0(01)$	$x_0(10)$	$\sqrt{3}$	0.0 ± 0.0
$x_0(00)$	$x_0(01)$	$y_0(10)$	$y_0(10)$	$y_0(10)$	$\sqrt{3}$	-1.9394 ± 0.0035
$x_0(00)$	$x_0(00)$	$x_0(00)$	$x_0(1\bar{1})$	$x_0(1\bar{1})$	$\sqrt{3}$	0.4791 ± 0.0014
$x_0(00)$	$x_0(00)$	$x_0(00)$	$y_1(\bar{1}0)$	$y_1(0\bar{1})$	$\sqrt{3}$	5.4058 ± 0.0045
$x_0(00)$	$x_0(01)$	$x_0(01)$	$x_0(01)$	$y_0(10)$	$\sqrt{3}$	-3.7078 ± 0.0045
$x_0(00)$	$x_0(00)$	$x_0(00)$	$x_1(\bar{1}0)$	$y_1(0\bar{1})$	$\sqrt{3}$	3.9271 ± 0.0041
$x_0(00)$	$x_0(00)$	$x_0(00)$	$y_0(1\bar{1})$	$y_0(1\bar{1})$	$\sqrt{3}$	-1.63 ± 0.0023
$x_0(00)$	$x_0(00)$	$x_0(00)$	$x_1(\bar{1}0)$	$x_1(0\bar{1})$	$\sqrt{3}$	-13.8761 ± 0.007
$x_0(00)$	$x_0(00)$	$x_0(01)$	$x_0(10)$	$y_0(01)$	$\sqrt{3}$	0.0 ± 0.0
$x_0(00)$	$x_0(00)$	$y_0(1\bar{1})$	$y_0(1\bar{1})$	$y_0(1\bar{1})$	$\sqrt{3}$	-3.8752 ± 0.0021

Coord.	Coord.	Coord.	Coord.	Coord.	Range/l_{nn}	Value (eV/Å^5)
$x_0(00)$	$x_0(00)$	$x_0(00)$	$y_0(01)$	$y_0(10)$	$\sqrt{3}$	2.6569 ± 0.0045
$x_0(00)$	$x_0(00)$	$x_0(01)$	$y_1(00)$	$y_1(00)$	2	-3.6919 ± 0.0043
$x_0(00)$	$y_1(00)$	$y_1(00)$	$y_1(00)$	$y_1(00)$	2	1.0632 ± 0.002
$x_0(00)$	$y_1(\bar{1}0)$	$y_1(\bar{1}0)$	$y_1(00)$	$y_1(00)$	2	-4.0304 ± 0.0049
$x_0(00)$	$x_0(00)$	$x_0(00)$	$x_0(00)$	$x_1(00)$	2	0.0 ± 0.0
$x_0(00)$	$x_0(00)$	$y_0(01)$	$x_1(00)$	$x_1(00)$	2	0.0 ± 0.0
$x_0(00)$	$x_0(00)$	$y_1(\bar{1}0)$	$y_1(00)$	$y_1(00)$	2	0.0 ± 0.0
$x_0(00)$	$x_1(\bar{1}0)$	$x_1(\bar{1}0)$	$y_1(00)$	$y_1(00)$	2	0.0 ± 0.0
$x_0(00)$	$x_0(00)$	$y_0(01)$	$y_1(00)$	$y_1(00)$	2	0.0 ± 0.0
$x_0(00)$	$x_0(00)$	$x_0(00)$	$x_1(00)$	$y_1(\bar{1}0)$	2	1.6963 ± 0.0038
$x_0(00)$	$x_0(00)$	$x_0(00)$	$x_1(\bar{1}0)$	$y_1(00)$	2	2.839 ± 0.0037
$x_0(00)$	$x_0(00)$	$x_1(\bar{1}0)$	$x_1(\bar{1}0)$	$y_1(00)$	2	-7.4933 ± 0.0059
$x_0(00)$	$x_0(00)$	$x_1(00)$	$y_1(\bar{1}0)$	$y_1(\bar{1}0)$	2	2.0796 ± 0.0049
$x_0(00)$	$x_0(00)$	$x_1(\bar{1}0)$	$x_1(\bar{1}0)$	$x_1(00)$	2	0.0 ± 0.0
$x_0(00)$	$y_0(01)$	$y_1(00)$	$y_1(00)$	$y_1(00)$	2	-3.0586 ± 0.004
$x_0(00)$	$x_0(00)$	$x_0(00)$	$x_1(00)$	$x_1(00)$	2	0.0 ± 0.0
$x_0(00)$	$x_0(00)$	$x_0(01)$	$x_1(00)$	$x_1(00)$	2	-3.5919 ± 0.0048
$x_0(00)$	$x_0(00)$	$x_0(01)$	$y_1(00)$	$y_1(00)$	2	0.0 ± 0.0
$x_0(00)$	$x_1(\bar{1}0)$	$y_1(00)$	$y_1(00)$	$y_1(00)$	2	-0.7717 ± 0.0055
$x_0(00)$	$y_1(\bar{1}0)$	$y_1(\bar{1}0)$	$y_1(\bar{1}0)$	$y_1(00)$	2	-2.0895 ± 0.0038
$x_0(00)$	$y_0(00)$	$y_1(00)$	$y_1(00)$	$y_1(00)$	2	-5.5951 ± 0.0045
$x_0(00)$	$x_0(01)$	$y_1(00)$	$y_1(00)$	$y_1(00)$	2	-1.5006 ± 0.0047
$x_0(00)$	$x_0(00)$	$x_0(00)$	$y_1(00)$	$y_1(00)$	2	0.0 ± 0.0
$x_0(00)$	$y_0(01)$	$y_0(01)$	$y_1(00)$	$y_1(00)$	2	1.6005 ± 0.005
$x_0(00)$	$x_0(00)$	$x_0(01)$	$y_0(10)$	$y_1(\bar{1}0)$	2	-4.3352 ± 0.0053
$x_0(00)$	$x_0(00)$	$x_0(01)$	$y_0(10)$	$x_1(0\bar{1})$	2	-3.5397 ± 0.0072
$x_0(00)$	$x_0(00)$	$x_0(01)$	$y_0(10)$	$y_1(0\bar{1})$	2	-7.2776 ± 0.0072
$x_0(00)$	$x_0(00)$	$y_0(0\bar{1})$	$y_1(0\bar{2})$	$y_1(0\bar{2})$	2	0.0 ± 0.0
$x_0(00)$	$x_0(00)$	$x_0(01)$	$x_1(0\bar{1})$	$y_1(0\bar{1})$	2	7.0392 ± 0.0073
$x_0(00)$	$x_0(00)$	$x_0(01)$	$x_1(0\bar{1})$	$y_1(\bar{1}0)$	2	-5.614 ± 0.0067
$x_0(00)$	$x_0(00)$	$y_0(01)$	$x_1(\bar{1}0)$	$y_1(0\bar{1})$	2	0.0 ± 0.0
$x_0(00)$	$x_0(00)$	$y_0(0\bar{1})$	$x_1(0\bar{2})$	$x_1(0\bar{2})$	2	2.1031 ± 0.0051
$x_0(00)$	$x_0(00)$	$y_0(0\bar{1})$	$y_0(0\bar{1})$	$y_1(0\bar{2})$	2	2.5459 ± 0.0046
$x_0(00)$	$x_0(00)$	$x_0(01)$	$y_0(01)$	$x_1(0\bar{1})$	2	0.0 ± 0.0
$x_0(00)$	$x_0(01)$	$x_0(01)$	$y_0(10)$	$y_1(\bar{1}0)$	2	0.0 ± 0.0
$x_0(00)$	$x_0(00)$	$x_0(1\bar{1})$	$y_1(0\bar{2})$	$y_1(0\bar{2})$	2	-2.0139 ± 0.0033
$x_0(00)$	$x_0(01)$	$x_0(01)$	$y_0(10)$	$y_1(0\bar{1})$	2	0.0 ± 0.0
$x_0(00)$	$x_0(00)$	$x_0(1\bar{1})$	$y_1(\bar{1}\bar{1})$	$y_1(\bar{1}\bar{1})$	2	0.0 ± 0.0
$x_0(00)$	$x_0(00)$	$x_0(1\bar{1})$	$x_1(\bar{1}\bar{1})$	$x_1(\bar{1}\bar{1})$	2	5.1321 ± 0.0065
$x_0(00)$	$x_0(01)$	$x_0(01)$	$x_0(10)$	$y_1(\bar{1}0)$	2	0.0 ± 0.0
$x_0(00)$	$x_0(00)$	$x_0(01)$	$y_0(10)$	$x_1(\bar{1}0)$	2	-3.0684 ± 0.0073
$x_0(00)$	$x_0(00)$	$x_0(01)$	$x_0(10)$	$y_1(\bar{1}0)$	2	-2.4177 ± 0.0064
$x_0(00)$	$x_0(00)$	$x_0(1\bar{1})$	$x_0(1\bar{1})$	$y_1(\bar{1}\bar{1})$	2	-2.0351 ± 0.0059
$x_0(00)$	$x_0(00)$	$x_0(00)$	$x_0(1\bar{1})$	$y_1(0\bar{2})$	2	-1.3304 ± 0.0045
$x_0(00)$	$y_0(01)$	$y_0(01)$	$x_1(0\bar{1})$	$x_1(0\bar{1})$	2	4.1129 ± 0.0033
$x_0(00)$	$y_0(01)$	$y_0(01)$	$y_0(01)$	$x_1(0\bar{1})$	2	0.0 ± 0.0
$x_0(00)$	$x_0(01)$	$y_1(0\bar{1})$	$y_1(0\bar{1})$	$y_1(0\bar{1})$	2	0.0 ± 0.0
$x_0(00)$	$x_0(01)$	$x_1(0\bar{1})$	$x_1(0\bar{1})$	$x_1(0\bar{1})$	2	2.5125 ± 0.004
$x_0(00)$	$x_0(01)$	$x_0(01)$	$x_0(01)$	$y_1(0\bar{1})$	2	5.7159 ± 0.0044

Coord.	Coord.	Coord.	Coord.	Coord.	Range/l_{nn}	Value (eV/Å^5)
$x_0(00)$	$x_0(01)$	$x_0(01)$	$x_0(01)$	$x_1(0\bar{1})$	2	-1.6531 ± 0.004
$x_0(00)$	$x_0(00)$	$x_0(00)$	$y_0(01)$	$y_1(0\bar{1})$	2	0.0 ± 0.0
$x_0(00)$	$y_0(01)$	$y_0(01)$	$y_0(01)$	$y_1(0\bar{1})$	2	0.0 ± 0.0
$x_0(00)$	$x_0(00)$	$x_0(00)$	$y_0(01)$	$x_1(0\bar{1})$	2	0.0 ± 0.0
$x_0(00)$	$x_0(00)$	$x_0(00)$	$x_0(01)$	$x_1(0\bar{1})$	2	0.5746 ± 0.0036
$x_0(00)$	$x_0(00)$	$y_1(0\bar{2})$	$y_1(0\bar{2})$	$y_1(0\bar{2})$	2	-0.9293 ± 0.0018
$x_0(00)$	$x_0(00)$	$x_0(00)$	$y_1(0\bar{2})$	$y_1(0\bar{2})$	2	1.3996 ± 0.0017
$x_0(00)$	$x_0(00)$	$x_0(00)$	$x_1(0\bar{2})$	$x_1(0\bar{2})$	2	-0.5067 ± 0.0028
$x_0(00)$	$x_0(00)$	$x_0(00)$	$x_0(00)$	$y_1(0\bar{2})$	2	0.2407 ± 0.0017
$x_0(00)$	$x_0(00)$	$x_0(00)$	$x_0(00)$	$x_1(0\bar{2})$	2	0.0 ± 0.0
$x_0(00)$	$x_0(00)$	$x_0(00)$	$x_0(01)$	$y_1(0\bar{1})$	2	-3.2879 ± 0.0048
$x_0(00)$	$y_0(01)$	$y_0(01)$	$y_1(0\bar{1})$	$y_1(0\bar{1})$	2	0.0 ± 0.0
$x_0(00)$	$y_0(01)$	$x_1(0\bar{1})$	$x_1(0\bar{1})$	$x_1(0\bar{1})$	2	0.0 ± 0.0
$x_0(00)$	$x_0(00)$	$x_0(00)$	$x_0(1\bar{1})$	$y_1(\bar{1}1)$	2	-4.218 ± 0.0052
$x_0(00)$	$x_0(01)$	$x_0(01)$	$y_1(0\bar{1})$	$y_1(0\bar{1})$	2	-1.5734 ± 0.003
$x_0(00)$	$x_0(01)$	$x_0(01)$	$x_1(0\bar{1})$	$x_1(0\bar{1})$	2	-0.4684 ± 0.0047
$x_0(00)$	$x_0(00)$	$y_0(01)$	$y_1(0\bar{1})$	$y_1(0\bar{1})$	2	3.2361 ± 0.0049
$x_0(00)$	$x_0(00)$	$y_0(01)$	$x_1(0\bar{1})$	$x_1(0\bar{1})$	2	0.0 ± 0.0
$x_0(00)$	$x_0(00)$	$y_0(01)$	$y_0(01)$	$y_1(0\bar{1})$	2	1.4582 ± 0.0047
$x_0(00)$	$x_0(00)$	$y_0(01)$	$y_0(01)$	$x_1(0\bar{1})$	2	-5.278 ± 0.005
$x_0(00)$	$y_0(01)$	$y_1(0\bar{1})$	$y_1(0\bar{1})$	$y_1(0\bar{1})$	2	0.3517 ± 0.0034
$x_0(00)$	$x_0(00)$	$x_0(01)$	$y_1(0\bar{1})$	$y_1(0\bar{1})$	2	0.0 ± 0.0
$x_0(00)$	$x_0(00)$	$x_0(01)$	$x_0(01)$	$y_1(0\bar{1})$	2	-4.3279 ± 0.006
$x_0(00)$	$x_0(00)$	$x_0(01)$	$x_0(01)$	$x_1(0\bar{1})$	2	0.0 ± 0.0
$x_0(00)$	$x_0(00)$	$x_0(00)$	$y_0(1\bar{1})$	$y_1(\bar{1}1)$	2	1.553 ± 0.0035
$x_0(00)$	$x_0(00)$	$x_0(00)$	$y_0(1\bar{1})$	$x_1(\bar{1}1)$	2	-6.6061 ± 0.0059
$x_0(00)$	$x_0(00)$	$x_0(00)$	$y_0(0\bar{1})$	$y_1(0\bar{2})$	2	-2.1484 ± 0.0041
$x_0(00)$	$x_0(01)$	$y_0(10)$	$y_0(10)$	$y_1(\bar{1}0)$	2	-3.8695 ± 0.0084
$x_0(00)$	$x_0(00)$	$x_0(01)$	$x_1(0\bar{1})$	$x_1(0\bar{1})$	2	-0.6716 ± 0.006
$x_0(00)$	$y_0(01)$	$y_0(01)$	$x_1(\bar{1}0)$	$y_1(0\bar{1})$	2	0.0 ± 0.0

Table 7.4: Fifth-order Cartesian coefficients for the single hexagon. All other interatomic force constants can be derived from these by symmetry.

Sym. Prod.	Polynomial	Value (eV/Å^2)
$[\![A_{10} \otimes A_{10}]\!]$	A_{10}^2	3.1515 ± 0.0018
$[\![A_{10} \otimes A_{11}]\!]$	$A_{10}A_{11}$	-2.1116 ± 0.0011
$[\![A_{10} \otimes A_{12}]\!]$	$A_{10}A_{12}$	-1.1716 ± 0.0002
$[\![A_{10} \otimes A_{13}]\!]$	$A_{10}A_{13}$	-0.2067 ± 0.0004
$[\![A_{11} \otimes A_{11}]\!]$	A_{11}^2	2.2266 ± 0.0007
$[\![A_{11} \otimes A_{12}]\!]$	$A_{11}A_{12}$	-1.5445 ± 0.004
$[\![A_{11} \otimes A_{13}]\!]$	$A_{11}A_{13}$	-1.7003 ± 0.0007
$[\![A_{12} \otimes A_{12}]\!]$	A_{12}^2	2.3034 ± 0.0023
$[\![A_{12} \otimes A_{13}]\!]$	$A_{12}A_{13}$	-2.315 ± 0.0018
$[\![A_{13} \otimes A_{13}]\!]$	A_{13}^2	3.7164 ± 0.0021
$[\![A_{20} \otimes A_{21}]\!]$	$1.00A_{20}^2 - 0.01A_{20}A_{21} + 0.01A_{20}A_{22} - 0.01A_{20}A_{23} - 0.02A_{21}^2 + 0.02A_{21}A_{22} - 0.02A_{21}A_{23} - 0.03A_{22}^2 + 0.03A_{22}A_{23} - 0.03A_{23}^2$	-0.9595 ± 0.0017
$[\![A_{20} \otimes A_{21}]\!]$	$-0.99A_{20}A_{21} - 0.02A_{20}A_{22} + 0.02A_{20}A_{23} + 0.03A_{21}^2 - 0.04A_{21}A_{22} + 0.05A_{21}A_{23} + 0.05A_{22}^2 - 0.06A_{22}A_{23} + 0.07A_{23}^2$	1.5415 ± 0.0012
$[\![A_{20} \otimes A_{23}]\!]$	$-0.99A_{20}A_{22} - 0.03A_{20}A_{23} - 0.04A_{21}^2 + 0.05A_{21}A_{22} - 0.06A_{21}A_{23} - 0.06A_{22}^2 + 0.07A_{22}A_{23} - 0.08A_{23}^2$	-0.2036 ± 0.0001
$[\![A_{20} \otimes A_{23}]\!]$	$0.98A_{20}A_{23} - 0.05A_{21}^2 + 0.06A_{21}A_{22} - 0.07A_{21}A_{23} - 0.08A_{22}^2 + 0.09A_{22}A_{23} - 0.10A_{23}^2$	0.3896 ± 0.0002
$[\![A_{22} \otimes A_{22}]\!]$	$-0.96A_{21}^2 - 0.09A_{21}A_{22} + 0.11A_{21}A_{23} + 0.11A_{22}^2 - 0.13A_{22}A_{23} + 0.15A_{23}^2$	-3.0391 ± 0.0005
$[\![A_{21} \otimes A_{22}]\!]$	$-0.94A_{21}A_{22} - 0.14A_{21}A_{23} - 0.15A_{22}^2 + 0.18A_{22}A_{23} - 0.20A_{23}^2$	-3.1168 ± 0.0001
$[\![A_{22} \otimes A_{23}]\!]$	$0.91A_{21}A_{23} - 0.21A_{22}^2 + 0.24A_{22}A_{23} - 0.28A_{23}^2$	-2.0897 ± 0.0035
$[\![A_{22} \otimes A_{23}]\!]$	$-0.87A_{22}^2 - 0.32A_{22}A_{23} + 0.37A_{23}^2$	-2.5082 ± 0.0008
$[\![A_{22} \otimes A_{23}]\!]$	$0.76A_{22}A_{23} + \frac{\sqrt{3}}{\sqrt{7}}A_{23}^2$	2.2461 ± 0.0039
$[\![B_{10} \otimes B_{10}]\!]$	B_{10}^2	4.8541 ± 0.0021
$[\![B_{10} \otimes B_{11}]\!]$	$B_{10}B_{11}$	-0.6234 ± 0.0007
$[\![B_{10} \otimes B_{12}]\!]$	$B_{10}B_{12}$	-0.1137 ± 0.0001
$[\![B_{10} \otimes B_{13}]\!]$	$B_{10}B_{13}$	-0.3422 ± 0.0006
$[\![B_{11} \otimes B_{11}]\!]$	B_{11}^2	2.518 ± 0.0006
$[\![B_{11} \otimes B_{12}]\!]$	$B_{11}B_{12}$	-2.6834 ± 0.0017
$[\![B_{11} \otimes B_{13}]\!]$	$B_{11}B_{13}$	0.1456 ± 0.0026
$[\![B_{12} \otimes B_{12}]\!]$	B_{12}^2	1.8193 ± 0.0029
$[\![B_{12} \otimes B_{13}]\!]$	$B_{12}B_{13}$	-1.2742 ± 0.001
$[\![B_{13} \otimes B_{13}]\!]$	B_{13}^2	3.323 ± 0.0054
$[\![B_{20} \otimes B_{20}]\!]$	B_{20}^2	3.884 ± 0.002
$[\![B_{20} \otimes B_{21}]\!]$	$B_{20}B_{21}$	-2.8564 ± 0.0008
$[\![B_{20} \otimes B_{22}]\!]$	$B_{20}B_{22}$	0.1906 ± 0.0003
$[\![B_{20} \otimes B_{23}]\!]$	$B_{20}B_{23}$	0.108 ± 0.0006
$[\![B_{21} \otimes B_{21}]\!]$	B_{21}^2	3.2068 ± 0.0008
$[\![B_{21} \otimes B_{22}]\!]$	$B_{21}B_{22}$	2.3124 ± 0.0014
$[\![B_{21} \otimes B_{23}]\!]$	$B_{21}B_{23}$	1.332 ± 0.0011
$[\![B_{22} \otimes B_{22}]\!]$	B_{22}^2	3.178 ± 0.0054
$[\![B_{22} \otimes B_{23}]\!]$	$B_{22}B_{23}$	1.8839 ± 0.0012
$[\![B_{23} \otimes B_{23}]\!]$	B_{23}^2	1.7492 ± 0.0018

Sym. Prod.	Polynomial	Value (eV/Å^2)
$[\![E_{10} \otimes E_{10}]\!]$	$\frac{1}{\sqrt{2}}E_{100}^2 + \frac{1}{\sqrt{2}}E_{101}^2$	4.3712 ± 0.0013
$[\![E_{10} \otimes E_{11}]\!]$	$\frac{1}{\sqrt{2}}E_{100}E_{110} + \frac{1}{\sqrt{2}}E_{101}E_{111}$	-2.9119 ± 0.0006
$[\![E_{10} \otimes E_{12}]\!]$	$\frac{1}{\sqrt{2}}E_{100}E_{120} + \frac{1}{\sqrt{2}}E_{101}E_{121}$	-2.811 ± 0.0008
$[\![E_{10} \otimes E_{13}]\!]$	$\frac{1}{\sqrt{2}}E_{100}E_{130} + \frac{1}{\sqrt{2}}E_{101}E_{131}$	1.1004 ± 0.0004
$[\![E_{10} \otimes E_{14}]\!]$	$\frac{1}{\sqrt{2}}E_{100}E_{140} + \frac{1}{\sqrt{2}}E_{101}E_{141}$	-0.3466 ± 0.0001
$[\![E_{10} \otimes E_{15}]\!]$	$\frac{1}{\sqrt{2}}E_{100}E_{150} + \frac{1}{\sqrt{2}}E_{101}E_{151}$	-0.0169 ± 0.0013
$[\![E_{10} \otimes E_{16}]\!]$	$\frac{1}{\sqrt{2}}E_{100}E_{160} + \frac{1}{\sqrt{2}}E_{101}E_{161}$	1.2292 ± 0.0005
$[\![E_{11} \otimes E_{11}]\!]$	$\frac{1}{\sqrt{2}}E_{110}^2 + \frac{1}{\sqrt{2}}E_{111}^2$	2.2464 ± 0.0018
$[\![E_{11} \otimes E_{12}]\!]$	$\frac{1}{\sqrt{2}}E_{110}E_{120} + \frac{1}{\sqrt{2}}E_{111}E_{121}$	-0.6596 ± 0.0005
$[\![E_{11} \otimes E_{13}]\!]$	$\frac{1}{\sqrt{2}}E_{110}E_{130} + \frac{1}{\sqrt{2}}E_{111}E_{131}$	-1.1092 ± 0.0002
$[\![E_{11} \otimes E_{14}]\!]$	$\frac{1}{\sqrt{2}}E_{110}E_{140} + \frac{1}{\sqrt{2}}E_{111}E_{141}$	-0.0595 ± 0.0013
$[\![E_{11} \otimes E_{15}]\!]$	$\frac{1}{\sqrt{2}}E_{110}E_{150} + \frac{1}{\sqrt{2}}E_{111}E_{151}$	-0.9951 ± 0.0012
$[\![E_{11} \otimes E_{16}]\!]$	$\frac{1}{\sqrt{2}}E_{110}E_{160} + \frac{1}{\sqrt{2}}E_{111}E_{161}$	0.2846 ± 0.0017
$[\![E_{12} \otimes E_{12}]\!]$	$\frac{1}{\sqrt{2}}E_{120}^2 + \frac{1}{\sqrt{2}}E_{121}^2$	4.0445 ± 0.0029
$[\![E_{12} \otimes E_{13}]\!]$	$\frac{1}{\sqrt{2}}E_{120}E_{130} + \frac{1}{\sqrt{2}}E_{121}E_{131}$	0.9199 ± 0.0007
$[\![E_{12} \otimes E_{14}]\!]$	$\frac{1}{\sqrt{2}}E_{120}E_{140} + \frac{1}{\sqrt{2}}E_{121}E_{141}$	0.595 ± 0.0021
$[\![E_{12} \otimes E_{15}]\!]$	$\frac{1}{\sqrt{2}}E_{120}E_{150} + \frac{1}{\sqrt{2}}E_{121}E_{151}$	-1.4879 ± 0.0
$[\![E_{12} \otimes E_{16}]\!]$	$\frac{1}{\sqrt{2}}E_{120}E_{160} + \frac{1}{\sqrt{2}}E_{121}E_{161}$	2.7457 ± 0.0036
$[\![E_{13} \otimes E_{13}]\!]$	$\frac{1}{\sqrt{2}}E_{130}^2 + \frac{1}{\sqrt{2}}E_{131}^2$	5.8475 ± 0.0023
$[\![E_{13} \otimes E_{14}]\!]$	$\frac{1}{\sqrt{2}}E_{130}E_{140} + \frac{1}{\sqrt{2}}E_{131}E_{141}$	-1.9063 ± 0.0019
$[\![E_{13} \otimes E_{15}]\!]$	$\frac{1}{\sqrt{2}}E_{130}E_{150} + \frac{1}{\sqrt{2}}E_{131}E_{151}$	0.311 ± 0.0034
$[\![E_{13} \otimes E_{16}]\!]$	$\frac{1}{\sqrt{2}}E_{130}E_{160} + \frac{1}{\sqrt{2}}E_{131}E_{161}$	-1.2441 ± 0.0013
$[\![E_{14} \otimes E_{14}]\!]$	$\frac{1}{\sqrt{2}}E_{140}^2 + \frac{1}{\sqrt{2}}E_{141}^2$	4.6594 ± 0.0038
$[\![E_{14} \otimes E_{15}]\!]$	$\frac{1}{\sqrt{2}}E_{140}E_{150} + \frac{1}{\sqrt{2}}E_{141}E_{151}$	-2.7988 ± 0.0003
$[\![E_{14} \otimes E_{16}]\!]$	$\frac{1}{\sqrt{2}}E_{140}E_{160} + \frac{1}{\sqrt{2}}E_{141}E_{161}$	0.4071 ± 0.0001
$[\![E_{15} \otimes E_{15}]\!]$	$\frac{1}{\sqrt{2}}E_{150}^2 + \frac{1}{\sqrt{2}}E_{151}^2$	4.4746 ± 0.0006
$[\![E_{15} \otimes E_{16}]\!]$	$\frac{1}{\sqrt{2}}E_{150}E_{160} + \frac{1}{\sqrt{2}}E_{151}E_{161}$	1.7136 ± 0.0017
$[\![E_{16} \otimes E_{16}]\!]$	$\frac{1}{\sqrt{2}}E_{160}^2 + \frac{1}{\sqrt{2}}E_{161}^2$	4.2786 ± 0.0007
$[\![E_{20} \otimes E_{20}]\!]$	$\frac{1}{\sqrt{2}}E_{200}^2 + \frac{1}{\sqrt{2}}E_{201}^2$	6.8466 ± 0.0017
$[\![E_{20} \otimes E_{21}]\!]$	$\frac{1}{\sqrt{2}}E_{200}E_{210} + \frac{1}{\sqrt{2}}E_{201}E_{211}$	-3.4081 ± 0.0004
$[\![E_{20} \otimes E_{22}]\!]$	$\frac{1}{\sqrt{2}}E_{200}E_{220} + \frac{1}{\sqrt{2}}E_{201}E_{221}$	-1.1338 ± 0.0009
$[\![E_{20} \otimes E_{23}]\!]$	$\frac{1}{\sqrt{2}}E_{200}E_{230} + \frac{1}{\sqrt{2}}E_{201}E_{231}$	-1.3066 ± 0.0013
$[\![E_{20} \otimes E_{24}]\!]$	$\frac{1}{\sqrt{2}}E_{200}E_{240} + \frac{1}{\sqrt{2}}E_{201}E_{241}$	0.3091 ± 0.0003

Sym. Prod.	Polynomial	Value (eV/Å^2)
$[\![E_{20} \otimes E_{25}]\!]$	$\frac{1}{\sqrt{2}} E_{200}E_{250} + \frac{1}{\sqrt{2}} E_{201}E_{251}$	-0.4408 ± 0.0004
$[\![E_{20} \otimes E_{26}]\!]$	$\frac{1}{\sqrt{2}} E_{200}E_{260} + \frac{1}{\sqrt{2}} E_{201}E_{261}$	0.4513 ± 0.0016
$[\![E_{20} \otimes E_{27}]\!]$	$\frac{1}{\sqrt{2}} E_{200}E_{270} + \frac{1}{\sqrt{2}} E_{201}E_{271}$	-0.5021 ± 0.0005
$[\![E_{21} \otimes E_{21}]\!]$	$\frac{1}{\sqrt{2}} E_{210}^2 + \frac{1}{\sqrt{2}} E_{211}^2$	3.4101 ± 0.0016
$[\![E_{21} \otimes E_{22}]\!]$	$\frac{1}{\sqrt{2}} E_{210}E_{220} + \frac{1}{\sqrt{2}} E_{211}E_{221}$	0.5948 ± 0.0011
$[\![E_{21} \otimes E_{23}]\!]$	$\frac{1}{\sqrt{2}} E_{210}E_{230} + \frac{1}{\sqrt{2}} E_{211}E_{231}$	-3.5982 ± 0.0007
$[\![E_{21} \otimes E_{24}]\!]$	$\frac{1}{\sqrt{2}} E_{210}E_{240} + \frac{1}{\sqrt{2}} E_{211}E_{241}$	-0.9469 ± 0.0013
$[\![E_{21} \otimes E_{25}]\!]$	$\frac{1}{\sqrt{2}} E_{210}E_{250} + \frac{1}{\sqrt{2}} E_{211}E_{251}$	-0.4241 ± 0.0001
$[\![E_{21} \otimes E_{26}]\!]$	$\frac{1}{\sqrt{2}} E_{210}E_{260} + \frac{1}{\sqrt{2}} E_{211}E_{261}$	-0.1384 ± 0.0006
$[\![E_{21} \otimes E_{27}]\!]$	$\frac{1}{\sqrt{2}} E_{210}E_{270} + \frac{1}{\sqrt{2}} E_{211}E_{271}$	0.4212 ± 0.0005
$[\![E_{22} \otimes E_{22}]\!]$	$\frac{1}{\sqrt{2}} E_{220}^2 + \frac{1}{\sqrt{2}} E_{221}^2$	3.7648 ± 0.0034
$[\![E_{22} \otimes E_{23}]\!]$	$\frac{1}{\sqrt{2}} E_{220}E_{230} + \frac{1}{\sqrt{2}} E_{221}E_{231}$	-0.2758 ± 0.0016
$[\![E_{22} \otimes E_{24}]\!]$	$\frac{1}{\sqrt{2}} E_{220}E_{240} + \frac{1}{\sqrt{2}} E_{221}E_{241}$	-2.3457 ± 0.0007
$[\![E_{22} \otimes E_{25}]\!]$	$\frac{1}{\sqrt{2}} E_{220}E_{250} + \frac{1}{\sqrt{2}} E_{221}E_{251}$	-1.1553 ± 0.0032
$[\![E_{22} \otimes E_{26}]\!]$	$\frac{1}{\sqrt{2}} E_{220}E_{260} + \frac{1}{\sqrt{2}} E_{221}E_{261}$	-2.918 ± 0.0001
$[\![E_{22} \otimes E_{27}]\!]$	$\frac{1}{\sqrt{2}} E_{220}E_{270} + \frac{1}{\sqrt{2}} E_{221}E_{271}$	-2.5999 ± 0.003
$[\![E_{23} \otimes E_{23}]\!]$	$\frac{1}{\sqrt{2}} E_{230}^2 + \frac{1}{\sqrt{2}} E_{231}^2$	3.8285 ± 0.0031
$[\![E_{23} \otimes E_{24}]\!]$	$\frac{1}{\sqrt{2}} E_{230}E_{240} + \frac{1}{\sqrt{2}} E_{231}E_{241}$	-2.0204 ± 0.001
$[\![E_{23} \otimes E_{25}]\!]$	$\frac{1}{\sqrt{2}} E_{230}E_{250} + \frac{1}{\sqrt{2}} E_{231}E_{251}$	-1.5655 ± 0.0018
$[\![E_{23} \otimes E_{26}]\!]$	$\frac{1}{\sqrt{2}} E_{230}E_{260} + \frac{1}{\sqrt{2}} E_{231}E_{261}$	0.1507 ± 0.0027
$[\![E_{23} \otimes E_{27}]\!]$	$\frac{1}{\sqrt{2}} E_{230}E_{270} + \frac{1}{\sqrt{2}} E_{231}E_{271}$	1.9622 ± 0.0017
$[\![E_{24} \otimes E_{24}]\!]$	$\frac{1}{\sqrt{2}} E_{240}^2 + \frac{1}{\sqrt{2}} E_{241}^2$	3.804 ± 0.0024
$[\![E_{24} \otimes E_{25}]\!]$	$\frac{1}{\sqrt{2}} E_{240}E_{250} + \frac{1}{\sqrt{2}} E_{241}E_{251}$	-1.6455 ± 0.0004
$[\![E_{24} \otimes E_{26}]\!]$	$\frac{1}{\sqrt{2}} E_{240}E_{260} + \frac{1}{\sqrt{2}} E_{241}E_{261}$	0.7746 ± 0.0024
$[\![E_{24} \otimes E_{27}]\!]$	$\frac{1}{\sqrt{2}} E_{240}E_{270} + \frac{1}{\sqrt{2}} E_{241}E_{271}$	-1.4986 ± 0.0031
$[\![E_{25} \otimes E_{25}]\!]$	$\frac{1}{\sqrt{2}} E_{250}^2 + \frac{1}{\sqrt{2}} E_{251}^2$	5.0424 ± 0.0018
$[\![E_{25} \otimes E_{26}]\!]$	$\frac{1}{\sqrt{2}} E_{250}E_{260} + \frac{1}{\sqrt{2}} E_{251}E_{261}$	-2.5512 ± 0.0029
$[\![E_{25} \otimes E_{27}]\!]$	$\frac{1}{\sqrt{2}} E_{250}E_{270} + \frac{1}{\sqrt{2}} E_{251}E_{271}$	-0.3748 ± 0.0042
$[\![E_{26} \otimes E_{26}]\!]$	$\frac{1}{\sqrt{2}} E_{260}^2 + \frac{1}{\sqrt{2}} E_{261}^2$	2.2274 ± 0.0027
$[\![E_{26} \otimes E_{27}]\!]$	$\frac{1}{\sqrt{2}} E_{260}E_{270} + \frac{1}{\sqrt{2}} E_{261}E_{271}$	-0.2369 ± 0.0006
$[\![E_{27} \otimes E_{27}]\!]$	$\frac{1}{\sqrt{2}} E_{270}^2 + \frac{1}{\sqrt{2}} E_{271}^2$	4.3472 ± 0.001

Sym. Prod.	Polynomial	Value (eV/Å^2)

Table 7.5: Second-order mode coefficients for the triple hexagon. When expanded in the provided basis, it constitutes a full Taylor expansion.

Sym. Prod.	Polynomial	Value (eV/Å^3)
$[\![A_{10} \otimes A_{10} \otimes A_{10}]\!]$	A_{10}^3	-3.4243 ± 0.0044
$[\![A_{10} \otimes A_{10} \otimes A_{11}]\!]$	$A_{10}^2 A_{11}$	-11.6475 ± 0.0172
$[\![A_{10} \otimes A_{11} \otimes A_{11}]\!]$	$A_{10} A_{11}^2$	9.7123 ± 0.0205
$[\![A_{10} \otimes A_{20} \otimes A_{20}]\!]$	$A_{10} A_{20}^2$	5.8738 ± 0.0061
$[\![A_{10} \otimes A_{20} \otimes A_{21}]\!]$	$A_{10} A_{20} A_{21}$	-0.3228 ± 0.0113
$[\![A_{10} \otimes A_{21} \otimes A_{21}]\!]$	$A_{10} A_{21}^2$	-1.0087 ± 0.0058
$[\![A_{10} \otimes B_{10} \otimes B_{10}]\!]$	$A_{10} B_{10}^2$	-31.8937 ± 0.001
$[\![A_{10} \otimes B_{10} \otimes B_{11}]\!]$	$A_{10} B_{10} B_{11}$	7.6109 ± 0.006
$[\![A_{10} \otimes B_{11} \otimes B_{11}]\!]$	$A_{10} B_{11}^2$	1.4776 ± 0.001
$[\![A_{10} \otimes B_{20} \otimes B_{20}]\!]$	$A_{10} B_{20}^2$	7.9886 ± 0.0005
$[\![A_{10} \otimes B_{20} \otimes B_{21}]\!]$	$A_{10} B_{20} B_{21}$	-20.0392 ± 0.0193
$[\![A_{10} \otimes B_{21} \otimes B_{21}]\!]$	$A_{10} B_{21}^2$	11.5841 ± 0.0072
$[\![A_{10} \otimes E_{10} \otimes E_{10}]\!]$	$\frac{1}{\sqrt{2}} A_{10} E_{100}^2 + \frac{1}{\sqrt{2}} A_{10} E_{101}^2$	-23.4919 ± 0.0013
$[\![A_{10} \otimes E_{10} \otimes E_{11}]\!]$	$\frac{1}{\sqrt{2}} A_{10} E_{100} E_{110} + \frac{1}{\sqrt{2}} A_{10} E_{101} E_{111}$	-11.1569 ± 0.0066
$[\![A_{10} \otimes E_{10} \otimes E_{12}]\!]$	$\frac{1}{\sqrt{2}} A_{10} E_{100} E_{120} + \frac{1}{\sqrt{2}} A_{10} E_{101} E_{121}$	16.6194 ± 0.0003
$[\![A_{10} \otimes E_{11} \otimes E_{11}]\!]$	$\frac{1}{\sqrt{2}} A_{10} E_{110}^2 + \frac{1}{\sqrt{2}} A_{10} E_{111}^2$	6.8044 ± 0.0048
$[\![A_{10} \otimes E_{11} \otimes E_{12}]\!]$	$\frac{1}{\sqrt{2}} A_{10} E_{110} E_{120} + \frac{1}{\sqrt{2}} A_{10} E_{111} E_{121}$	-20.2348 ± 0.0051
$[\![A_{10} \otimes E_{12} \otimes E_{12}]\!]$	$\frac{1}{\sqrt{2}} A_{10} E_{120}^2 + \frac{1}{\sqrt{2}} A_{10} E_{121}^2$	17.5137 ± 0.0025
$[\![A_{10} \otimes E_{20} \otimes E_{20}]\!]$	$\frac{1}{\sqrt{2}} A_{10} E_{200}^2 + \frac{1}{\sqrt{2}} A_{10} E_{201}^2$	-46.7134 ± 0.0039
$[\![A_{10} \otimes E_{20} \otimes E_{21}]\!]$	$\frac{1}{\sqrt{2}} A_{10} E_{200} E_{210} + \frac{1}{\sqrt{2}} A_{10} E_{201} E_{211}$	18.766 ± 0.0042
$[\![A_{10} \otimes E_{20} \otimes E_{22}]\!]$	$\frac{1}{\sqrt{2}} A_{10} E_{200} E_{220} + \frac{1}{\sqrt{2}} A_{10} E_{201} E_{221}$	1.7688 ± 0.0068
$[\![A_{10} \otimes E_{20} \otimes E_{23}]\!]$	$\frac{1}{\sqrt{2}} A_{10} E_{200} E_{230} + \frac{1}{\sqrt{2}} A_{10} E_{201} E_{231}$	-0.7308 ± 0.0135
$[\![A_{10} \otimes E_{21} \otimes E_{21}]\!]$	$\frac{1}{\sqrt{2}} A_{10} E_{210}^2 + \frac{1}{\sqrt{2}} A_{10} E_{211}^2$	7.9198 ± 0.0009
$[\![A_{10} \otimes E_{21} \otimes E_{22}]\!]$	$\frac{1}{\sqrt{2}} A_{10} E_{210} E_{220} + \frac{1}{\sqrt{2}} A_{10} E_{211} E_{221}$	-3.5322 ± 0.0024
$[\![A_{10} \otimes E_{21} \otimes E_{23}]\!]$	$\frac{1}{\sqrt{2}} A_{10} E_{210} E_{230} + \frac{1}{\sqrt{2}} A_{10} E_{211} E_{231}$	-25.9067 ± 0.0113
$[\![A_{10} \otimes E_{22} \otimes E_{22}]\!]$	$\frac{1}{\sqrt{2}} A_{10} E_{220}^2 + \frac{1}{\sqrt{2}} A_{10} E_{221}^2$	1.6653 ± 0.0058
$[\![A_{10} \otimes E_{22} \otimes E_{23}]\!]$	$\frac{1}{\sqrt{2}} A_{10} E_{220} E_{230} + \frac{1}{\sqrt{2}} A_{10} E_{221} E_{231}$	3.6802 ± 0.0058
$[\![A_{10} \otimes E_{23} \otimes E_{23}]\!]$	$\frac{1}{\sqrt{2}} A_{10} E_{230}^2 + \frac{1}{\sqrt{2}} A_{10} E_{231}^2$	11.9831 ± 0.0061
$[\![A_{11} \otimes A_{11} \otimes A_{11}]\!]$	A_{11}^3	-2.6852 ± 0.0004
$[\![A_{11} \otimes A_{20} \otimes A_{20}]\!]$	$A_{11} A_{20}^2$	-3.9409 ± 0.0293
$[\![A_{11} \otimes A_{20} \otimes A_{21}]\!]$	$A_{11} A_{20} A_{21}$	-1.2251 ± 0.0078

Sym. Prod.	Polynomial	Value (eV/Å^3)
$[\![A_{11} \otimes A_{21} \otimes A_{21}]\!]$	$A_{11}A_{21}^2$	2.0962 ± 0.0076
$[\![A_{11} \otimes B_{10} \otimes B_{10}]\!]$	$A_{11}B_{10}^2$	-3.9989 ± 0.0078
$[\![A_{11} \otimes B_{10} \otimes B_{11}]\!]$	$A_{11}B_{10}B_{11}$	-3.6388 ± 0.0009
$[\![A_{11} \otimes B_{11} \otimes B_{11}]\!]$	$A_{11}B_{11}^2$	1.5325 ± 0.0036
$[\![A_{11} \otimes B_{20} \otimes B_{20}]\!]$	$A_{11}B_{20}^2$	-14.9985 ± 0.0055
$[\![A_{11} \otimes B_{20} \otimes B_{21}]\!]$	$A_{11}B_{20}B_{21}$	15.9322 ± 0.0166
$[\![A_{11} \otimes B_{21} \otimes B_{21}]\!]$	$A_{11}B_{21}^2$	-12.1274 ± 0.0009
$[\![A_{11} \otimes E_{10} \otimes E_{10}]\!]$	$\frac{1}{\sqrt{2}}A_{11}E_{100}^2 + \frac{1}{\sqrt{2}}A_{11}E_{101}^2$	-6.5968 ± 0.0223
$[\![A_{11} \otimes E_{10} \otimes E_{11}]\!]$	$\frac{1}{\sqrt{2}}A_{11}E_{100}E_{110} + \frac{1}{\sqrt{2}}A_{11}E_{101}E_{111}$	16.6855 ± 0.0011
$[\![A_{11} \otimes E_{10} \otimes E_{12}]\!]$	$\frac{1}{\sqrt{2}}A_{11}E_{100}E_{120} + \frac{1}{\sqrt{2}}A_{11}E_{101}E_{121}$	-17.825 ± 0.0004
$[\![A_{11} \otimes E_{11} \otimes E_{11}]\!]$	$\frac{1}{\sqrt{2}}A_{11}E_{110}^2 + \frac{1}{\sqrt{2}}A_{11}E_{111}^2$	-2.247 ± 0.0043
$[\![A_{11} \otimes E_{11} \otimes E_{12}]\!]$	$\frac{1}{\sqrt{2}}A_{11}E_{110}E_{120} + \frac{1}{\sqrt{2}}A_{11}E_{111}E_{121}$	21.8085 ± 0.0036
$[\![A_{11} \otimes E_{12} \otimes E_{12}]\!]$	$\frac{1}{\sqrt{2}}A_{11}E_{120}^2 + \frac{1}{\sqrt{2}}A_{11}E_{121}^2$	-12.9633 ± 0.0072
$[\![A_{11} \otimes E_{20} \otimes E_{20}]\!]$	$\frac{1}{\sqrt{2}}A_{11}E_{200}^2 + \frac{1}{\sqrt{2}}A_{11}E_{201}^2$	0.439 ± 0.0138
$[\![A_{11} \otimes E_{20} \otimes E_{21}]\!]$	$\frac{1}{\sqrt{2}}A_{11}E_{200}E_{210} + \frac{1}{\sqrt{2}}A_{11}E_{201}E_{211}$	-2.5186 ± 0.0074
$[\![A_{11} \otimes E_{20} \otimes E_{22}]\!]$	$\frac{1}{\sqrt{2}}A_{11}E_{200}E_{220} + \frac{1}{\sqrt{2}}A_{11}E_{201}E_{221}$	-0.4642 ± 0.0102
$[\![A_{11} \otimes E_{20} \otimes E_{23}]\!]$	$\frac{1}{\sqrt{2}}A_{11}E_{200}E_{230} + \frac{1}{\sqrt{2}}A_{11}E_{201}E_{231}$	1.1713 ± 0.0048
$[\![A_{11} \otimes E_{21} \otimes E_{21}]\!]$	$\frac{1}{\sqrt{2}}A_{11}E_{210}^2 + \frac{1}{\sqrt{2}}A_{11}E_{211}^2$	-17.9266 ± 0.0099
$[\![A_{11} \otimes E_{21} \otimes E_{22}]\!]$	$\frac{1}{\sqrt{2}}A_{11}E_{210}E_{220} + \frac{1}{\sqrt{2}}A_{11}E_{211}E_{221}$	-1.1823 ± 0.0059
$[\![A_{11} \otimes E_{21} \otimes E_{23}]\!]$	$\frac{1}{\sqrt{2}}A_{11}E_{210}E_{230} + \frac{1}{\sqrt{2}}A_{11}E_{211}E_{231}$	25.3935 ± 0.0128
$[\![A_{11} \otimes E_{22} \otimes E_{22}]\!]$	$\frac{1}{\sqrt{2}}A_{11}E_{220}^2 + \frac{1}{\sqrt{2}}A_{11}E_{221}^2$	3.7491 ± 0.0087
$[\![A_{11} \otimes E_{22} \otimes E_{23}]\!]$	$\frac{1}{\sqrt{2}}A_{11}E_{220}E_{230} + \frac{1}{\sqrt{2}}A_{11}E_{221}E_{231}$	-3.9953 ± 0.0022
$[\![A_{11} \otimes E_{23} \otimes E_{23}]\!]$	$\frac{1}{\sqrt{2}}A_{11}E_{230}^2 + \frac{1}{\sqrt{2}}A_{11}E_{231}^2$	-12.1569 ± 0.0014
$[\![A_{20} \otimes B_{10} \otimes B_{20}]\!]$	$A_{20}B_{10}B_{20}$	5.4224 ± 0.0061
$[\![A_{20} \otimes B_{10} \otimes B_{21}]\!]$	$A_{20}B_{10}B_{21}$	1.0255 ± 0.0162
$[\![A_{20} \otimes B_{11} \otimes B_{20}]\!]$	$A_{20}B_{11}B_{20}$	1.9866 ± 0.0055
$[\![A_{20} \otimes B_{11} \otimes B_{21}]\!]$	$A_{20}B_{11}B_{21}$	-1.9135 ± 0.0083
$[\![A_{20} \otimes E_{10} \otimes E_{11}]\!]$	$\frac{1}{\sqrt{2}}A_{20}E_{100}E_{111} - \frac{1}{\sqrt{2}}A_{20}E_{101}E_{110}$	-0.1224 ± 0.013
$[\![A_{20} \otimes E_{10} \otimes E_{12}]\!]$	$\frac{1}{\sqrt{2}}A_{20}E_{100}E_{121} - \frac{1}{\sqrt{2}}A_{20}E_{101}E_{120}$	4.2435 ± 0.0071
$[\![A_{20} \otimes E_{11} \otimes E_{12}]\!]$	$\frac{1}{\sqrt{2}}A_{20}E_{110}E_{121} - \frac{1}{\sqrt{2}}A_{20}E_{111}E_{120}$	1.563 ± 0.0105
$[\![A_{20} \otimes E_{20} \otimes E_{21}]\!]$	$\frac{1}{\sqrt{2}}A_{20}E_{200}E_{211} - \frac{1}{\sqrt{2}}A_{20}E_{201}E_{210}$	5.5974 ± 0.0042
$[\![A_{20} \otimes E_{20} \otimes E_{22}]\!]$	$\frac{1}{\sqrt{2}}A_{20}E_{200}E_{221} - \frac{1}{\sqrt{2}}A_{20}E_{201}E_{220}$	4.1716 ± 0.0053
$[\![A_{20} \otimes E_{20} \otimes E_{23}]\!]$	$\frac{1}{\sqrt{2}}A_{20}E_{200}E_{231} - \frac{1}{\sqrt{2}}A_{20}E_{201}E_{230}$	8.2595 ± 0.0014
$[\![A_{20} \otimes E_{21} \otimes E_{22}]\!]$	$\frac{1}{\sqrt{2}}A_{20}E_{210}E_{221} - \frac{1}{\sqrt{2}}A_{20}E_{211}E_{220}$	-3.3333 ± 0.0225
$[\![A_{20} \otimes E_{21} \otimes E_{23}]\!]$	$\frac{1}{\sqrt{2}}A_{20}E_{210}E_{231} - \frac{1}{\sqrt{2}}A_{20}E_{211}E_{230}$	-2.9509 ± 0.0041
$[\![A_{20} \otimes E_{22} \otimes E_{23}]\!]$	$\frac{1}{\sqrt{2}}A_{20}E_{220}E_{231} - \frac{1}{\sqrt{2}}A_{20}E_{221}E_{230}$	-4.7424 ± 0.0079

Sym. Prod.	Polynomial	Value (eV/Å^3)
$[\![A_{21} \otimes B_{10} \otimes B_{20}]\!]$	$A_{21}B_{10}B_{20}$	0.3377 ± 0.0128
$[\![A_{21} \otimes B_{10} \otimes B_{21}]\!]$	$A_{21}B_{10}B_{21}$	-0.5143 ± 0.0054
$[\![A_{21} \otimes B_{11} \otimes B_{20}]\!]$	$A_{21}B_{11}B_{20}$	-0.4921 ± 0.0032
$[\![A_{21} \otimes B_{11} \otimes B_{21}]\!]$	$A_{21}B_{11}B_{21}$	8.4854 ± 0.0036
$[\![A_{21} \otimes E_{10} \otimes E_{11}]\!]$	$\frac{1}{\sqrt{2}}A_{21}E_{100}E_{111} - \frac{1}{\sqrt{2}}A_{21}E_{101}E_{110}$	7.9844 ± 0.001
$[\![A_{21} \otimes E_{10} \otimes E_{12}]\!]$	$\frac{1}{\sqrt{2}}A_{21}E_{100}E_{121} - \frac{1}{\sqrt{2}}A_{21}E_{101}E_{120}$	0.0319 ± 0.0115
$[\![A_{21} \otimes E_{11} \otimes E_{12}]\!]$	$\frac{1}{\sqrt{2}}A_{21}E_{110}E_{121} - \frac{1}{\sqrt{2}}A_{21}E_{111}E_{120}$	-14.0082 ± 0.0021
$[\![A_{21} \otimes E_{20} \otimes E_{21}]\!]$	$\frac{1}{\sqrt{2}}A_{21}E_{200}E_{211} - \frac{1}{\sqrt{2}}A_{21}E_{201}E_{210}$	5.5324 ± 0.0087
$[\![A_{21} \otimes E_{20} \otimes E_{22}]\!]$	$\frac{1}{\sqrt{2}}A_{21}E_{200}E_{221} - \frac{1}{\sqrt{2}}A_{21}E_{201}E_{220}$	0.5404 ± 0.0023
$[\![A_{21} \otimes E_{20} \otimes E_{23}]\!]$	$\frac{1}{\sqrt{2}}A_{21}E_{200}E_{231} - \frac{1}{\sqrt{2}}A_{21}E_{201}E_{230}$	-3.551 ± 0.0135
$[\![A_{21} \otimes E_{21} \otimes E_{22}]\!]$	$\frac{1}{\sqrt{2}}A_{21}E_{210}E_{221} - \frac{1}{\sqrt{2}}A_{21}E_{211}E_{220}$	1.8297 ± 0.0063
$[\![A_{21} \otimes E_{21} \otimes E_{23}]\!]$	$\frac{1}{\sqrt{2}}A_{21}E_{210}E_{231} - \frac{1}{\sqrt{2}}A_{21}E_{211}E_{230}$	-0.8133 ± 0.0102
$[\![A_{21} \otimes E_{22} \otimes E_{23}]\!]$	$\frac{1}{\sqrt{2}}A_{21}E_{220}E_{231} - \frac{1}{\sqrt{2}}A_{21}E_{221}E_{230}$	10.9279 ± 0.0081
$[\![B_{10} \otimes E_{10} \otimes E_{20}]\!]$	$\frac{1}{\sqrt{2}}E_{200}B_{10}E_{100} + \frac{1}{\sqrt{2}}E_{201}B_{10}E_{101}$	-90.0209 ± 0.0013
$[\![B_{10} \otimes E_{10} \otimes E_{21}]\!]$	$\frac{1}{\sqrt{2}}E_{210}B_{10}E_{100} + \frac{1}{\sqrt{2}}E_{211}B_{10}E_{101}$	28.4168 ± 0.0022
$[\![B_{10} \otimes E_{10} \otimes E_{22}]\!]$	$\frac{1}{\sqrt{2}}E_{220}B_{10}E_{100} + \frac{1}{\sqrt{2}}E_{221}B_{10}E_{101}$	2.2698 ± 0.0149
$[\![B_{10} \otimes E_{10} \otimes E_{23}]\!]$	$\frac{1}{\sqrt{2}}E_{230}B_{10}E_{100} + \frac{1}{\sqrt{2}}E_{231}B_{10}E_{101}$	0.1698 ± 0.0011
$[\![B_{10} \otimes E_{11} \otimes E_{20}]\!]$	$\frac{1}{\sqrt{2}}E_{200}B_{10}E_{110} + \frac{1}{\sqrt{2}}E_{201}B_{10}E_{111}$	1.2373 ± 0.0015
$[\![B_{10} \otimes E_{11} \otimes E_{21}]\!]$	$\frac{1}{\sqrt{2}}E_{210}B_{10}E_{110} + \frac{1}{\sqrt{2}}E_{211}B_{10}E_{111}$	2.3305 ± 0.0219
$[\![B_{10} \otimes E_{11} \otimes E_{22}]\!]$	$\frac{1}{\sqrt{2}}E_{220}B_{10}E_{110} + \frac{1}{\sqrt{2}}E_{221}B_{10}E_{111}$	-1.7447 ± 0.0052
$[\![B_{10} \otimes E_{11} \otimes E_{23}]\!]$	$\frac{1}{\sqrt{2}}E_{230}B_{10}E_{110} + \frac{1}{\sqrt{2}}E_{231}B_{10}E_{111}$	-5.6654 ± 0.0027
$[\![B_{10} \otimes E_{12} \otimes E_{20}]\!]$	$\frac{1}{\sqrt{2}}E_{200}B_{10}E_{120} + \frac{1}{\sqrt{2}}E_{201}B_{10}E_{121}$	1.6025 ± 0.004
$[\![B_{10} \otimes E_{12} \otimes E_{21}]\!]$	$\frac{1}{\sqrt{2}}E_{210}B_{10}E_{120} + \frac{1}{\sqrt{2}}E_{211}B_{10}E_{121}$	-1.6635 ± 0.0077
$[\![B_{10} \otimes E_{12} \otimes E_{22}]\!]$	$\frac{1}{\sqrt{2}}E_{220}B_{10}E_{120} + \frac{1}{\sqrt{2}}E_{221}B_{10}E_{121}$	4.0629 ± 0.0031
$[\![B_{10} \otimes E_{12} \otimes E_{23}]\!]$	$\frac{1}{\sqrt{2}}E_{230}B_{10}E_{120} + \frac{1}{\sqrt{2}}E_{231}B_{10}E_{121}$	8.7754 ± 0.0054
$[\![B_{11} \otimes E_{10} \otimes E_{20}]\!]$	$\frac{1}{\sqrt{2}}E_{200}B_{11}E_{100} + \frac{1}{\sqrt{2}}E_{201}B_{11}E_{101}$	6.1073 ± 0.0112
$[\![B_{11} \otimes E_{10} \otimes E_{21}]\!]$	$\frac{1}{\sqrt{2}}E_{210}B_{11}E_{100} + \frac{1}{\sqrt{2}}E_{211}B_{11}E_{101}$	-4.8614 ± 0.0097
$[\![B_{11} \otimes E_{10} \otimes E_{22}]\!]$	$\frac{1}{\sqrt{2}}E_{220}B_{11}E_{100} + \frac{1}{\sqrt{2}}E_{221}B_{11}E_{101}$	5.5236 ± 0.0035
$[\![B_{11} \otimes E_{10} \otimes E_{23}]\!]$	$\frac{1}{\sqrt{2}}E_{230}B_{11}E_{100} + \frac{1}{\sqrt{2}}E_{231}B_{11}E_{101}$	3.8501 ± 0.0113
$[\![B_{11} \otimes E_{11} \otimes E_{20}]\!]$	$\frac{1}{\sqrt{2}}E_{200}B_{11}E_{110} + \frac{1}{\sqrt{2}}E_{201}B_{11}E_{111}$	1.3569 ± 0.007
$[\![B_{11} \otimes E_{11} \otimes E_{21}]\!]$	$\frac{1}{\sqrt{2}}E_{210}B_{11}E_{110} + \frac{1}{\sqrt{2}}E_{211}B_{11}E_{111}$	1.2799 ± 0.0065
$[\![B_{11} \otimes E_{11} \otimes E_{22}]\!]$	$\frac{1}{\sqrt{2}}E_{220}B_{11}E_{110} + \frac{1}{\sqrt{2}}E_{221}B_{11}E_{111}$	6.4595 ± 0.0051
$[\![B_{11} \otimes E_{11} \otimes E_{23}]\!]$	$\frac{1}{\sqrt{2}}E_{230}B_{11}E_{110} + \frac{1}{\sqrt{2}}E_{231}B_{11}E_{111}$	-10.4598 ± 0.0022
$[\![B_{11} \otimes E_{12} \otimes E_{20}]\!]$	$\frac{1}{\sqrt{2}}E_{200}B_{11}E_{120} + \frac{1}{\sqrt{2}}E_{201}B_{11}E_{121}$	8.2456 ± 0.0039

Sym. Prod.	Polynomial	Value (eV/Å^3)
$[\![B_{11} \otimes E_{12} \otimes E_{21}]\!]$	$\frac{1}{\sqrt{2}} E_{210} B_{11} E_{120} + \frac{1}{\sqrt{2}} E_{211} B_{11} E_{121}$	2.85 ± 0.0107
$[\![B_{11} \otimes E_{12} \otimes E_{22}]\!]$	$\frac{1}{\sqrt{2}} E_{220} B_{11} E_{120} + \frac{1}{\sqrt{2}} E_{221} B_{11} E_{121}$	-6.8366 ± 0.003
$[\![B_{11} \otimes E_{12} \otimes E_{23}]\!]$	$\frac{1}{\sqrt{2}} E_{230} B_{11} E_{120} + \frac{1}{\sqrt{2}} E_{231} B_{11} E_{121}$	-6.538 ± 0.007
$[\![B_{20} \otimes E_{10} \otimes E_{20}]\!]$	$\frac{1}{\sqrt{2}} E_{201} B_{20} E_{100} - \frac{1}{\sqrt{2}} E_{200} B_{20} E_{101}$	-10.9852 ± 0.0021
$[\![B_{20} \otimes E_{10} \otimes E_{21}]\!]$	$\frac{1}{\sqrt{2}} E_{211} B_{20} E_{100} - \frac{1}{\sqrt{2}} E_{210} B_{20} E_{101}$	23.1815 ± 0.0034
$[\![B_{20} \otimes E_{10} \otimes E_{22}]\!]$	$\frac{1}{\sqrt{2}} E_{221} B_{20} E_{100} - \frac{1}{\sqrt{2}} E_{220} B_{20} E_{101}$	-2.9093 ± 0.0023
$[\![B_{20} \otimes E_{10} \otimes E_{23}]\!]$	$\frac{1}{\sqrt{2}} E_{231} B_{20} E_{100} - \frac{1}{\sqrt{2}} E_{230} B_{20} E_{101}$	-15.2864 ± 0.0255
$[\![B_{20} \otimes E_{11} \otimes E_{20}]\!]$	$\frac{1}{\sqrt{2}} E_{201} B_{20} E_{110} - \frac{1}{\sqrt{2}} E_{200} B_{20} E_{111}$	1.6541 ± 0.0002
$[\![B_{20} \otimes E_{11} \otimes E_{21}]\!]$	$\frac{1}{\sqrt{2}} E_{211} B_{20} E_{110} - \frac{1}{\sqrt{2}} E_{210} B_{20} E_{111}$	-26.7808 ± 0.0079
$[\![B_{20} \otimes E_{11} \otimes E_{22}]\!]$	$\frac{1}{\sqrt{2}} E_{221} B_{20} E_{110} - \frac{1}{\sqrt{2}} E_{220} B_{20} E_{111}$	-2.5478 ± 0.0059
$[\![B_{20} \otimes E_{11} \otimes E_{23}]\!]$	$\frac{1}{\sqrt{2}} E_{231} B_{20} E_{110} - \frac{1}{\sqrt{2}} E_{230} B_{20} E_{111}$	20.8351 ± 0.0055
$[\![B_{20} \otimes E_{12} \otimes E_{20}]\!]$	$\frac{1}{\sqrt{2}} E_{201} B_{20} E_{120} - \frac{1}{\sqrt{2}} E_{200} B_{20} E_{121}$	-2.1873 ± 0.0044
$[\![B_{20} \otimes E_{12} \otimes E_{21}]\!]$	$\frac{1}{\sqrt{2}} E_{211} B_{20} E_{120} - \frac{1}{\sqrt{2}} E_{210} B_{20} E_{121}$	28.8885 ± 0.0038
$[\![B_{20} \otimes E_{12} \otimes E_{22}]\!]$	$\frac{1}{\sqrt{2}} E_{221} B_{20} E_{120} - \frac{1}{\sqrt{2}} E_{220} B_{20} E_{121}$	-4.1005 ± 0.002
$[\![B_{20} \otimes E_{12} \otimes E_{23}]\!]$	$\frac{1}{\sqrt{2}} E_{231} B_{20} E_{120} - \frac{1}{\sqrt{2}} E_{230} B_{20} E_{121}$	-27.0139 ± 0.012
$[\![B_{21} \otimes E_{10} \otimes E_{20}]\!]$	$\frac{1}{\sqrt{2}} E_{201} B_{21} E_{100} - \frac{1}{\sqrt{2}} E_{200} B_{21} E_{101}$	6.6178 ± 0.0264
$[\![B_{21} \otimes E_{10} \otimes E_{21}]\!]$	$\frac{1}{\sqrt{2}} E_{211} B_{21} E_{100} - \frac{1}{\sqrt{2}} E_{210} B_{21} E_{101}$	-25.0065 ± 0.0079
$[\![B_{21} \otimes E_{10} \otimes E_{22}]\!]$	$\frac{1}{\sqrt{2}} E_{221} B_{21} E_{100} - \frac{1}{\sqrt{2}} E_{220} B_{21} E_{101}$	1.1548 ± 0.0011
$[\![B_{21} \otimes E_{10} \otimes E_{23}]\!]$	$\frac{1}{\sqrt{2}} E_{231} B_{21} E_{100} - \frac{1}{\sqrt{2}} E_{230} B_{21} E_{101}$	13.3326 ± 0.0082
$[\![B_{21} \otimes E_{11} \otimes E_{20}]\!]$	$\frac{1}{\sqrt{2}} E_{201} B_{21} E_{110} - \frac{1}{\sqrt{2}} E_{200} B_{21} E_{111}$	-4.5041 ± 0.0024
$[\![B_{21} \otimes E_{11} \otimes E_{21}]\!]$	$\frac{1}{\sqrt{2}} E_{211} B_{21} E_{110} - \frac{1}{\sqrt{2}} E_{210} B_{21} E_{111}$	13.4174 ± 0.0123
$[\![B_{21} \otimes E_{11} \otimes E_{22}]\!]$	$\frac{1}{\sqrt{2}} E_{221} B_{21} E_{110} - \frac{1}{\sqrt{2}} E_{220} B_{21} E_{111}$	5.9681 ± 0.0034
$[\![B_{21} \otimes E_{11} \otimes E_{23}]\!]$	$\frac{1}{\sqrt{2}} E_{231} B_{21} E_{110} - \frac{1}{\sqrt{2}} E_{230} B_{21} E_{111}$	-13.271 ± 0.0007
$[\![B_{21} \otimes E_{12} \otimes E_{20}]\!]$	$\frac{1}{\sqrt{2}} E_{201} B_{21} E_{120} - \frac{1}{\sqrt{2}} E_{200} B_{21} E_{121}$	-4.442 ± 0.0078
$[\![B_{21} \otimes E_{12} \otimes E_{21}]\!]$	$\frac{1}{\sqrt{2}} E_{211} B_{21} E_{120} - \frac{1}{\sqrt{2}} E_{210} B_{21} E_{121}$	-34.1876 ± 0.0234
$[\![B_{21} \otimes E_{12} \otimes E_{22}]\!]$	$\frac{1}{\sqrt{2}} E_{221} B_{21} E_{120} - \frac{1}{\sqrt{2}} E_{220} B_{21} E_{121}$	15.419 ± 0.0064
$[\![B_{21} \otimes E_{12} \otimes E_{23}]\!]$	$\frac{1}{\sqrt{2}} E_{231} B_{21} E_{120} - \frac{1}{\sqrt{2}} E_{230} B_{21} E_{121}$	26.5004 ± 0.0035
$[\![E_{10} \otimes E_{10} \otimes E_{20}]\!]$	$\frac{1}{\sqrt{6}} E_{201} E_{100}^2 + \frac{\sqrt{2}}{\sqrt{3}} E_{200} E_{100} E_{101} - \frac{1}{\sqrt{6}} E_{201} E_{101}^2$	43.2477 ± 0.0048
$[\![E_{10} \otimes E_{10} \otimes E_{21}]\!]$	$\frac{1}{\sqrt{6}} E_{211} E_{100}^2 + \frac{\sqrt{2}}{\sqrt{3}} E_{210} E_{100} E_{101} - \frac{1}{\sqrt{6}} E_{211} E_{101}^2$	-2.6876 ± 0.0022
$[\![E_{10} \otimes E_{10} \otimes E_{22}]\!]$	$\frac{1}{\sqrt{6}} E_{221} E_{100}^2 + \frac{\sqrt{2}}{\sqrt{3}} E_{220} E_{100} E_{101} - \frac{1}{\sqrt{6}} E_{221} E_{101}^2$	-2.9162 ± 0.0018
$[\![E_{10} \otimes E_{10} \otimes E_{23}]\!]$	$\frac{1}{\sqrt{6}} E_{231} E_{100}^2 + \frac{\sqrt{2}}{\sqrt{3}} E_{230} E_{100} E_{101} - \frac{1}{\sqrt{6}} E_{231} E_{101}^2$	-11.1784 ± 0.0174
$[\![E_{10} \otimes E_{11} \otimes E_{20}]\!]$	$\frac{1}{2} E_{201} E_{100} E_{110} + \frac{1}{2} E_{200} E_{100} E_{111} + \frac{1}{2} E_{200} E_{101} E_{110} - \frac{1}{2} E_{201} E_{101} E_{111}$	-0.8568 ± 0.0058

Sym. Prod.	Polynomial	Value (eV/Å^3)
$[\![E_{10} \otimes E_{11} \otimes E_{21}]\!]$	$\frac{1}{2}E_{211}E_{100}E_{110} + \frac{1}{2}E_{210}E_{100}E_{111} + \frac{1}{2}E_{210}E_{101}E_{110} - \frac{1}{2}E_{211}E_{101}E_{111}$	-16.2574 ± 0.0087
$[\![E_{10} \otimes E_{11} \otimes E_{22}]\!]$	$\frac{1}{2}E_{221}E_{100}E_{110} + \frac{1}{2}E_{220}E_{100}E_{111} + \frac{1}{2}E_{220}E_{101}E_{110} - \frac{1}{2}E_{221}E_{101}E_{111}$	1.6996 ± 0.0003
$[\![E_{10} \otimes E_{11} \otimes E_{23}]\!]$	$\frac{1}{2}E_{231}E_{100}E_{110} + \frac{1}{2}E_{230}E_{100}E_{111} + \frac{1}{2}E_{230}E_{101}E_{110} - \frac{1}{2}E_{231}E_{101}E_{111}$	9.0296 ± 0.0129
$[\![E_{10} \otimes E_{12} \otimes E_{20}]\!]$	$\frac{1}{2}E_{201}E_{100}E_{120} + \frac{1}{2}E_{200}E_{100}E_{121} + \frac{1}{2}E_{200}E_{101}E_{120} - \frac{1}{2}E_{201}E_{101}E_{121}$	3.9247 ± 0.0104
$[\![E_{10} \otimes E_{12} \otimes E_{21}]\!]$	$\frac{1}{2}E_{211}E_{100}E_{120} + \frac{1}{2}E_{210}E_{100}E_{121} + \frac{1}{2}E_{210}E_{101}E_{120} - \frac{1}{2}E_{211}E_{101}E_{121}$	21.8705 ± 0.0108
$[\![E_{10} \otimes E_{12} \otimes E_{22}]\!]$	$\frac{1}{2}E_{221}E_{100}E_{120} + \frac{1}{2}E_{220}E_{100}E_{121} + \frac{1}{2}E_{220}E_{101}E_{120} - \frac{1}{2}E_{221}E_{101}E_{121}$	-3.4913 ± 0.0035
$[\![E_{10} \otimes E_{12} \otimes E_{23}]\!]$	$\frac{1}{2}E_{231}E_{100}E_{120} + \frac{1}{2}E_{230}E_{100}E_{121} + \frac{1}{2}E_{230}E_{101}E_{120} - \frac{1}{2}E_{231}E_{101}E_{121}$	-20.9385 ± 0.0066
$[\![E_{11} \otimes E_{11} \otimes E_{20}]\!]$	$\frac{1}{\sqrt{6}}E_{201}E_{110}^2 + \frac{\sqrt{2}}{\sqrt{3}}E_{200}E_{110}E_{111} - \frac{1}{\sqrt{6}}E_{201}E_{111}^2$	2.5439 ± 0.001
$[\![E_{11} \otimes E_{11} \otimes E_{21}]\!]$	$\frac{1}{\sqrt{6}}E_{211}E_{110}^2 + \frac{\sqrt{2}}{\sqrt{3}}E_{210}E_{110}E_{111} - \frac{1}{\sqrt{6}}E_{211}E_{111}^2$	10.61 ± 0.0045
$[\![E_{11} \otimes E_{11} \otimes E_{22}]\!]$	$\frac{1}{\sqrt{6}}E_{221}E_{110}^2 + \frac{\sqrt{2}}{\sqrt{3}}E_{220}E_{110}E_{111} - \frac{1}{\sqrt{6}}E_{221}E_{111}^2$	-7.7942 ± 0.0005
$[\![E_{11} \otimes E_{11} \otimes E_{23}]\!]$	$\frac{1}{\sqrt{6}}E_{231}E_{110}^2 + \frac{\sqrt{2}}{\sqrt{3}}E_{230}E_{110}E_{111} - \frac{1}{\sqrt{6}}E_{231}E_{111}^2$	-7.3703 ± 0.0018
$[\![E_{11} \otimes E_{12} \otimes E_{20}]\!]$	$\frac{1}{2}E_{201}E_{110}E_{120} + \frac{1}{2}E_{200}E_{110}E_{121} + \frac{1}{2}E_{200}E_{111}E_{120} - \frac{1}{2}E_{201}E_{111}E_{121}$	-3.0516 ± 0.0009
$[\![E_{11} \otimes E_{12} \otimes E_{21}]\!]$	$\frac{1}{2}E_{211}E_{110}E_{120} + \frac{1}{2}E_{210}E_{110}E_{121} + \frac{1}{2}E_{210}E_{111}E_{120} - \frac{1}{2}E_{211}E_{111}E_{121}$	-15.2987 ± 0.0025
$[\![E_{11} \otimes E_{12} \otimes E_{22}]\!]$	$\frac{1}{2}E_{221}E_{110}E_{120} + \frac{1}{2}E_{220}E_{110}E_{121} + \frac{1}{2}E_{220}E_{111}E_{120} - \frac{1}{2}E_{221}E_{111}E_{121}$	5.9937 ± 0.007
$[\![E_{11} \otimes E_{12} \otimes E_{23}]\!]$	$\frac{1}{2}E_{231}E_{110}E_{120} + \frac{1}{2}E_{230}E_{110}E_{121} + \frac{1}{2}E_{230}E_{111}E_{120} - \frac{1}{2}E_{231}E_{111}E_{121}$	8.2274 ± 0.0077
$[\![E_{12} \otimes E_{12} \otimes E_{20}]\!]$	$\frac{1}{\sqrt{6}}E_{201}E_{120}^2 + \frac{\sqrt{2}}{\sqrt{3}}E_{200}E_{120}E_{121} - \frac{1}{\sqrt{6}}E_{201}E_{121}^2$	-2.0895 ± 0.0013
$[\![E_{12} \otimes E_{12} \otimes E_{21}]\!]$	$\frac{1}{\sqrt{6}}E_{211}E_{120}^2 + \frac{\sqrt{2}}{\sqrt{3}}E_{210}E_{120}E_{121} - \frac{1}{\sqrt{6}}E_{211}E_{121}^2$	16.897 ± 0.0094
$[\![E_{12} \otimes E_{12} \otimes E_{22}]\!]$	$\frac{1}{\sqrt{6}}E_{221}E_{120}^2 + \frac{\sqrt{2}}{\sqrt{3}}E_{220}E_{120}E_{121} - \frac{1}{\sqrt{6}}E_{221}E_{121}^2$	7.4968 ± 0.0087
$[\![E_{12} \otimes E_{12} \otimes E_{23}]\!]$	$\frac{1}{\sqrt{6}}E_{231}E_{120}^2 + \frac{\sqrt{2}}{\sqrt{3}}E_{230}E_{120}E_{121} - \frac{1}{\sqrt{6}}E_{231}E_{121}^2$	-26.6043 ± 0.0057
$[\![E_{20} \otimes E_{20} \otimes E_{20}]\!]$	$\frac{3}{\sqrt{10}}E_{200}^2E_{201} - \frac{1}{\sqrt{10}}E_{201}^3$	36.4031 ± 0.004
$[\![E_{20} \otimes E_{20} \otimes E_{21}]\!]$	$\frac{1}{\sqrt{6}}E_{200}^2E_{211} + \frac{\sqrt{2}}{\sqrt{3}}E_{200}E_{201}E_{210} - \frac{1}{\sqrt{6}}E_{201}^2E_{211}$	-19.1816 ± 0.0081
$[\![E_{20} \otimes E_{20} \otimes E_{22}]\!]$	$\frac{1}{\sqrt{6}}E_{200}^2E_{221} + \frac{\sqrt{2}}{\sqrt{3}}E_{200}E_{201}E_{220} - \frac{1}{\sqrt{6}}E_{201}^2E_{221}$	-0.8948 ± 0.0004
$[\![E_{20} \otimes E_{20} \otimes E_{23}]\!]$	$\frac{1}{\sqrt{6}}E_{200}^2E_{231} + \frac{\sqrt{2}}{\sqrt{3}}E_{200}E_{201}E_{230} - \frac{1}{\sqrt{6}}E_{201}^2E_{231}$	3.0891 ± 0.0161
$[\![E_{20} \otimes E_{21} \otimes E_{21}]\!]$	$\frac{\sqrt{2}}{\sqrt{3}}E_{200}E_{210}E_{211} + \frac{1}{\sqrt{6}}E_{201}E_{210}^2 - \frac{1}{\sqrt{6}}E_{201}E_{211}^2$	10.7765 ± 0.0031
$[\![E_{20} \otimes E_{21} \otimes E_{22}]\!]$	$\frac{1}{2}E_{200}E_{210}E_{221} + \frac{1}{2}E_{200}E_{211}E_{220} + \frac{1}{2}E_{201}E_{210}E_{220} - \frac{1}{2}E_{201}E_{211}E_{221}$	0.4224 ± 0.0031
$[\![E_{20} \otimes E_{21} \otimes E_{23}]\!]$	$\frac{1}{2}E_{200}E_{210}E_{231} + \frac{1}{2}E_{200}E_{211}E_{230} + \frac{1}{2}E_{201}E_{210}E_{230} - \frac{1}{2}E_{201}E_{211}E_{231}$	-1.1994 ± 0.011
$[\![E_{20} \otimes E_{22} \otimes E_{22}]\!]$	$\frac{\sqrt{2}}{\sqrt{3}}E_{200}E_{220}E_{221} + \frac{1}{\sqrt{6}}E_{201}E_{220}^2 - \frac{1}{\sqrt{6}}E_{201}E_{221}^2$	-1.77 ± 0.0023
$[\![E_{20} \otimes E_{22} \otimes E_{23}]\!]$	$\frac{1}{2}E_{200}E_{220}E_{231} + \frac{1}{2}E_{200}E_{221}E_{230} + \frac{1}{2}E_{201}E_{220}E_{230} - \frac{1}{2}E_{201}E_{221}E_{231}$	-4.7891 ± 0.0075
$[\![E_{20} \otimes E_{23} \otimes E_{23}]\!]$	$\frac{\sqrt{2}}{\sqrt{3}}E_{200}E_{230}E_{231} + \frac{1}{\sqrt{6}}E_{201}E_{230}^2 - \frac{1}{\sqrt{6}}E_{201}E_{231}^2$	-3.5307 ± 0.0016
$[\![E_{21} \otimes E_{21} \otimes E_{21}]\!]$	$\frac{3}{\sqrt{10}}E_{210}^2E_{211} - \frac{1}{\sqrt{10}}E_{211}^3$	-9.9204 ± 0.0043
$[\![E_{21} \otimes E_{21} \otimes E_{22}]\!]$	$\frac{1}{\sqrt{6}}E_{210}^2E_{221} + \frac{\sqrt{2}}{\sqrt{3}}E_{210}E_{211}E_{220} - \frac{1}{\sqrt{6}}E_{211}^2E_{221}$	2.7483 ± 0.0054
$[\![E_{21} \otimes E_{21} \otimes E_{23}]\!]$	$\frac{1}{\sqrt{6}}E_{210}^2E_{231} + \frac{\sqrt{2}}{\sqrt{3}}E_{210}E_{211}E_{230} - \frac{1}{\sqrt{6}}E_{211}^2E_{231}$	12.1823 ± 0.0367

Sym. Prod.	Polynomial	Value (eV/Å^3)
$[\![E_{21} \otimes E_{22} \otimes E_{22}]\!]$	$\frac{\sqrt{2}}{\sqrt{3}} E_{210}E_{220}E_{221} + \frac{1}{\sqrt{6}} E_{211}E_{220}^2 - \frac{1}{\sqrt{6}} E_{211}E_{221}^2$	$-3.01 \quad \pm 0.0047$
$[\![E_{21} \otimes E_{22} \otimes E_{23}]\!]$	$\frac{1}{2} E_{210}E_{220}E_{231} + \frac{1}{2} E_{210}E_{221}E_{230} + \frac{1}{2} E_{211}E_{220}E_{230} - \frac{1}{2} E_{211}E_{221}E_{231}$	-4.7959 ± 0.0078
$[\![E_{21} \otimes E_{23} \otimes E_{23}]\!]$	$\frac{\sqrt{2}}{\sqrt{3}} E_{210}E_{230}E_{231} + \frac{1}{\sqrt{6}} E_{211}E_{230}^2 - \frac{1}{\sqrt{6}} E_{211}E_{231}^2$	-11.7172 ± 0.0252
$[\![E_{22} \otimes E_{22} \otimes E_{22}]\!]$	$\frac{3}{\sqrt{10}} E_{220}^2E_{221} - \frac{1}{\sqrt{10}} E_{221}^3$	-0.4041 ± 0.0057
$[\![E_{22} \otimes E_{22} \otimes E_{23}]\!]$	$\frac{1}{\sqrt{6}} E_{220}^2E_{231} + \frac{\sqrt{2}}{\sqrt{3}} E_{220}E_{221}E_{230} - \frac{1}{\sqrt{6}} E_{221}^2E_{231}$	6.6931 ± 0.0064
$[\![E_{22} \otimes E_{23} \otimes E_{23}]\!]$	$\frac{\sqrt{2}}{\sqrt{3}} E_{220}E_{230}E_{231} + \frac{1}{\sqrt{6}} E_{221}E_{230}^2 - \frac{1}{\sqrt{6}} E_{221}E_{231}^2$	0.3958 ± 0.0034
$[\![E_{23} \otimes E_{23} \otimes E_{23}]\!]$	$\frac{3}{\sqrt{10}} E_{230}^2E_{231} - \frac{1}{\sqrt{10}} E_{231}^3$	4.9912 ± 0.0004

Table 7.6: Third-order mode coefficients for the double hexagon. When expanded in the provided basis, it constitutes a full Taylor expansion.

Sym. Prod.	Polynomial	Value (eV/Å^4)
$[\![A_1 \otimes A_1 \otimes A_1 \otimes A_1]\!]$	A_1^4	4.7601 ± 0.0043
$[\![A_1 \otimes A_1 \otimes A_2 \otimes A_2]\!]$	$A_1^2A_2^2$	$1.387 \quad \pm 0.016$
$[\![A_1 \otimes A_1 \otimes B_1 \otimes B_1]\!]$	$A_1^2B_1^2$	68.1573 ± 0.0296
$[\![A_1 \otimes A_1 \otimes B_2 \otimes B_2]\!]$	$A_1^2B_2^2$	-9.0902 ± 0.0046
$[\![A_1 \otimes A_1 \otimes E_1 \otimes E_1]\!]$	$\frac{1}{\sqrt{2}} A_1^2E_{10}^2 + \frac{1}{\sqrt{2}} A_1^2E_{11}^2$	39.7426 ± 0.0063
$[\![A_1 \otimes A_1 \otimes E_{20} \otimes E_{20}]\!]$	$\frac{1}{\sqrt{2}} A_1^2E_{200}^2 + \frac{1}{\sqrt{2}} A_1^2E_{201}^2$	74.9797 ± 0.004
$[\![A_1 \otimes A_1 \otimes E_{20} \otimes E_{21}]\!]$	$\frac{1}{\sqrt{2}} A_1^2E_{200}E_{210} + \frac{1}{\sqrt{2}} A_1^2E_{201}E_{211}$	-40.4034 ± 0.0237
$[\![A_1 \otimes A_1 \otimes E_{21} \otimes E_{21}]\!]$	$\frac{1}{\sqrt{2}} A_1^2E_{210}^2 + \frac{1}{\sqrt{2}} A_1^2E_{211}^2$	3.1299 ± 0.0026
$[\![A_1 \otimes A_2 \otimes B_1 \otimes B_2]\!]$	$A_1A_2B_1B_2$	6.1872 ± 0.0048
$[\![A_1 \otimes A_2 \otimes E_{20} \otimes E_{21}]\!]$	$\frac{1}{\sqrt{2}} A_1A_2E_{200}E_{211} - \frac{1}{\sqrt{2}} A_1A_2E_{201}E_{210}$	45.5439 ± 0.0032
$[\![A_1 \otimes B_1 \otimes E_1 \otimes E_{20}]\!]$	$\frac{1}{\sqrt{2}} A_1E_{200}B_1E_{10} + \frac{1}{\sqrt{2}} A_1E_{201}B_1E_{11}$	410.6974 ± 0.033
$[\![A_1 \otimes B_1 \otimes E_1 \otimes E_{21}]\!]$	$\frac{1}{\sqrt{2}} A_1E_{210}B_1E_{10} + \frac{1}{\sqrt{2}} A_1E_{211}B_1E_{11}$	-170.9959 ± 0.013
$[\![A_1 \otimes B_2 \otimes E_1 \otimes E_{20}]\!]$	$\frac{1}{\sqrt{2}} A_1E_{201}B_2E_{10} - \frac{1}{\sqrt{2}} A_1E_{200}B_2E_{11}$	99.9982 ± 0.0065
$[\![A_1 \otimes B_2 \otimes E_1 \otimes E_{21}]\!]$	$\frac{1}{\sqrt{2}} A_1E_{211}B_2E_{10} - \frac{1}{\sqrt{2}} A_1E_{210}B_2E_{11}$	-105.2989 ± 0.0114
$[\![A_1 \otimes E_1 \otimes E_1 \otimes E_{20}]\!]$	$\frac{1}{\sqrt{6}} A_1E_{201}E_{10}^2 + \frac{\sqrt{2}}{\sqrt{3}} A_1E_{200}E_{10}E_{11} - \frac{1}{\sqrt{6}} A_1E_{201}E_{11}^2$	-190.4262 ± 0.0207
$[\![A_1 \otimes E_1 \otimes E_1 \otimes E_{21}]\!]$	$\frac{1}{\sqrt{6}} A_1E_{211}E_{10}^2 + \frac{\sqrt{2}}{\sqrt{3}} A_1E_{210}E_{10}E_{11} - \frac{1}{\sqrt{6}} A_1E_{211}E_{11}^2$	-5.3516 ± 0.0111
$[\![A_1 \otimes E_{20} \otimes E_{20} \otimes E_{20}]\!]$	$\frac{3}{\sqrt{10}} A_1E_{200}^2E_{201} - \frac{1}{\sqrt{10}} A_1E_{201}^3$	-132.1719 ± 0.0141
$[\![A_1 \otimes E_{20} \otimes E_{20} \otimes E_{21}]\!]$	$\frac{1}{\sqrt{6}} A_1E_{200}^2E_{211} + \frac{\sqrt{2}}{\sqrt{3}} A_1E_{200}E_{201}E_{210} - \frac{1}{\sqrt{6}} A_1E_{201}^2E_{211}$	118.8596 ± 0.021
$[\![A_1 \otimes E_{20} \otimes E_{21} \otimes E_{21}]\!]$	$\frac{\sqrt{2}}{\sqrt{3}} A_1E_{200}E_{210}E_{211} + \frac{1}{\sqrt{6}} A_1E_{201}E_{210}^2 - \frac{1}{\sqrt{6}} A_1E_{201}E_{211}^2$	$-73.426 \quad \pm 0.0141$
$[\![A_1 \otimes E_{21} \otimes E_{21} \otimes E_{21}]\!]$	$\frac{3}{\sqrt{10}} A_1E_{210}^2E_{211} - \frac{1}{\sqrt{10}} A_1E_{211}^3$	19.4806 ± 0.0046
$[\![A_2 \otimes A_2 \otimes A_2 \otimes A_2]\!]$	A_2^4	-0.2665 ± 0.0339

Sym. Prod.	Polynomial	Value (eV/Å^4)
$[\![A_2 \otimes A_2 \otimes B_1 \otimes B_1]\!]$	$A_2^2 B_1^2$	-6.8396 ± 0.0547
$[\![A_2 \otimes A_2 \otimes B_2 \otimes B_2]\!]$	$A_2^2 B_2^2$	-3.4287 ± 0.0142
$[\![A_2 \otimes A_2 \otimes E_1 \otimes E_1]\!]$	$\frac{1}{\sqrt{2}} A_2^2 E_{10}^2 + \frac{1}{\sqrt{2}} A_2^2 E_{11}^2$	-11.1224 ± 0.0824
$[\![A_2 \otimes A_2 \otimes E_{20} \otimes E_{20}]\!]$	$\frac{1}{\sqrt{2}} A_2^2 E_{200}^2 + \frac{1}{\sqrt{2}} A_2^2 E_{201}^2$	-8.8378 ± 0.0346
$[\![A_2 \otimes A_2 \otimes E_{20} \otimes E_{21}]\!]$	$\frac{1}{\sqrt{2}} A_2^2 E_{200} E_{210} + \frac{1}{\sqrt{2}} A_2^2 E_{201} E_{211}$	-2.0766 ± 0.0149
$[\![A_2 \otimes A_2 \otimes E_{21} \otimes E_{21}]\!]$	$\frac{1}{\sqrt{2}} A_2^2 E_{210}^2 + \frac{1}{\sqrt{2}} A_2^2 E_{211}^2$	3.2794 ± 0.0399
$[\![A_2 \otimes B_1 \otimes E_1 \otimes E_{20}]\!]$	$\frac{1}{\sqrt{2}} A_2 E_{201} B_1 E_{10} - \frac{1}{\sqrt{2}} A_2 E_{200} B_1 E_{11}$	-75.0497 ± 0.097
$[\![A_2 \otimes B_1 \otimes E_1 \otimes E_{21}]\!]$	$\frac{1}{\sqrt{2}} A_2 E_{211} B_1 E_{10} - \frac{1}{\sqrt{2}} A_2 E_{210} B_1 E_{11}$	77.0028 ± 0.0156
$[\![A_2 \otimes B_2 \otimes E_1 \otimes E_{20}]\!]$	$\frac{1}{\sqrt{2}} A_2 E_{200} B_2 E_{10} + \frac{1}{\sqrt{2}} A_2 E_{201} B_2 E_{11}$	49.0276 ± 0.0137
$[\![A_2 \otimes B_2 \otimes E_1 \otimes E_{21}]\!]$	$\frac{1}{\sqrt{2}} A_2 E_{210} B_2 E_{10} + \frac{1}{\sqrt{2}} A_2 E_{211} B_2 E_{11}$	-29.6959 ± 0.0073
$[\![A_2 \otimes E_1 \otimes E_1 \otimes E_{20}]\!]$	$\frac{1}{\sqrt{6}} A_2 E_{200} E_{10}^2 - \frac{\sqrt{2}}{\sqrt{3}} A_2 E_{201} E_{10} E_{11} - \frac{1}{\sqrt{6}} A_2 E_{200} E_{11}^2$	59.2005 ± 0.0348
$[\![A_2 \otimes E_1 \otimes E_1 \otimes E_{21}]\!]$	$\frac{1}{\sqrt{6}} A_2 E_{210} E_{10}^2 - \frac{\sqrt{2}}{\sqrt{3}} A_2 E_{211} E_{10} E_{11} - \frac{1}{\sqrt{6}} A_2 E_{210} E_{11}^2$	2.8352 ± 0.0143
$[\![A_2 \otimes E_{20} \otimes E_{20} \otimes E_{20}]\!]$	$\frac{1}{\sqrt{10}} A_2 E_{200}^3 - \frac{3}{\sqrt{10}} A_2 E_{200} E_{201}^2$	-18.6718 ± 0.0076
$[\![A_2 \otimes E_{20} \otimes E_{20} \otimes E_{21}]\!]$	$\frac{1}{\sqrt{6}} A_2 E_{200}^2 E_{210} - \frac{\sqrt{2}}{\sqrt{3}} A_2 E_{200} E_{201} E_{211} - \frac{1}{\sqrt{6}} A_2 E_{201}^2 E_{210}$	57.7021 ± 0.0855
$[\![A_2 \otimes E_{20} \otimes E_{21} \otimes E_{21}]\!]$	$\frac{1}{\sqrt{6}} A_2 E_{200} E_{210}^2 - \frac{1}{\sqrt{6}} A_2 E_{200} E_{211}^2 - \frac{\sqrt{2}}{\sqrt{3}} A_2 E_{201} E_{210} E_{211}$	-35.1844 ± 0.0029
$[\![A_2 \otimes E_{21} \otimes E_{21} \otimes E_{21}]\!]$	$\frac{1}{\sqrt{10}} A_2 E_{210}^3 - \frac{3}{\sqrt{10}} A_2 E_{210} E_{211}^2$	13.348 ± 0.0095
$[\![B_1 \otimes B_1 \otimes B_1 \otimes B_1]\!]$	B_1^4	31.7046 ± 0.0104
$[\![B_1 \otimes B_1 \otimes B_2 \otimes B_2]\!]$	$B_1^2 B_2^2$	-34.9746 ± 0.0208
$[\![B_1 \otimes B_1 \otimes E_1 \otimes E_1]\!]$	$\frac{1}{\sqrt{2}} B_1^2 E_{10}^2 + \frac{1}{\sqrt{2}} B_1^2 E_{11}^2$	106.9487 ± 0.0228
$[\![B_1 \otimes B_1 \otimes E_{20} \otimes E_{20}]\!]$	$\frac{1}{\sqrt{2}} E_{200}^2 B_1^2 + \frac{1}{\sqrt{2}} E_{201}^2 B_1^2$	213.4746 ± 0.0184
$[\![B_1 \otimes B_1 \otimes E_{20} \otimes E_{21}]\!]$	$\frac{1}{\sqrt{2}} E_{200} E_{210} B_1^2 + \frac{1}{\sqrt{2}} E_{201} E_{211} B_1^2$	-91.7163 ± 0.0408
$[\![B_1 \otimes B_1 \otimes E_{21} \otimes E_{21}]\!]$	$\frac{1}{\sqrt{2}} E_{210}^2 B_1^2 + \frac{1}{\sqrt{2}} E_{211}^2 B_1^2$	-20.7257 ± 0.0102
$[\![B_1 \otimes B_2 \otimes E_{20} \otimes E_{21}]\!]$	$\frac{1}{\sqrt{2}} E_{200} E_{211} B_1 B_2 - \frac{1}{\sqrt{2}} E_{201} E_{210} B_1 B_2$	-127.4032 ± 0.0646
$[\![B_1 \otimes E_1 \otimes E_1 \otimes E_1]\!]$	$\frac{3}{\sqrt{10}} B_1 E_{10}^2 E_{11} - \frac{1}{\sqrt{10}} B_1 E_{11}^3$	-180.8014 ± 0.0292
$[\![B_1 \otimes E_1 \otimes E_{20} \otimes E_{20}]\!]$	$\frac{\sqrt{2}}{\sqrt{3}} E_{200} E_{201} B_1 E_{10} + \frac{1}{\sqrt{6}} E_{200}^2 B_1 E_{11} - \frac{1}{\sqrt{6}} E_{201}^2 B_1 E_{11}$	-352.8748 ± 0.0868
$[\![B_1 \otimes E_1 \otimes E_{20} \otimes E_{21}]\!]$	$\frac{1}{2} E_{200} E_{211} B_1 E_{10} + \frac{1}{2} E_{201} E_{210} B_1 E_{10} + \frac{1}{2} E_{200} E_{210} B_1 E_{11} - \frac{1}{2} E_{201} E_{211} B_1 E_{11}$	120.5995 ± 0.0313
$[\![B_1 \otimes E_1 \otimes E_{21} \otimes E_{21}]\!]$	$\frac{\sqrt{2}}{\sqrt{3}} E_{210} E_{211} B_1 E_{10} + \frac{1}{\sqrt{6}} E_{210}^2 B_1 E_{11} - \frac{1}{\sqrt{6}} E_{211}^2 B_1 E_{11}$	-35.7348 ± 0.0103
$[\![B_2 \otimes B_2 \otimes B_2 \otimes B_2]\!]$	B_2^4	-2.5794 ± 0.0019
$[\![B_2 \otimes B_2 \otimes E_1 \otimes E_1]\!]$	$\frac{1}{\sqrt{2}} B_2^2 E_{10}^2 + \frac{1}{\sqrt{2}} B_2^2 E_{11}^2$	-16.3963 ± 0.0192
$[\![B_2 \otimes B_2 \otimes E_{20} \otimes E_{20}]\!]$	$\frac{1}{\sqrt{2}} E_{200}^2 B_2^2 + \frac{1}{\sqrt{2}} E_{201}^2 B_2^2$	-52.7487 ± 0.0102
$[\![B_2 \otimes B_2 \otimes E_{20} \otimes E_{21}]\!]$	$\frac{1}{\sqrt{2}} E_{200} E_{210} B_2^2 + \frac{1}{\sqrt{2}} E_{201} E_{211} B_2^2$	27.0601 ± 0.0034
$[\![B_2 \otimes B_2 \otimes E_{21} \otimes E_{21}]\!]$	$\frac{1}{\sqrt{2}} E_{210}^2 B_2^2 + \frac{1}{\sqrt{2}} E_{211}^2 B_2^2$	-8.1474 ± 0.0147

Sym. Prod.	Polynomial	Value (eV/Å^4)
$[\![B_2 \otimes E_1 \otimes E_1 \otimes E_1]\!]$	$\frac{1}{\sqrt{10}} B_2 E_{10}^3 - \frac{3}{\sqrt{10}} B_2 E_{10} E_{11}^2$	-56.3908 ± 0.0157
$[\![B_2 \otimes E_1 \otimes E_{20} \otimes E_{20}]\!]$	$\frac{1}{\sqrt{6}} E_{200}^2 B_2 E_{10} - \frac{1}{\sqrt{6}} E_{201}^2 B_2 E_{10} - \frac{\sqrt{2}}{\sqrt{3}} E_{200} E_{201} B_2 E_{11}$	1.0953 ± 0.022
$[\![B_2 \otimes E_1 \otimes E_{20} \otimes E_{21}]\!]$	$\frac{1}{2} E_{200} E_{210} B_2 E_{10} - \frac{1}{2} E_{201} E_{211} B_2 E_{10} - \frac{1}{2} E_{200} E_{211} B_2 E_{11} - \frac{1}{2} E_{201} E_{210} B_2 E_{11}$	-79.5335 ± 0.0181
$[\![B_2 \otimes E_1 \otimes E_{21} \otimes E_{21}]\!]$	$\frac{1}{\sqrt{6}} E_{210}^2 B_2 E_{10} - \frac{1}{\sqrt{6}} E_{211}^2 B_2 E_{10} - \frac{\sqrt{2}}{\sqrt{3}} E_{210} E_{211} B_2 E_{11}$	33.8153 ± 0.0049
$[\![E_1 \otimes E_1 \otimes E_1 \otimes E_1]\!]$	$\frac{1}{\sqrt{6}} E_{10}^4 + \frac{\sqrt{2}}{\sqrt{3}} E_{10}^2 E_{11}^2 + \frac{1}{\sqrt{6}} E_{11}^4$	20.0229 ± 0.0011
$[\![E_1 \otimes E_1 \otimes E_{20} \otimes E_{20}]\!]$	$\frac{1}{2} E_{200}^2 E_{10}^2 + \frac{1}{6} E_{201}^2 E_{10}^2 + \frac{2}{3} E_{200} E_{201} E_{10} E_{11} + \frac{1}{6} E_{200}^2 E_{11}^2 + \frac{1}{2} E_{201}^2 E_{11}^2$	215.9695 ± 0.1077
$[\![E_1 \otimes E_1 \otimes E_{20} \otimes E_{20}]\!]$	$\frac{1}{\sqrt{6}} E_{201}^2 E_{10}^2 - \frac{\sqrt{2}}{\sqrt{3}} E_{200} E_{201} E_{10} E_{11} + \frac{1}{\sqrt{6}} E_{200}^2 E_{11}^2$	-57.8836 ± 0.0587
$[\![E_1 \otimes E_1 \otimes E_{20} \otimes E_{21}]\!]$	$\frac{3}{\sqrt{28}} E_{200} E_{210} E_{10}^2 + \frac{1}{\sqrt{28}} E_{201} E_{211} E_{10}^2 + \frac{1}{\sqrt{7}} E_{200} E_{211} E_{10} E_{11} + \frac{1}{\sqrt{7}} E_{201} E_{210} E_{10} E_{11} + \frac{1}{\sqrt{28}} E_{200} E_{210} E_{11}^2 + \frac{3}{\sqrt{28}} E_{201} E_{211} E_{11}^2$	-143.6045 ± 0.0017
$[\![E_1 \otimes E_1 \otimes E_{20} \otimes E_{21}]\!]$	$\frac{1}{2} E_{201} E_{211} E_{10}^2 - \frac{1}{2} E_{200} E_{211} E_{10} E_{11} - \frac{1}{2} E_{201} E_{210} E_{10} E_{11} + \frac{1}{2} E_{200} E_{210} E_{11}^2$	112.1211 ± 0.0197
$[\![E_1 \otimes E_1 \otimes E_{21} \otimes E_{21}]\!]$	$\frac{1}{2} E_{210}^2 E_{10}^2 + \frac{1}{6} E_{211}^2 E_{10}^2 + \frac{2}{3} E_{210} E_{211} E_{10} E_{11} + \frac{1}{6} E_{210}^2 E_{11}^2 + \frac{1}{2} E_{211}^2 E_{11}^2$	15.8049 ± 0.0199
$[\![E_1 \otimes E_1 \otimes E_{21} \otimes E_{21}]\!]$	$\frac{1}{\sqrt{6}} E_{211}^2 E_{10}^2 - \frac{\sqrt{2}}{\sqrt{3}} E_{210} E_{211} E_{10} E_{11} + \frac{1}{\sqrt{6}} E_{210}^2 E_{11}^2$	-78.2174 ± 0.0216
$[\![E_{20} \otimes E_{20} \otimes E_{20} \otimes E_{20}]\!]$	$\frac{1}{\sqrt{6}} E_{200}^4 + \frac{\sqrt{2}}{\sqrt{3}} E_{200}^2 E_{201}^2 + \frac{1}{\sqrt{6}} E_{201}^4$	62.3753 ± 0.0102
$[\![E_{20} \otimes E_{20} \otimes E_{20} \otimes E_{21}]\!]$	$\frac{1}{2} E_{200}^3 E_{210} + \frac{1}{2} E_{200}^2 E_{201} E_{211} + \frac{1}{2} E_{200} E_{201}^2 E_{210} + \frac{1}{2} E_{201}^3 E_{211}$	-47.7797 ± 0.002
$[\![E_{20} \otimes E_{20} \otimes E_{21} \otimes E_{21}]\!]$	$\frac{1}{2} E_{200}^2 E_{210}^2 + \frac{1}{6} E_{200}^2 E_{211}^2 + \frac{2}{3} E_{200} E_{201} E_{210} E_{211} + \frac{1}{6} E_{201}^2 E_{210}^2 + \frac{1}{2} E_{201}^2 E_{211}^2$	-9.482 ± 0.0245
$[\![E_{20} \otimes E_{20} \otimes E_{21} \otimes E_{21}]\!]$	$\frac{1}{\sqrt{6}} E_{200}^2 E_{211}^2 - \frac{\sqrt{2}}{\sqrt{3}} E_{200} E_{201} E_{210} E_{211} + \frac{1}{\sqrt{6}} E_{201}^2 E_{210}^2$	-43.3499 ± 0.0203
$[\![E_{20} \otimes E_{21} \otimes E_{21} \otimes E_{21}]\!]$	$\frac{1}{2} E_{200} E_{210}^3 + \frac{1}{2} E_{200} E_{210} E_{211}^2 + \frac{1}{2} E_{201} E_{210}^2 E_{211} + \frac{1}{2} E_{201} E_{211}^3$	17.1415 ± 0.004
$[\![E_{21} \otimes E_{21} \otimes E_{21} \otimes E_{21}]\!]$	$\frac{1}{\sqrt{6}} E_{210}^4 + \frac{\sqrt{2}}{\sqrt{3}} E_{210}^2 E_{211}^2 + \frac{1}{\sqrt{6}} E_{211}^4$	-4.3945 ± 0.004

Table 7.7: Fourth-order mode coefficients for the hexagon. When expanded in the provided basis, it constitutes a full Taylor expansion.

Sym. Prod.	Polynomial	Value (eV/Å^5)
$[\![A_1 \otimes A_1 \otimes A_1 \otimes A_1 \otimes A_1]\!]$	A_1^5	-0.241 ± 0.4139
$[\![A_1 \otimes A_1 \otimes A_1 \otimes A_2 \otimes A_2]\!]$	$A_1^3 A_2^2$	14.7051 ± 0.8301
$[\![A_1 \otimes A_1 \otimes A_1 \otimes B_1 \otimes B_1]\!]$	$A_1^3 B_1^2$	-41.2798 ± 2.9657
$[\![A_1 \otimes A_1 \otimes A_1 \otimes B_2 \otimes B_2]\!]$	$A_1^3 B_2^2$	14.5041 ± 0.3865
$[\![A_1 \otimes A_1 \otimes A_1 \otimes E_1 \otimes E_1]\!]$	$\frac{1}{\sqrt{2}} A_1^3 E_{10}^2 + \frac{1}{\sqrt{2}} A_1^3 E_{11}^2$	-21.2799 ± 0.2063
$[\![A_1 \otimes A_1 \otimes A_1 \otimes E_{20} \otimes E_{20}]\!]$	$\frac{1}{\sqrt{2}} A_1^3 E_{200}^2 + \frac{1}{\sqrt{2}} A_1^3 E_{201}^2$	-43.2479 ± 0.6774
$[\![A_1 \otimes A_1 \otimes A_1 \otimes E_{20} \otimes E_{21}]\!]$	$\frac{1}{\sqrt{2}} A_1^3 E_{200} E_{210} + \frac{1}{\sqrt{2}} A_1^3 E_{201} E_{211}$	16.1848 ± 0.3468
$[\![A_1 \otimes A_1 \otimes A_1 \otimes E_{21} \otimes E_{21}]\!]$	$\frac{1}{\sqrt{2}} A_1^3 E_{210}^2 + \frac{1}{\sqrt{2}} A_1^3 E_{211}^2$	-2.1881 ± 0.2055
$[\![A_1 \otimes A_1 \otimes A_2 \otimes B_1 \otimes B_2]\!]$	$A_1^2 A_2 B_1 B_2$	-51.7823 ± 2.1242
$[\![A_1 \otimes A_1 \otimes A_2 \otimes E_{20} \otimes E_{21}]\!]$	$\frac{1}{\sqrt{2}} A_1^2 A_2 E_{200} E_{211} - \frac{1}{\sqrt{2}} A_1^2 A_2 E_{201} E_{210}$	-63.748 ± 2.361

Sym. Prod.	Polynomial	Value (eV/Å^5)
$[\![A_1 \otimes A_1 \otimes B_1 \otimes E_1 \otimes E_{20}]\!]$	$\frac{1}{\sqrt{2}} A_1^2 E_{200} B_1 E_{10} + \frac{1}{\sqrt{2}} A_1^2 E_{201} B_1 E_{11}$	-444.5141 ± 0.0819
$[\![A_1 \otimes A_1 \otimes B_1 \otimes E_1 \otimes E_{21}]\!]$	$\frac{1}{\sqrt{2}} A_1^2 E_{210} B_1 E_{10} + \frac{1}{\sqrt{2}} A_1^2 E_{211} B_1 E_{11}$	210.4021 ± 0.1614
$[\![A_1 \otimes A_1 \otimes B_2 \otimes E_1 \otimes E_{20}]\!]$	$\frac{1}{\sqrt{2}} A_1^2 E_{201} B_2 E_{10} - \frac{1}{\sqrt{2}} A_1^2 E_{200} B_2 E_{11}$	-117.8629 ± 0.5415
$[\![A_1 \otimes A_1 \otimes B_2 \otimes E_1 \otimes E_{21}]\!]$	$\frac{1}{\sqrt{2}} A_1^2 E_{211} B_2 E_{10} - \frac{1}{\sqrt{2}} A_1^2 E_{210} B_2 E_{11}$	93.3863 ± 0.7898
$[\![A_1 \otimes A_1 \otimes E_1 \otimes E_1 \otimes E_{20}]\!]$	$\frac{1}{\sqrt{6}} A_1^2 E_{201} E_{10}^2 + \frac{\sqrt{2}}{\sqrt{3}} A_1^2 E_{200} E_{10} E_{11} - \frac{1}{\sqrt{6}} A_1^2 E_{201} E_{11}^2$	169.0053 ± 1.3098
$[\![A_1 \otimes A_1 \otimes E_1 \otimes E_1 \otimes E_{21}]\!]$	$\frac{1}{\sqrt{6}} A_1^2 E_{211} E_{10}^2 + \frac{\sqrt{2}}{\sqrt{3}} A_1^2 E_{210} E_{10} E_{11} - \frac{1}{\sqrt{6}} A_1^2 E_{211} E_{11}^2$	26.1847 ± 1.2647
$[\![A_1 \otimes A_1 \otimes E_{20} \otimes E_{20} \otimes E_{20}]\!]$	$\frac{3}{\sqrt{10}} A_1^2 E_{200}^2 E_{201} - \frac{1}{\sqrt{10}} A_1^2 E_{201}^3$	135.1636 ± 1.4745
$[\![A_1 \otimes A_1 \otimes E_{20} \otimes E_{20} \otimes E_{21}]\!]$	$\frac{1}{\sqrt{6}} A_1^2 E_{200}^2 E_{211} + \frac{\sqrt{2}}{\sqrt{3}} A_1^2 E_{200} E_{201} E_{210} - \frac{1}{\sqrt{6}} A_1^2 E_{201}^2 E_{211}$	-130.3353 ± 0.8417
$[\![A_1 \otimes A_1 \otimes E_{20} \otimes E_{21} \otimes E_{21}]\!]$	$\frac{\sqrt{2}}{\sqrt{3}} A_1^2 E_{200} E_{210} E_{211} + \frac{1}{\sqrt{6}} A_1^2 E_{201} E_{210}^2 - \frac{1}{\sqrt{6}} A_1^2 E_{201} E_{211}^2$	94.599 ± 2.7329
$[\![A_1 \otimes A_1 \otimes E_{21} \otimes E_{21} \otimes E_{21}]\!]$	$\frac{3}{\sqrt{10}} A_1^2 E_{210}^2 E_{211} - \frac{1}{\sqrt{10}} A_1^2 E_{211}^3$	-27.525 ± 0.063
$[\![A_1 \otimes A_2 \otimes A_2 \otimes A_2 \otimes A_2]\!]$	$A_1 A_2^4$	5.1565 ± 0.9244
$[\![A_1 \otimes A_2 \otimes A_2 \otimes B_1 \otimes B_1]\!]$	$A_1 A_2^2 B_1^2$	12.1496 ± 4.446
$[\![A_1 \otimes A_2 \otimes A_2 \otimes B_2 \otimes B_2]\!]$	$A_1 A_2^2 B_2^2$	-1.2486 ± 1.3594
$[\![A_1 \otimes A_2 \otimes A_2 \otimes E_1 \otimes E_1]\!]$	$\frac{1}{\sqrt{2}} A_1 A_2^2 E_{10}^2 + \frac{1}{\sqrt{2}} A_1 A_2^2 E_{11}^2$	15.6756 ± 2.7976
$[\![A_1 \otimes A_2 \otimes A_2 \otimes E_{20} \otimes E_{20}]\!]$	$\frac{1}{\sqrt{2}} A_1 A_2^2 E_{200}^2 + \frac{1}{\sqrt{2}} A_1 A_2^2 E_{201}^2$	18.5294 ± 1.2038
$[\![A_1 \otimes A_2 \otimes A_2 \otimes E_{20} \otimes E_{21}]\!]$	$\frac{1}{\sqrt{2}} A_1 A_2^2 E_{200} E_{210} + \frac{1}{\sqrt{2}} A_1 A_2^2 E_{201} E_{211}$	-16.0008 ± 4.0144
$[\![A_1 \otimes A_2 \otimes A_2 \otimes E_{21} \otimes E_{21}]\!]$	$\frac{1}{\sqrt{2}} A_1 A_2^2 E_{210}^2 + \frac{1}{\sqrt{2}} A_1 A_2^2 E_{211}^2$	-11.7768 ± 1.344
$[\![A_1 \otimes A_2 \otimes B_1 \otimes E_1 \otimes E_{20}]\!]$	$\frac{1}{\sqrt{2}} A_1 A_2 E_{201} B_1 E_{10} - \frac{1}{\sqrt{2}} A_1 A_2 E_{200} B_1 E_{11}$	230.0386 ± 12.2397
$[\![A_1 \otimes A_2 \otimes B_1 \otimes E_1 \otimes E_{21}]\!]$	$\frac{1}{\sqrt{2}} A_1 A_2 E_{211} B_1 E_{10} - \frac{1}{\sqrt{2}} A_1 A_2 E_{210} B_1 E_{11}$	-201.2566 ± 5.1647
$[\![A_1 \otimes A_2 \otimes B_2 \otimes E_1 \otimes E_{20}]\!]$	$\frac{1}{\sqrt{2}} A_1 A_2 E_{200} B_2 E_{10} + \frac{1}{\sqrt{2}} A_1 A_2 E_{201} B_2 E_{11}$	-211.3226 ± 0.6149
$[\![A_1 \otimes A_2 \otimes B_2 \otimes E_1 \otimes E_{21}]\!]$	$\frac{1}{\sqrt{2}} A_1 A_2 E_{210} B_2 E_{10} + \frac{1}{\sqrt{2}} A_1 A_2 E_{211} B_2 E_{11}$	152.3057 ± 0.2136
$[\![A_1 \otimes A_2 \otimes E_1 \otimes E_1 \otimes E_{20}]\!]$	$\frac{1}{\sqrt{6}} A_1 A_2 E_{200} E_{10}^2 - \frac{\sqrt{2}}{\sqrt{3}} A_1 A_2 E_{201} E_{10} E_{11} - \frac{1}{\sqrt{6}} A_1 A_2 E_{200} E_{11}^2$	-143.6468 ± 0.0903
$[\![A_1 \otimes A_2 \otimes E_1 \otimes E_1 \otimes E_{21}]\!]$	$\frac{1}{\sqrt{6}} A_1 A_2 E_{210} E_{10}^2 - \frac{\sqrt{2}}{\sqrt{3}} A_1 A_2 E_{211} E_{10} E_{11} - \frac{1}{\sqrt{6}} A_1 A_2 E_{210} E_{11}^2$	-67.2121 ± 0.4605
$[\![A_1 \otimes A_2 \otimes E_{20} \otimes E_{20} \otimes E_{20}]\!]$	$\frac{1}{\sqrt{10}} A_1 A_2 E_{200}^3 - \frac{3}{\sqrt{10}} A_1 A_2 E_{200} E_{201}^2$	33.1042 ± 1.2928
$[\![A_1 \otimes A_2 \otimes E_{20} \otimes E_{20} \otimes E_{21}]\!]$	$\frac{1}{\sqrt{6}} A_1 A_2 E_{200}^2 E_{210} - \frac{\sqrt{2}}{\sqrt{3}} A_1 A_2 E_{200} E_{201} E_{211} - \frac{1}{\sqrt{6}} A_1 A_2 E_{201}^2 E_{210}$	-98.2672 ± 2.8492
$[\![A_1 \otimes A_2 \otimes E_{20} \otimes E_{21} \otimes E_{21}]\!]$	$\frac{1}{\sqrt{6}} A_1 A_2 E_{200} E_{210}^2 - \frac{1}{\sqrt{6}} A_1 A_2 E_{200} E_{211}^2 - \frac{\sqrt{2}}{\sqrt{3}} A_1 A_2 E_{201} E_{210} E_{211}$	68.2071 ± 1.7636
$[\![A_1 \otimes A_2 \otimes E_{21} \otimes E_{21} \otimes E_{21}]\!]$	$\frac{1}{\sqrt{10}} A_1 A_2 E_{210}^3 - \frac{3}{\sqrt{10}} A_1 A_2 E_{210} E_{211}^2$	-38.5307 ± 1.0642
$[\![A_1 \otimes B_1 \otimes B_1 \otimes B_1 \otimes B_1]\!]$	$A_1 B_1^4$	-79.5381 ± 2.7287
$[\![A_1 \otimes B_1 \otimes B_1 \otimes B_2 \otimes B_2]\!]$	$A_1 B_1^2 B_2^2$	88.8282 ± 2.1781
$[\![A_1 \otimes B_1 \otimes B_1 \otimes E_1 \otimes E_1]\!]$	$\frac{1}{\sqrt{2}} A_1 B_1^2 E_{10}^2 + \frac{1}{\sqrt{2}} A_1 B_1^2 E_{11}^2$	-199.6491 ± 4.7623
$[\![A_1 \otimes B_1 \otimes B_1 \otimes E_{20} \otimes E_{20}]\!]$	$\frac{1}{\sqrt{2}} A_1 E_{200}^2 B_1^2 + \frac{1}{\sqrt{2}} A_1 E_{201}^2 B_1^2$	-458.6065 ± 1.845
$[\![A_1 \otimes B_1 \otimes B_1 \otimes E_{20} \otimes E_{21}]\!]$	$\frac{1}{\sqrt{2}} A_1 E_{200} E_{210} B_1^2 + \frac{1}{\sqrt{2}} A_1 E_{201} E_{211} B_1^2$	243.9344 ± 2.0466
$[\![A_1 \otimes B_1 \otimes B_1 \otimes E_{21} \otimes E_{21}]\!]$	$\frac{1}{\sqrt{2}} A_1 E_{210}^2 B_1^2 + \frac{1}{\sqrt{2}} A_1 E_{211}^2 B_1^2$	26.3823 ± 3.4129

Sym. Prod.	Polynomial	Value (eV/Å^5)
$[\![A_1 \otimes B_1 \otimes B_2 \otimes E_{20} \otimes E_{21}]\!]$	$\frac{1}{\sqrt{2}} A_1 E_{200} E_{211} B_1 B_2 - \frac{1}{\sqrt{2}} A_1 E_{201} E_{210} B_1 B_2$	319.7559 ± 0.4885
$[\![A_1 \otimes B_1 \otimes E_1 \otimes E_1 \otimes E_1]\!]$	$\frac{3}{\sqrt{10}} A_1 B_1 E_{10}^2 E_{11} - \frac{1}{\sqrt{10}} A_1 B_1 E_{11}^3$	365.3509 ± 0.2296
$[\![A_1 \otimes B_1 \otimes E_1 \otimes E_{20} \otimes E_{20}]\!]$	$\frac{\sqrt{2}}{\sqrt{3}} A_1 E_{200} E_{201} B_1 E_{10} + \frac{1}{\sqrt{6}} A_1 E_{200}^2 B_1 E_{11} - \frac{1}{\sqrt{6}} A_1 E_{201}^2 B_1 E_{11}$	684.4644 ± 3.464
$[\![A_1 \otimes B_1 \otimes E_1 \otimes E_{20} \otimes E_{21}]\!]$	$\frac{1}{2} A_1 E_{200} E_{211} B_1 E_{10} + \frac{1}{2} A_1 E_{201} E_{210} B_1 E_{10} + \frac{1}{2} A_1 E_{200} E_{210} B_1 E_{11} - \frac{1}{2} A_1 E_{201} E_{211} B_1 E_{11}$	−219.6879 ± 2.8887
$[\![A_1 \otimes B_1 \otimes E_1 \otimes E_{21} \otimes E_{21}]\!]$	$\frac{\sqrt{2}}{\sqrt{3}} A_1 E_{210} E_{211} B_1 E_{10} + \frac{1}{\sqrt{6}} A_1 E_{210}^2 B_1 E_{11} - \frac{1}{\sqrt{6}} A_1 E_{211}^2 B_1 E_{11}$	104.3304 ± 0.9589
$[\![A_1 \otimes B_2 \otimes B_2 \otimes B_2 \otimes B_2]\!]$	$A_1 B_2^4$	4.103 ± 0.0183
$[\![A_1 \otimes B_2 \otimes B_2 \otimes E_1 \otimes E_1]\!]$	$\frac{1}{\sqrt{2}} A_1 B_2^2 E_{10}^2 + \frac{1}{\sqrt{2}} A_1 B_2^2 E_{11}^2$	24.316 ± 0.3569
$[\![A_1 \otimes B_2 \otimes B_2 \otimes E_{20} \otimes E_{20}]\!]$	$\frac{1}{\sqrt{2}} A_1 E_{200}^2 B_2^2 + \frac{1}{\sqrt{2}} A_1 E_{201}^2 B_2^2$	73.5707 ± 1.5351
$[\![A_1 \otimes B_2 \otimes B_2 \otimes E_{20} \otimes E_{21}]\!]$	$\frac{1}{\sqrt{2}} A_1 E_{200} E_{210} B_2^2 + \frac{1}{\sqrt{2}} A_1 E_{201} E_{211} B_2^2$	−14.522 ± 0.7979
$[\![A_1 \otimes B_2 \otimes B_2 \otimes E_{21} \otimes E_{21}]\!]$	$\frac{1}{\sqrt{2}} A_1 E_{210}^2 B_2^2 + \frac{1}{\sqrt{2}} A_1 E_{211}^2 B_2^2$	−6.8806 ± 0.4117
$[\![A_1 \otimes B_2 \otimes E_1 \otimes E_1 \otimes E_1]\!]$	$\frac{1}{\sqrt{10}} A_1 B_2 E_{10}^3 - \frac{3}{\sqrt{10}} A_1 B_2 E_{10} E_{11}^2$	186.468 ± 2.1322
$[\![A_1 \otimes B_2 \otimes E_1 \otimes E_{20} \otimes E_{20}]\!]$	$\frac{1}{\sqrt{6}} A_1 E_{200}^2 B_2 E_{10} - \frac{1}{\sqrt{6}} A_1 E_{201}^2 B_2 E_{10} - \frac{\sqrt{2}}{\sqrt{3}} A_1 E_{200} E_{201} B_2 E_{11}$	16.686 ± 1.7983
$[\![A_1 \otimes B_2 \otimes E_1 \otimes E_{20} \otimes E_{21}]\!]$	$\frac{1}{2} A_1 E_{200} E_{210} B_2 E_{10} - \frac{1}{2} A_1 E_{201} E_{211} B_2 E_{10} - \frac{1}{2} A_1 E_{200} E_{211} B_2 E_{11} - \frac{1}{2} A_1 E_{201} E_{210} B_2 E_{11}$	182.9759 ± 4.5375
$[\![A_1 \otimes B_2 \otimes E_1 \otimes E_{21} \otimes E_{21}]\!]$	$\frac{1}{\sqrt{6}} A_1 E_{210}^2 B_2 E_{10} - \frac{1}{\sqrt{6}} A_1 E_{211}^2 B_2 E_{10} - \frac{\sqrt{2}}{\sqrt{3}} A_1 E_{210} E_{211} B_2 E_{11}$	−53.252 ± 3.2416
$[\![A_1 \otimes E_1 \otimes E_1 \otimes E_1 \otimes E_1]\!]$	$\frac{1}{\sqrt{6}} A_1 E_{10}^4 + \frac{\sqrt{2}}{\sqrt{3}} A_1 E_{10}^2 E_{11}^2 + \frac{1}{\sqrt{6}} A_1 E_{11}^4$	−19.5465 ± 0.983
$[\![A_1 \otimes E_1 \otimes E_1 \otimes E_{20} \otimes E_{20}]\!]$	$\frac{1}{2} A_1 E_{200}^2 E_{10}^2 + \frac{1}{6} A_1 E_{201}^2 E_{10}^2 + \frac{2}{3} A_1 E_{200} E_{201} E_{10} E_{11} + \frac{1}{6} A_1 E_{200}^2 E_{11}^2 + \frac{1}{2} A_1 E_{201}^2 E_{11}^2$	−408.7572 ± 2.0399
$[\![A_1 \otimes E_1 \otimes E_1 \otimes E_{20} \otimes E_{20}]\!]$	$\frac{1}{\sqrt{6}} A_1 E_{201}^2 E_{10}^2 - \frac{\sqrt{2}}{\sqrt{3}} A_1 E_{200} E_{201} E_{10} E_{11} + \frac{1}{\sqrt{6}} A_1 E_{200}^2 E_{11}^2$	211.597 ± 1.0327
$[\![A_1 \otimes E_1 \otimes E_1 \otimes E_{20} \otimes E_{21}]\!]$	$\frac{3}{\sqrt{28}} A_1 E_{200} E_{210} E_{10}^2 + \frac{1}{\sqrt{28}} A_1 E_{201} E_{211} E_{10}^2 + \frac{1}{\sqrt{7}} A_1 E_{200} E_{211} E_{10} E_{11} + \frac{1}{\sqrt{7}} A_1 E_{201} E_{210} E_{10} E_{11} + \frac{1}{\sqrt{28}} A_1 E_{200} E_{210} E_{11}^2 + \frac{3}{\sqrt{28}} A_1 E_{201} E_{211} E_{11}^2$	299.0186 ± 1.4011
$[\![A_1 \otimes E_1 \otimes E_1 \otimes E_{20} \otimes E_{21}]\!]$	$\frac{1}{2} A_1 E_{201} E_{211} E_{10}^2 - \frac{1}{2} A_1 E_{200} E_{211} E_{10} E_{11} - \frac{1}{2} A_1 E_{201} E_{210} E_{10} E_{11} + \frac{1}{2} A_1 E_{200} E_{210} E_{11}^2$	−280.771 ± 1.9671
$[\![A_1 \otimes E_1 \otimes E_1 \otimes E_{21} \otimes E_{21}]\!]$	$\frac{1}{2} A_1 E_{210}^2 E_{10}^2 + \frac{1}{6} A_1 E_{211}^2 E_{10}^2 + \frac{2}{3} A_1 E_{210} E_{211} E_{10} E_{11} + \frac{1}{6} A_1 E_{210}^2 E_{11}^2 + \frac{1}{2} A_1 E_{211}^2 E_{11}^2$	−56.0281 ± 0.0895
$[\![A_1 \otimes E_1 \otimes E_1 \otimes E_{21} \otimes E_{21}]\!]$	$\frac{1}{\sqrt{6}} A_1 E_{211}^2 E_{10}^2 - \frac{\sqrt{2}}{\sqrt{3}} A_1 E_{210} E_{211} E_{10} E_{11} + \frac{1}{\sqrt{6}} A_1 E_{210}^2 E_{11}^2$	187.5521 ± 1.9022
$[\![A_1 \otimes E_{20} \otimes E_{20} \otimes E_{20} \otimes E_{20}]\!]$	$\frac{1}{\sqrt{6}} A_1 E_{200}^4 + \frac{\sqrt{2}}{\sqrt{3}} A_1 E_{200}^2 E_{201}^2 + \frac{1}{\sqrt{6}} A_1 E_{201}^4$	−123.2919 ± 0.0164
$[\![A_1 \otimes E_{20} \otimes E_{20} \otimes E_{20} \otimes E_{21}]\!]$	$\frac{1}{2} A_1 E_{200}^3 E_{210} + \frac{1}{2} A_1 E_{200}^2 E_{201} E_{211} + \frac{1}{2} A_1 E_{200} E_{201}^2 E_{210} + \frac{1}{2} A_1 E_{201}^3 E_{211}$	97.7471 ± 2.0621
$[\![A_1 \otimes E_{20} \otimes E_{20} \otimes E_{21} \otimes E_{21}]\!]$	$\frac{1}{2} A_1 E_{200}^2 E_{210}^2 + \frac{1}{6} A_1 E_{200}^2 E_{211}^2 + \frac{2}{3} A_1 E_{200} E_{201} E_{210} E_{211} + \frac{1}{6} A_1 E_{201}^2 E_{210}^2 + \frac{1}{2} A_1 E_{201}^2 E_{211}^2$	32.7288 ± 1.1306
$[\![A_1 \otimes E_{20} \otimes E_{20} \otimes E_{21} \otimes E_{21}]\!]$	$\frac{1}{\sqrt{6}} A_1 E_{200}^2 E_{211}^2 - \frac{\sqrt{2}}{\sqrt{3}} A_1 E_{200} E_{201} E_{210} E_{211} + \frac{1}{\sqrt{6}} A_1 E_{201}^2 E_{210}^2$	128.3519 ± 0.3635
$[\![A_1 \otimes E_{20} \otimes E_{21} \otimes E_{21} \otimes E_{21}]\!]$	$\frac{1}{2} A_1 E_{200} E_{210}^3 + \frac{1}{2} A_1 E_{200} E_{210} E_{211}^2 + \frac{1}{2} A_1 E_{201} E_{210}^2 E_{211} + \frac{1}{2} A_1 E_{201} E_{211}^3$	−29.132 ± 0.1469

Sym. Prod.	Polynomial	Value (eV/Å^5)
$[\![A_1 \otimes E_{21} \otimes E_{21} \otimes E_{21} \otimes E_{21}]\!]$	$\frac{1}{\sqrt{6}} A_1 E_{210}^4 + \frac{\sqrt{2}}{\sqrt{3}} A_1 E_{210}^2 E_{211}^2 + \frac{1}{\sqrt{6}} A_1 E_{211}^4$	-0.4699 ± 0.7537
$[\![A_2 \otimes A_2 \otimes A_2 \otimes B_1 \otimes B_2]\!]$	$A_2^3 B_1 B_2$	12.3982 ± 1.545
$[\![A_2 \otimes A_2 \otimes A_2 \otimes E_{20} \otimes E_{21}]\!]$	$\frac{1}{\sqrt{2}} A_2^3 E_{200} E_{211} - \frac{1}{\sqrt{2}} A_2^3 E_{201} E_{210}$	-0.3027 ± 0.2297
$[\![A_2 \otimes A_2 \otimes B_1 \otimes E_1 \otimes E_{20}]\!]$	$\frac{1}{\sqrt{2}} A_2^2 E_{200} B_1 E_{10} + \frac{1}{\sqrt{2}} A_2^2 E_{201} B_1 E_{11}$	140.9608 ± 0.9576
$[\![A_2 \otimes A_2 \otimes B_1 \otimes E_1 \otimes E_{21}]\!]$	$\frac{1}{\sqrt{2}} A_2^2 E_{210} B_1 E_{10} + \frac{1}{\sqrt{2}} A_2^2 E_{211} B_1 E_{11}$	-72.0117 ± 3.2642
$[\![A_2 \otimes A_2 \otimes B_2 \otimes E_1 \otimes E_{20}]\!]$	$\frac{1}{\sqrt{2}} A_2^2 E_{201} B_2 E_{10} - \frac{1}{\sqrt{2}} A_2^2 E_{200} B_2 E_{11}$	22.2374 ± 2.7962
$[\![A_2 \otimes A_2 \otimes B_2 \otimes E_1 \otimes E_{21}]\!]$	$\frac{1}{\sqrt{2}} A_2^2 E_{211} B_2 E_{10} - \frac{1}{\sqrt{2}} A_2^2 E_{210} B_2 E_{11}$	-40.9328 ± 1.3943
$[\![A_2 \otimes A_2 \otimes E_1 \otimes E_1 \otimes E_{20}]\!]$	$\frac{1}{\sqrt{6}} A_2^2 E_{201} E_{10}^2 + \frac{\sqrt{2}}{\sqrt{3}} A_2^2 E_{200} E_{10} E_{11} - \frac{1}{\sqrt{6}} A_2^2 E_{201} E_{11}^2$	-59.9315 ± 0.8494
$[\![A_2 \otimes A_2 \otimes E_1 \otimes E_1 \otimes E_{21}]\!]$	$\frac{1}{\sqrt{6}} A_2^2 E_{211} E_{10}^2 + \frac{\sqrt{2}}{\sqrt{3}} A_2^2 E_{210} E_{10} E_{11} - \frac{1}{\sqrt{6}} A_2^2 E_{211} E_{11}^2$	-5.129 ± 1.3073
$[\![A_2 \otimes A_2 \otimes E_{20} \otimes E_{20} \otimes E_{20}]\!]$	$\frac{3}{\sqrt{10}} A_2^2 E_{200}^2 E_{201} - \frac{1}{\sqrt{10}} A_2^2 E_{201}^3$	-42.7005 ± 0.0586
$[\![A_2 \otimes A_2 \otimes E_{20} \otimes E_{20} \otimes E_{21}]\!]$	$\frac{1}{\sqrt{6}} A_2^2 E_{200}^2 E_{211} + \frac{\sqrt{2}}{\sqrt{3}} A_2^2 E_{200} E_{201} E_{210} - \frac{1}{\sqrt{6}} A_2^2 E_{201}^2 E_{211}$	44.8214 ± 1.2348
$[\![A_2 \otimes A_2 \otimes E_{20} \otimes E_{21} \otimes E_{21}]\!]$	$\frac{\sqrt{2}}{\sqrt{3}} A_2^2 E_{200} E_{210} E_{211} + \frac{1}{\sqrt{6}} A_2^2 E_{201} E_{210}^2 - \frac{1}{\sqrt{6}} A_2^2 E_{201} E_{211}^2$	-16.8254 ± 2.927
$[\![A_2 \otimes A_2 \otimes E_{21} \otimes E_{21} \otimes E_{21}]\!]$	$\frac{3}{\sqrt{10}} A_2^2 E_{210}^2 E_{211} - \frac{1}{\sqrt{10}} A_2^2 E_{211}^3$	18.9071 ± 1.6784
$[\![A_2 \otimes B_1 \otimes B_1 \otimes B_1 \otimes B_2]\!]$	$A_2 B_1^3 B_2$	-84.3345 ± 0.7028
$[\![A_2 \otimes B_1 \otimes B_1 \otimes E_{20} \otimes E_{21}]\!]$	$\frac{1}{\sqrt{2}} A_2 E_{200} E_{211} B_1^2 - \frac{1}{\sqrt{2}} A_2 E_{201} E_{210} B_1^2$	-162.314 ± 2.1621
$[\![A_2 \otimes B_1 \otimes B_2 \otimes B_2 \otimes B_2]\!]$	$A_2 B_1 B_2^3$	13.6703 ± 1.8812
$[\![A_2 \otimes B_1 \otimes B_2 \otimes E_1 \otimes E_1]\!]$	$\frac{1}{\sqrt{2}} A_2 B_1 B_2 E_{10}^2 + \frac{1}{\sqrt{2}} A_2 B_1 B_2 E_{11}^2$	-95.4851 ± 1.7495
$[\![A_2 \otimes B_1 \otimes B_2 \otimes E_{20} \otimes E_{20}]\!]$	$\frac{1}{\sqrt{2}} A_2 E_{200}^2 B_1 B_2 + \frac{1}{\sqrt{2}} A_2 E_{201}^2 B_1 B_2$	-221.8874 ± 2.989
$[\![A_2 \otimes B_1 \otimes B_2 \otimes E_{20} \otimes E_{21}]\!]$	$\frac{1}{\sqrt{2}} A_2 E_{200} E_{210} B_1 B_2 + \frac{1}{\sqrt{2}} A_2 E_{201} E_{211} B_1 B_2$	120.5734 ± 3.319
$[\![A_2 \otimes B_1 \otimes B_2 \otimes E_{21} \otimes E_{21}]\!]$	$\frac{1}{\sqrt{2}} A_2 E_{210}^2 B_1 B_2 + \frac{1}{\sqrt{2}} A_2 E_{211}^2 B_1 B_2$	61.7384 ± 1.4827
$[\![A_2 \otimes B_1 \otimes E_1 \otimes E_1 \otimes E_1]\!]$	$\frac{1}{\sqrt{10}} A_2 B_1 E_{10}^3 - \frac{3}{\sqrt{10}} A_2 B_1 E_{10} E_{11}^2$	-152.5628 ± 0.695
$[\![A_2 \otimes B_1 \otimes E_1 \otimes E_{20} \otimes E_{20}]\!]$	$\frac{1}{\sqrt{6}} A_2 E_{200}^2 B_1 E_{10} - \frac{1}{\sqrt{6}} A_2 E_{201}^2 B_1 E_{10} - \frac{\sqrt{2}}{\sqrt{3}} A_2 E_{200} E_{201} B_1 E_{11}$	-32.1461 ± 0.3949
$[\![A_2 \otimes B_1 \otimes E_1 \otimes E_{20} \otimes E_{21}]\!]$	$\frac{1}{2} A_2 E_{200} E_{210} B_1 E_{10} - \frac{1}{2} A_2 E_{201} E_{211} B_1 E_{10} - \frac{1}{2} A_2 E_{200} E_{211} B_1 E_{11} - \frac{1}{2} A_2 E_{201} E_{210} B_1 E_{11}$	-197.9223 ± 5.6396
$[\![A_2 \otimes B_1 \otimes E_1 \otimes E_{21} \otimes E_{21}]\!]$	$\frac{1}{\sqrt{6}} A_2 E_{210}^2 B_1 E_{10} - \frac{1}{\sqrt{6}} A_2 E_{211}^2 B_1 E_{10} - \frac{\sqrt{2}}{\sqrt{3}} A_2 E_{210} E_{211} B_1 E_{11}$	50.8136 ± 1.2618
$[\![A_2 \otimes B_2 \otimes B_2 \otimes E_{20} \otimes E_{21}]\!]$	$\frac{1}{\sqrt{2}} A_2 E_{200} E_{211} B_2^2 - \frac{1}{\sqrt{2}} A_2 E_{201} E_{210} B_2^2$	93.4781 ± 1.9751
$[\![A_2 \otimes B_2 \otimes E_1 \otimes E_1 \otimes E_1]\!]$	$\frac{3}{\sqrt{10}} A_2 B_2 E_{10}^2 E_{11} - \frac{1}{\sqrt{10}} A_2 B_2 E_{11}^3$	105.4065 ± 1.8098
$[\![A_2 \otimes B_2 \otimes E_1 \otimes E_{20} \otimes E_{20}]\!]$	$\frac{\sqrt{2}}{\sqrt{3}} A_2 E_{200} E_{201} B_2 E_{10} + \frac{1}{\sqrt{6}} A_2 E_{200}^2 B_2 E_{11} - \frac{1}{\sqrt{6}} A_2 E_{201}^2 B_2 E_{11}$	159.2783 ± 4.0763
$[\![A_2 \otimes B_2 \otimes E_1 \otimes E_{20} \otimes E_{21}]\!]$	$\frac{1}{2} A_2 E_{200} E_{211} B_2 E_{10} + \frac{1}{2} A_2 E_{201} E_{210} B_2 E_{10} + \frac{1}{2} A_2 E_{200} E_{210} B_2 E_{11} - \frac{1}{2} A_2 E_{201} E_{211} B_2 E_{11}$	-24.0987 ± 1.6757
$[\![A_2 \otimes B_2 \otimes E_1 \otimes E_{21} \otimes E_{21}]\!]$	$\frac{\sqrt{2}}{\sqrt{3}} A_2 E_{210} E_{211} B_2 E_{10} + \frac{1}{\sqrt{6}} A_2 E_{210}^2 B_2 E_{11} - \frac{1}{\sqrt{6}} A_2 E_{211}^2 B_2 E_{11}$	43.3279 ± 1.6082
$[\![A_2 \otimes E_1 \otimes E_1 \otimes E_{20} \otimes E_{20}]\!]$	$\frac{1}{2} A_2 E_{200} E_{201} E_{10}^2 - \frac{1}{2} A_2 E_{200}^2 E_{10} E_{11} + \frac{1}{2} A_2 E_{201}^2 E_{10} E_{11} - \frac{1}{2} A_2 E_{200} E_{201} E_{11}^2$	227.6899 ± 0.8069

Sym. Prod.	Polynomial	Value (eV/Å^5)
$[\![A_2 \otimes E_1 \otimes E_1 \otimes E_{20} \otimes E_{21}]\!]$	$\frac{3}{\sqrt{28}} A_2 E_{200} E_{211} E_{10}^2 - \frac{1}{\sqrt{28}} A_2 E_{201} E_{210} E_{10}^2 - \frac{1}{\sqrt{7}} A_2 E_{200} E_{210} E_{10} E_{11} + \frac{1}{\sqrt{7}} A_2 E_{201} E_{211} E_{10} E_{11} + \frac{1}{\sqrt{28}} A_2 E_{200} E_{211} E_{11}^2 - \frac{3}{\sqrt{28}} A_2 E_{201} E_{210} E_{11}^2$	-192.0805 ± 0.6134
$[\![A_2 \otimes E_1 \otimes E_1 \otimes E_{20} \otimes E_{21}]\!]$	$\frac{1}{2} A_2 E_{201} E_{210} E_{10}^2 - \frac{1}{2} A_2 E_{200} E_{210} E_{10} E_{11} + \frac{1}{2} A_2 E_{201} E_{211} E_{10} E_{11} - \frac{1}{2} A_2 E_{200} E_{211} E_{11}^2$	-156.6331 ± 2.0558
$[\![A_2 \otimes E_1 \otimes E_1 \otimes E_{21} \otimes E_{21}]\!]$	$\frac{1}{2} A_2 E_{210} E_{211} E_{10}^2 - \frac{1}{2} A_2 E_{210}^2 E_{10} E_{11} + \frac{1}{2} A_2 E_{211}^2 E_{10} E_{11} - \frac{1}{2} A_2 E_{210} E_{211} E_{11}^2$	104.2736 ± 0.3845
$[\![A_2 \otimes E_{20} \otimes E_{20} \otimes E_{20} \otimes E_{21}]\!]$	$\frac{1}{2} A_2 E_{200}^3 E_{211} - \frac{1}{2} A_2 E_{200}^2 E_{201} E_{210} + \frac{1}{2} A_2 E_{200} E_{201}^2 E_{211} - \frac{1}{2} A_2 E_{201}^3 E_{210}$	-93.9108 ± 0.7845
$[\![A_2 \otimes E_{20} \otimes E_{20} \otimes E_{21} \otimes E_{21}]\!]$	$\frac{1}{2} A_2 E_{200}^2 E_{210} E_{211} - \frac{1}{2} A_2 E_{200} E_{201} E_{210}^2 + \frac{1}{2} A_2 E_{200} E_{201} E_{211}^2 - \frac{1}{2} A_2 E_{201}^2 E_{210} E_{211}$	29.7312 ± 1.8915
$[\![A_2 \otimes E_{20} \otimes E_{21} \otimes E_{21} \otimes E_{21}]\!]$	$\frac{1}{2} A_2 E_{200} E_{210}^2 E_{211} + \frac{1}{2} A_2 E_{200} E_{211}^3 - \frac{1}{2} A_2 E_{201} E_{210}^3 - \frac{1}{2} A_2 E_{201} E_{210} E_{211}^2$	15.3225 ± 0.261
$[\![B_1 \otimes B_1 \otimes B_1 \otimes E_1 \otimes E_{20}]\!]$	$\frac{1}{\sqrt{2}} E_{200} B_1^3 E_{10} + \frac{1}{\sqrt{2}} E_{201} B_1^3 E_{11}$	-486.2814 ± 0.0832
$[\![B_1 \otimes B_1 \otimes B_1 \otimes E_1 \otimes E_{21}]\!]$	$\frac{1}{\sqrt{2}} E_{210} B_1^3 E_{10} + \frac{1}{\sqrt{2}} E_{211} B_1^3 E_{11}$	233.0267 ± 0.877
$[\![B_1 \otimes B_1 \otimes B_2 \otimes E_1 \otimes E_{20}]\!]$	$\frac{1}{\sqrt{2}} E_{201} B_1^2 B_2 E_{10} - \frac{1}{\sqrt{2}} E_{200} B_1^2 B_2 E_{11}$	-401.4273 ± 0.1444
$[\![B_1 \otimes B_1 \otimes B_2 \otimes E_1 \otimes E_{21}]\!]$	$\frac{1}{\sqrt{2}} E_{211} B_1^2 B_2 E_{10} - \frac{1}{\sqrt{2}} E_{210} B_1^2 B_2 E_{11}$	352.385 ± 5.1802
$[\![B_1 \otimes B_1 \otimes E_1 \otimes E_1 \otimes E_{20}]\!]$	$\frac{1}{\sqrt{6}} E_{201} B_1^2 E_{10}^2 + \frac{\sqrt{2}}{\sqrt{3}} E_{200} B_1^2 E_{10} E_{11} - \frac{1}{\sqrt{6}} E_{201} B_1^2 E_{11}^2$	580.0431 ± 0.0731
$[\![B_1 \otimes B_1 \otimes E_1 \otimes E_1 \otimes E_{21}]\!]$	$\frac{1}{\sqrt{6}} E_{211} B_1^2 E_{10}^2 + \frac{\sqrt{2}}{\sqrt{3}} E_{210} B_1^2 E_{10} E_{11} - \frac{1}{\sqrt{6}} E_{211} B_1^2 E_{11}^2$	4.4957 ± 0.8271
$[\![B_1 \otimes B_1 \otimes E_{20} \otimes E_{20} \otimes E_{20}]\!]$	$\frac{3}{\sqrt{10}} E_{200}^2 E_{201} B_1^2 - \frac{1}{\sqrt{10}} E_{201}^3 B_1^2$	393.113 ± 0.0216
$[\![B_1 \otimes B_1 \otimes E_{20} \otimes E_{20} \otimes E_{21}]\!]$	$\frac{1}{\sqrt{6}} E_{200}^2 E_{211} B_1^2 + \frac{\sqrt{2}}{\sqrt{3}} E_{200} E_{201} E_{210} B_1^2 - \frac{1}{\sqrt{6}} E_{201}^2 E_{211} B_1^2$	-429.026 ± 2.4873
$[\![B_1 \otimes B_1 \otimes E_{20} \otimes E_{21} \otimes E_{21}]\!]$	$\frac{\sqrt{2}}{\sqrt{3}} E_{200} E_{210} E_{211} B_1^2 + \frac{1}{\sqrt{6}} E_{201} E_{210}^2 B_1^2 - \frac{1}{\sqrt{6}} E_{201} E_{211}^2 B_1^2$	370.6661 ± 1.156
$[\![B_1 \otimes B_1 \otimes E_{21} \otimes E_{21} \otimes E_{21}]\!]$	$\frac{3}{\sqrt{10}} E_{210}^2 E_{211} B_1^2 - \frac{1}{\sqrt{10}} E_{211}^3 B_1^2$	-88.3211 ± 1.4338
$[\![B_1 \otimes B_2 \otimes B_2 \otimes E_1 \otimes E_{20}]\!]$	$\frac{1}{\sqrt{2}} E_{200} B_1 B_2^2 E_{10} + \frac{1}{\sqrt{2}} E_{201} B_1 B_2^2 E_{11}$	253.1729 ± 0.1311
$[\![B_1 \otimes B_2 \otimes B_2 \otimes E_1 \otimes E_{21}]\!]$	$\frac{1}{\sqrt{2}} E_{210} B_1 B_2^2 E_{10} + \frac{1}{\sqrt{2}} E_{211} B_1 B_2^2 E_{11}$	-166.8274 ± 0.8092
$[\![B_1 \otimes B_2 \otimes E_1 \otimes E_1 \otimes E_{20}]\!]$	$\frac{1}{\sqrt{6}} E_{200} B_1 B_2 E_{10}^2 - \frac{\sqrt{2}}{\sqrt{3}} E_{201} B_1 B_2 E_{10} E_{11} - \frac{1}{\sqrt{6}} E_{200} B_1 B_2 E_{11}^2$	311.7269 ± 3.6367
$[\![B_1 \otimes B_2 \otimes E_1 \otimes E_1 \otimes E_{21}]\!]$	$\frac{1}{\sqrt{6}} E_{210} B_1 B_2 E_{10}^2 - \frac{\sqrt{2}}{\sqrt{3}} E_{211} B_1 B_2 E_{10} E_{11} - \frac{1}{\sqrt{6}} E_{210} B_1 B_2 E_{11}^2$	100.3495 ± 1.2226
$[\![B_1 \otimes B_2 \otimes E_{20} \otimes E_{20} \otimes E_{20}]\!]$	$\frac{1}{\sqrt{10}} E_{200}^3 B_1 B_2 - \frac{3}{\sqrt{10}} E_{200} E_{201}^2 B_1 B_2$	-201.5291 ± 4.0396
$[\![B_1 \otimes B_2 \otimes E_{20} \otimes E_{20} \otimes E_{21}]\!]$	$\frac{1}{\sqrt{6}} E_{200}^2 E_{210} B_1 B_2 - \frac{\sqrt{2}}{\sqrt{3}} E_{200} E_{201} E_{211} B_1 B_2 - \frac{1}{\sqrt{6}} E_{201}^2 E_{210} B_1 B_2$	457.2553 ± 0.5972
$[\![B_1 \otimes B_2 \otimes E_{20} \otimes E_{21} \otimes E_{21}]\!]$	$\frac{1}{\sqrt{6}} E_{200} E_{210}^2 B_1 B_2 - \frac{1}{\sqrt{6}} E_{200} E_{211}^2 B_1 B_2 - \frac{\sqrt{2}}{\sqrt{3}} E_{201} E_{210} E_{211} B_1 B_2$	-246.2959 ± 0.0474
$[\![B_1 \otimes B_2 \otimes E_{21} \otimes E_{21} \otimes E_{21}]\!]$	$\frac{1}{\sqrt{10}} E_{210}^3 B_1 B_2 - \frac{3}{\sqrt{10}} E_{210} E_{211}^2 B_1 B_2$	114.0732 ± 0.1052
$[\![B_1 \otimes E_1 \otimes E_1 \otimes E_1 \otimes E_{20}]\!]$	$\frac{1}{2} E_{200} B_1 E_{10}^3 + \frac{1}{2} E_{201} B_1 E_{10}^2 E_{11} + \frac{1}{2} E_{200} B_1 E_{10} E_{11}^2 + \frac{1}{2} E_{201} B_1 E_{11}^3$	-342.2306 ± 0.1501
$[\![B_1 \otimes E_1 \otimes E_1 \otimes E_1 \otimes E_{21}]\!]$	$\frac{1}{2} E_{210} B_1 E_{10}^3 + \frac{1}{2} E_{211} B_1 E_{10}^2 E_{11} + \frac{1}{2} E_{210} B_1 E_{10} E_{11}^2 + \frac{1}{2} E_{211} B_1 E_{11}^3$	147.8287 ± 1.1821
$[\![B_1 \otimes E_1 \otimes E_{20} \otimes E_{20} \otimes E_{20}]\!]$	$\frac{1}{2} E_{200}^3 B_1 E_{10} + \frac{1}{2} E_{200} E_{201}^2 B_1 E_{10} + \frac{1}{2} E_{200}^2 E_{201} B_1 E_{11} + \frac{1}{2} E_{201}^3 B_1 E_{11}$	-684.2408 ± 0.997
$[\![B_1 \otimes E_1 \otimes E_{20} \otimes E_{20} \otimes E_{21}]\!]$	$\frac{3}{\sqrt{28}} E_{200}^2 E_{210} B_1 E_{10} + \frac{1}{\sqrt{7}} E_{200} E_{201} E_{211} B_1 E_{10} + \frac{1}{\sqrt{28}} E_{201}^2 E_{210} B_1 E_{10} + \frac{1}{\sqrt{28}} E_{200}^2 E_{211} B_1 E_{11} + \frac{1}{\sqrt{7}} E_{200} E_{201} E_{210} B_1 E_{11} + \frac{3}{\sqrt{28}} E_{201}^2 E_{211} B_1 E_{11}$	636.6104 ± 4.3507

Sym. Prod.	Polynomial	Value (eV/Å^5)
$[\![B_1 \otimes E_1 \otimes E_{20} \otimes E_{20} \otimes E_{21}]\!]$	$\frac{1}{2}E_{200}E_{201}E_{211}B_1E_{10} - \frac{1}{2}E_{201}^2E_{210}B_1E_{10} - \frac{1}{2}E_{200}^2E_{211}B_1E_{11} + \frac{1}{2}E_{200}E_{201}E_{210}B_1E_{11}$	-476.558 ± 1.179
$[\![B_1 \otimes E_1 \otimes E_{20} \otimes E_{21} \otimes E_{21}]\!]$	$\frac{3}{\sqrt{28}}E_{200}E_{210}^2B_1E_{10} + \frac{1}{\sqrt{28}}E_{200}E_{211}^2B_1E_{10} + \frac{1}{\sqrt{7}}E_{201}E_{210}E_{211}B_1E_{10} + \frac{1}{\sqrt{7}}E_{200}E_{210}E_{211}B_1E_{11} + \frac{1}{\sqrt{28}}E_{201}E_{210}^2B_1E_{11} + \frac{3}{\sqrt{28}}E_{201}E_{211}^2B_1E_{11}$	-105.6205 ± 0.3616
$[\![B_1 \otimes E_1 \otimes E_{20} \otimes E_{21} \otimes E_{21}]\!]$	$\frac{1}{2}E_{200}E_{211}^2B_1E_{10} - \frac{1}{2}E_{201}E_{210}E_{211}B_1E_{10} - \frac{1}{2}E_{200}E_{210}E_{211}B_1E_{11} + \frac{1}{2}E_{201}E_{210}^2B_1E_{11}$	396.4581 ± 0.9442
$[\![B_1 \otimes E_1 \otimes E_{21} \otimes E_{21} \otimes E_{21}]\!]$	$\frac{1}{2}E_{210}^3B_1E_{10} + \frac{1}{2}E_{210}E_{211}^2B_1E_{10} + \frac{1}{2}E_{210}^2E_{211}B_1E_{11} + \frac{1}{2}E_{211}^3B_1E_{11}$	-49.7448 ± 0.4605
$[\![B_2 \otimes B_2 \otimes B_2 \otimes E_1 \otimes E_{20}]\!]$	$\frac{1}{\sqrt{2}}E_{201}B_2^3E_{10} - \frac{1}{\sqrt{2}}E_{200}B_2^3E_{11}$	45.2895 ± 0.9282
$[\![B_2 \otimes B_2 \otimes B_2 \otimes E_1 \otimes E_{21}]\!]$	$\frac{1}{\sqrt{2}}E_{211}B_2^3E_{10} - \frac{1}{\sqrt{2}}E_{210}B_2^3E_{11}$	-26.166 ± 0.7834
$[\![B_2 \otimes B_2 \otimes E_1 \otimes E_1 \otimes E_{20}]\!]$	$\frac{1}{\sqrt{6}}E_{201}B_2^2E_{10}^2 + \frac{\sqrt{2}}{\sqrt{3}}E_{200}B_2^2E_{10}E_{11} - \frac{1}{\sqrt{6}}E_{201}B_2^2E_{11}^2$	-123.2315 ± 0.7548
$[\![B_2 \otimes B_2 \otimes E_1 \otimes E_1 \otimes E_{21}]\!]$	$\frac{1}{\sqrt{6}}E_{211}B_2^2E_{10}^2 + \frac{\sqrt{2}}{\sqrt{3}}E_{210}B_2^2E_{10}E_{11} - \frac{1}{\sqrt{6}}E_{211}B_2^2E_{11}^2$	-16.9186 ± 2.7209
$[\![B_2 \otimes B_2 \otimes E_{20} \otimes E_{20} \otimes E_{20}]\!]$	$\frac{3}{\sqrt{10}}E_{200}^2E_{201}B_2^2 - \frac{1}{\sqrt{10}}E_{201}^3B_2^2$	-68.4365 ± 0.5654
$[\![B_2 \otimes B_2 \otimes E_{20} \otimes E_{20} \otimes E_{21}]\!]$	$\frac{1}{\sqrt{6}}E_{200}^2E_{211}B_2^2 + \frac{\sqrt{2}}{\sqrt{3}}E_{200}E_{201}E_{210}B_2^2 - \frac{1}{\sqrt{6}}E_{201}^2E_{211}B_2^2$	104.0596 ± 2.229
$[\![B_2 \otimes B_2 \otimes E_{20} \otimes E_{21} \otimes E_{21}]\!]$	$\frac{\sqrt{2}}{\sqrt{3}}E_{200}E_{210}E_{211}B_2^2 + \frac{1}{\sqrt{6}}E_{201}E_{210}^2B_2^2 - \frac{1}{\sqrt{6}}E_{201}E_{211}^2B_2^2$	-91.4389 ± 0.2483
$[\![B_2 \otimes B_2 \otimes E_{21} \otimes E_{21} \otimes E_{21}]\!]$	$\frac{3}{\sqrt{10}}E_{210}^2E_{211}B_2^2 - \frac{1}{\sqrt{10}}E_{211}^3B_2^2$	7.7689 ± 1.2093
$[\![B_2 \otimes E_1 \otimes E_1 \otimes E_1 \otimes E_{20}]\!]$	$\frac{1}{2}E_{201}B_2E_{10}^3 - \frac{1}{2}E_{200}B_2E_{10}^2E_{11} + \frac{1}{2}E_{201}B_2E_{10}E_{11}^2 - \frac{1}{2}E_{200}B_2E_{11}^3$	-102.2057 ± 0.7514
$[\![B_2 \otimes E_1 \otimes E_1 \otimes E_1 \otimes E_{21}]\!]$	$\frac{1}{2}E_{211}B_2E_{10}^3 - \frac{1}{2}E_{210}B_2E_{10}^2E_{11} + \frac{1}{2}E_{211}B_2E_{10}E_{11}^2 - \frac{1}{2}E_{210}B_2E_{11}^3$	83.6905 ± 0.4824
$[\![B_2 \otimes E_1 \otimes E_{20} \otimes E_{20} \otimes E_{20}]\!]$	$\frac{1}{2}E_{200}^2E_{201}B_2E_{10} + \frac{1}{2}E_{201}^3B_2E_{10} - \frac{1}{2}E_{200}^3B_2E_{11} - \frac{1}{2}E_{200}E_{201}^2B_2E_{11}$	-190.2154 ± 0.5268
$[\![B_2 \otimes E_1 \otimes E_{20} \otimes E_{20} \otimes E_{21}]\!]$	$\frac{3}{\sqrt{28}}E_{200}^2E_{211}B_2E_{10} - \frac{1}{\sqrt{7}}E_{200}E_{201}E_{210}B_2E_{10} + \frac{1}{\sqrt{28}}E_{201}^2E_{211}B_2E_{10} - \frac{1}{\sqrt{28}}E_{200}^2E_{210}B_2E_{11} + \frac{1}{\sqrt{7}}E_{200}E_{201}E_{211}B_2E_{11} - \frac{3}{\sqrt{28}}E_{201}^2E_{210}B_2E_{11}$	390.3143 ± 1.799
$[\![B_2 \otimes E_1 \otimes E_{20} \otimes E_{20} \otimes E_{21}]\!]$	$\frac{1}{2}E_{200}E_{201}E_{210}B_2E_{10} + \frac{1}{2}E_{201}^2E_{211}B_2E_{10} - \frac{1}{2}E_{200}^2E_{210}B_2E_{11} - \frac{1}{2}E_{200}E_{201}E_{211}B_2E_{11}$	142.6822 ± 2.5037
$[\![B_2 \otimes E_1 \otimes E_{20} \otimes E_{21} \otimes E_{21}]\!]$	$\frac{1}{\sqrt{3}}E_{200}E_{210}E_{211}B_2E_{10} - \frac{1}{\sqrt{12}}E_{201}E_{210}^2B_2E_{10} + \frac{1}{\sqrt{12}}E_{201}E_{211}^2B_2E_{10} - \frac{1}{\sqrt{12}}E_{200}E_{210}^2B_2E_{11} + \frac{1}{\sqrt{12}}E_{200}E_{211}^2B_2E_{11} - \frac{1}{\sqrt{3}}E_{201}E_{210}E_{211}B_2E_{11}$	-260.0511 ± 0.7266
$[\![B_2 \otimes E_1 \otimes E_{20} \otimes E_{21} \otimes E_{21}]\!]$	$\frac{1}{2}E_{201}E_{210}^2B_2E_{10} + \frac{1}{2}E_{201}E_{211}^2B_2E_{10} - \frac{1}{2}E_{200}E_{210}^2B_2E_{11} - \frac{1}{2}E_{200}E_{211}^2B_2E_{11}$	71.6683 ± 2.1037
$[\![B_2 \otimes E_1 \otimes E_{21} \otimes E_{21} \otimes E_{21}]\!]$	$\frac{1}{2}E_{210}^2E_{211}B_2E_{10} + \frac{1}{2}E_{211}^3B_2E_{10} - \frac{1}{2}E_{210}^3B_2E_{11} - \frac{1}{2}E_{210}E_{211}^2B_2E_{11}$	-35.4554 ± 0.2838
$[\![E_1 \otimes E_1 \otimes E_1 \otimes E_1 \otimes E_{20}]\!]$	$\frac{\sqrt{5}}{\sqrt{46}}E_{201}E_{10}^4 + \frac{\sqrt{8}}{\sqrt{115}}E_{200}E_{10}^3E_{11} - \frac{3\sqrt{2}}{\sqrt{115}}E_{201}E_{10}^2E_{11}^2 + \frac{6\sqrt{2}}{\sqrt{115}}E_{200}E_{10}E_{11}^3 - \frac{3}{\sqrt{230}}E_{201}E_{11}^4$	-8.8179 ± 0.2467
$[\![E_1 \otimes E_1 \otimes E_1 \otimes E_1 \otimes E_{20}]\!]$	$\frac{3}{2\sqrt{5}}E_{200}E_{10}^3E_{11} + \frac{3}{2\sqrt{5}}E_{201}E_{10}^2E_{11}^2 - \frac{1}{2\sqrt{5}}E_{200}E_{10}E_{11}^3 - \frac{1}{2\sqrt{5}}E_{201}E_{11}^4$	217.2351 ± 1.0985
$[\![E_1 \otimes E_1 \otimes E_1 \otimes E_1 \otimes E_{21}]\!]$	$\frac{\sqrt{5}}{\sqrt{46}}E_{211}E_{10}^4 + \frac{\sqrt{8}}{\sqrt{115}}E_{210}E_{10}^3E_{11} - \frac{3\sqrt{2}}{\sqrt{115}}E_{211}E_{10}^2E_{11}^2 + \frac{6\sqrt{2}}{\sqrt{115}}E_{210}E_{10}E_{11}^3 - \frac{3}{\sqrt{230}}E_{211}E_{11}^4$	55.3584 ± 0.786
$[\![E_1 \otimes E_1 \otimes E_1 \otimes E_1 \otimes E_{21}]\!]$	$\frac{3}{2\sqrt{5}}E_{210}E_{10}^3E_{11} + \frac{3}{2\sqrt{5}}E_{211}E_{10}^2E_{11}^2 - \frac{1}{2\sqrt{5}}E_{210}E_{10}E_{11}^3 - \frac{1}{2\sqrt{5}}E_{211}E_{11}^4$	-138.0518 ± 1.8803

Sym. Prod.	Polynomial	Value (eV/Å^5)
$[\![E_1 \otimes E_1 \otimes E_{20} \otimes E_{20} \otimes E_{20}]\!]$	$\frac{7}{2\sqrt{23}}E_{200}^2E_{201}E_{10}^2 - \frac{1}{2\sqrt{23}}E_{201}^3E_{10}^2 + \frac{1}{\sqrt{23}}E_{200}^3E_{10}E_{11} + \frac{1}{\sqrt{23}}E_{200}E_{201}^2E_{10}E_{11} + \frac{5}{2\sqrt{23}}E_{200}^2E_{201}E_{11}^2 - \frac{3}{2\sqrt{23}}E_{201}^3E_{11}^2$	313.8636 ± 1.715
$[\![E_1 \otimes E_1 \otimes E_{20} \otimes E_{20} \otimes E_{20}]\!]$	$\frac{1}{\sqrt{8}}E_{201}^3E_{10}^2 + \frac{3}{\sqrt{32}}E_{200}^3E_{10}E_{11} + \frac{3}{\sqrt{32}}E_{200}E_{201}^2E_{10}E_{11} - \frac{3}{\sqrt{32}}E_{200}^2E_{201}E_{11}^2 - \frac{1}{\sqrt{32}}E_{201}^3E_{11}^2$	160.666 ± 0.8557
$[\![E_1 \otimes E_1 \otimes E_{20} \otimes E_{20} \otimes E_{21}]\!]$	$\frac{5}{2\sqrt{33}}E_{200}^2E_{211}E_{10}^2 + \frac{1}{\sqrt{33}}E_{200}E_{201}E_{210}E_{10}^2 - \frac{1}{2\sqrt{33}}E_{201}^2E_{211}E_{10}^2 + \frac{1}{\sqrt{33}}E_{200}^2E_{210}E_{10}E_{11} - \frac{2}{\sqrt{33}}E_{200}E_{201}E_{211}E_{10}E_{11} + \frac{\sqrt{3}}{\sqrt{11}}E_{201}^2E_{210}E_{10}E_{11} - \frac{1}{2\sqrt{33}}E_{200}^2E_{211}E_{11}^2 + \frac{\sqrt{3}}{\sqrt{11}}E_{200}E_{201}E_{210}E_{11}^2 - \frac{\sqrt{3}}{2\sqrt{11}}E_{201}^2E_{211}E_{11}^2$	-30.4451 ± 0.6959
$[\![E_1 \otimes E_1 \otimes E_{20} \otimes E_{20} \otimes E_{21}]\!]$	$\frac{7}{2\sqrt{33}}E_{200}E_{201}E_{210}E_{10}^2 - \frac{1}{2\sqrt{33}}E_{201}^2E_{211}E_{10}^2 + \frac{1}{\sqrt{33}}E_{200}^2E_{210}E_{10}E_{11} + \frac{\sqrt{3}}{\sqrt{11}}E_{200}E_{201}E_{211}E_{10}E_{11} - \frac{2}{\sqrt{33}}E_{201}^2E_{210}E_{10}E_{11} + \frac{2}{\sqrt{33}}E_{200}^2E_{211}E_{11}^2 + \frac{1}{2\sqrt{33}}E_{200}E_{201}E_{210}E_{11}^2 - \frac{\sqrt{3}}{2\sqrt{11}}E_{201}^2E_{211}E_{11}^2$	-333.9295 ± 4.3245
$[\![E_1 \otimes E_1 \otimes E_{20} \otimes E_{20} \otimes E_{21}]\!]$	$\frac{1}{\sqrt{6}}E_{201}^2E_{211}E_{10}^2 + \frac{\sqrt{3}}{\sqrt{8}}E_{200}^2E_{210}E_{10}E_{11} + \frac{1}{\sqrt{6}}E_{200}E_{201}E_{211}E_{10}E_{11} + \frac{1}{\sqrt{24}}E_{201}^2E_{210}E_{10}E_{11} - \frac{1}{\sqrt{24}}E_{200}^2E_{211}E_{11}^2 - \frac{1}{\sqrt{6}}E_{200}E_{201}E_{210}E_{11}^2 - \frac{1}{\sqrt{24}}E_{201}^2E_{211}E_{11}^2$	46.2841 ± 1.0756
$[\![E_1 \otimes E_1 \otimes E_{20} \otimes E_{21} \otimes E_{21}]\!]$	$\frac{\sqrt{3}}{\sqrt{7}}E_{200}E_{210}E_{211}E_{10}^2 + \frac{1}{2\sqrt{21}}E_{201}E_{210}^2E_{10}^2 - \frac{1}{2\sqrt{21}}E_{201}E_{211}^2E_{10}^2 + \frac{1}{\sqrt{21}}E_{200}E_{210}^2E_{10}E_{11} - \frac{1}{\sqrt{21}}E_{200}E_{211}^2E_{10}E_{11} + \frac{2}{\sqrt{21}}E_{201}E_{210}E_{211}E_{10}E_{11} + \frac{1}{\sqrt{21}}E_{200}E_{210}E_{211}E_{11}^2 + \frac{\sqrt{3}}{\sqrt{28}}E_{201}E_{210}^2E_{11}^2 - \frac{\sqrt{3}}{\sqrt{28}}E_{201}E_{211}^2E_{11}^2$	149.5052 ± 0.1672
$[\![E_1 \otimes E_1 \otimes E_{20} \otimes E_{21} \otimes E_{21}]\!]$	$\frac{7}{10\sqrt{3}}E_{201}E_{210}^2E_{10}^2 - \frac{1}{10\sqrt{3}}E_{201}E_{211}^2E_{10}^2 + \frac{1}{5\sqrt{3}}E_{200}E_{210}^2E_{10}E_{11} + \frac{1}{\sqrt{3}}E_{200}E_{211}^2E_{10}E_{11} - \frac{4}{5\sqrt{3}}E_{201}E_{210}E_{211}E_{10}E_{11} + \frac{4}{5\sqrt{3}}E_{200}E_{210}E_{211}E_{11}^2 - \frac{\sqrt{3}}{10}E_{201}E_{210}^2E_{11}^2 - \frac{\sqrt{3}}{10}E_{201}E_{211}^2E_{11}^2$	8.2128 ± 0.3181
$[\![E_1 \otimes E_1 \otimes E_{20} \otimes E_{21} \otimes E_{21}]\!]$	$\frac{1}{\sqrt{6}}E_{201}E_{211}^2E_{10}^2 + \frac{\sqrt{3}}{\sqrt{8}}E_{200}E_{210}^2E_{10}E_{11} + \frac{1}{\sqrt{24}}E_{200}E_{211}^2E_{10}E_{11} + \frac{1}{\sqrt{6}}E_{201}E_{210}E_{211}E_{10}E_{11} - \frac{1}{\sqrt{6}}E_{200}E_{210}E_{211}E_{11}^2 - \frac{1}{\sqrt{24}}E_{201}E_{210}^2E_{11}^2 - \frac{1}{\sqrt{24}}E_{201}E_{211}^2E_{11}^2$	-111.7611 ± 0.7513
$[\![E_1 \otimes E_1 \otimes E_{21} \otimes E_{21} \otimes E_{21}]\!]$	$\frac{7}{2\sqrt{23}}E_{210}^2E_{211}E_{10}^2 - \frac{1}{2\sqrt{23}}E_{211}^3E_{10}^2 + \frac{1}{\sqrt{23}}E_{210}^3E_{10}E_{11} + \frac{1}{\sqrt{23}}E_{210}E_{211}^2E_{10}E_{11} + \frac{5}{2\sqrt{23}}E_{210}^2E_{211}E_{11}^2 - \frac{3}{2\sqrt{23}}E_{211}^3E_{11}^2$	-31.8663 ± 1.9014
$[\![E_1 \otimes E_1 \otimes E_{21} \otimes E_{21} \otimes E_{21}]\!]$	$\frac{1}{\sqrt{8}}E_{211}^3E_{10}^2 + \frac{3}{\sqrt{32}}E_{210}^3E_{10}E_{11} + \frac{3}{\sqrt{32}}E_{210}E_{211}^2E_{10}E_{11} - \frac{3}{\sqrt{32}}E_{210}^2E_{211}E_{11}^2 - \frac{1}{\sqrt{32}}E_{211}^3E_{11}^2$	14.2003 ± 0.8711
$[\![E_{20} \otimes E_{20} \otimes E_{20} \otimes E_{20} \otimes E_{20}]\!]$	$\frac{3}{\sqrt{14}}E_{200}^4E_{201} + \frac{\sqrt{2}}{\sqrt{7}}E_{200}^2E_{201}^3 - \frac{1}{\sqrt{14}}E_{201}^5$	74.0341 ± 0.1828

Sym. Prod.	Polynomial	Value (eV/Å^5)
$[\![E_{20}\otimes E_{20}\otimes E_{20}\otimes E_{20}\otimes E_{21}]\!]$	$\frac{\sqrt{5}}{\sqrt{46}}E_{200}^4E_{211} + \frac{\sqrt{8}}{\sqrt{115}}E_{200}^3E_{201}E_{210} - \frac{3\sqrt{2}}{\sqrt{115}}E_{200}^2E_{201}^2E_{211} + \frac{6\sqrt{2}}{\sqrt{115}}E_{200}E_{201}^3E_{210} - \frac{3}{\sqrt{230}}E_{201}^4E_{211}$	-117.1412 ± 1.2082
$[\![E_{20}\otimes E_{20}\otimes E_{20}\otimes E_{20}\otimes E_{21}]\!]$	$\frac{3}{2\sqrt{5}}E_{200}^3E_{201}E_{210} + \frac{3}{2\sqrt{5}}E_{200}^2E_{201}^2E_{211} - \frac{1}{2\sqrt{5}}E_{200}E_{201}^3E_{210} - \frac{1}{2\sqrt{5}}E_{201}^4E_{211}$	-66.6549 ± 0.4851
$[\![E_{20}\otimes E_{20}\otimes E_{20}\otimes E_{21}\otimes E_{21}]\!]$	$\frac{1}{\sqrt{3}}E_{200}^3E_{210}E_{211} + \frac{1}{\sqrt{12}}E_{200}^2E_{201}E_{210}^2 - \frac{1}{\sqrt{12}}E_{200}^2E_{201}E_{211}^2 + \frac{1}{\sqrt{3}}E_{200}E_{201}^2E_{210}E_{211} + \frac{1}{\sqrt{12}}E_{201}^3E_{210}^2 - \frac{1}{\sqrt{12}}E_{201}^3E_{211}^2$	161.9853 ± 1.6329
$[\![E_{20}\otimes E_{20}\otimes E_{20}\otimes E_{21}\otimes E_{21}]\!]$	$\frac{3}{2\sqrt{5}}E_{200}^2E_{201}E_{210}^2 + \frac{3}{2\sqrt{5}}E_{200}^2E_{201}E_{211}^2 - \frac{1}{2\sqrt{5}}E_{201}^3E_{210}^2 - \frac{1}{2\sqrt{5}}E_{201}^3E_{211}^2$	-42.022 ± 1.6258
$[\![E_{20}\otimes E_{20}\otimes E_{21}\otimes E_{21}\otimes E_{21}]\!]$	$\frac{7}{2\sqrt{23}}E_{200}^2E_{210}^2E_{211} - \frac{1}{2\sqrt{23}}E_{200}^2E_{211}^3 + \frac{1}{\sqrt{23}}E_{200}E_{201}E_{210}^3 + \frac{1}{\sqrt{23}}E_{200}E_{201}E_{210}E_{211}^2 + \frac{5}{2\sqrt{23}}E_{201}^2E_{210}^2E_{211} - \frac{3}{2\sqrt{23}}E_{201}^2E_{211}^3$	-71.2029 ± 1.5416
$[\![E_{20}\otimes E_{20}\otimes E_{21}\otimes E_{21}\otimes E_{21}]\!]$	$\frac{1}{\sqrt{8}}E_{200}^2E_{211}^3 + \frac{3}{\sqrt{32}}E_{200}E_{201}E_{210}^3 + \frac{3}{\sqrt{32}}E_{200}E_{201}E_{210}E_{211}^2 - \frac{3}{\sqrt{32}}E_{201}^2E_{210}^2E_{211} - \frac{1}{\sqrt{32}}E_{201}^2E_{211}^3$	43.8516 ± 1.06
$[\![E_{20}\otimes E_{21}\otimes E_{21}\otimes E_{21}\otimes E_{21}]\!]$	$\frac{4\sqrt{2}}{\sqrt{55}}E_{200}E_{210}^3E_{211} + \frac{1}{\sqrt{110}}E_{201}E_{210}^4 + \frac{3\sqrt{2}}{\sqrt{55}}E_{201}E_{210}^2E_{211}^2 - \frac{3}{\sqrt{110}}E_{201}E_{211}^4$	13.8655 ± 1.6635
$[\![E_{20}\otimes E_{21}\otimes E_{21}\otimes E_{21}\otimes E_{21}]\!]$	$\frac{4\sqrt{2}}{\sqrt{55}}E_{200}E_{210}E_{211}^3 + \frac{3}{\sqrt{110}}E_{201}E_{210}^4 - \frac{3\sqrt{2}}{\sqrt{55}}E_{201}E_{210}^2E_{211}^2 - \frac{1}{\sqrt{110}}E_{201}E_{211}^4$	-46.9735 ± 0.2326
$[\![E_{21}\otimes E_{21}\otimes E_{21}\otimes E_{21}\otimes E_{21}]\!]$	$\frac{3}{\sqrt{14}}E_{210}^4E_{211} + \frac{\sqrt{2}}{\sqrt{7}}E_{210}^2E_{211}^3 - \frac{1}{\sqrt{14}}E_{211}^5$	-2.4813 ± 0.6851

Table 7.8: Fifth-order mode coefficients for the hexagon. When expanded in the provided basis, it constitutes a full Taylor expansion.

Bibliography

[1] Anubhav Jain, Yongwoo Shin, and Kristin A. Persson. Computational predictions of energy materials using density functional theory. *Nature Reviews Materials*, 1(1):15004, Jan 2016.

[2] G. Leibfried and W. Ludwig. Theory of Anharmonic Effects in Crystals. In *Solid State Physics*, pages 275–444. Elsevier BV, 1961.

[3] K. H. Michel, S. Costamagna, and F. M. Peeters. Theory of anharmonic phonons in two-dimensional crystals. *Physical Review B*, 91(13), Apr 2015.

[4] A. Hmiel, J. M. Winey, Y. M. Gupta, and M. P. Desjarlais. Nonlinear elastic response of strong solids: First-principles calculations of the third-order elastic constants of diamond. *Physical Review B*, 93(17), May 2016.

[5] Xiaoding Wei, Benjamin Fragneaud, Chris A. Marianetti, and Jeffrey W. Kysar. Nonlinear elastic behavior of graphene: Ab initio calculations to continuum description. *Physical Review B*, 80(20), Nov 2009.

[6] Sandeep Kumar and David M. Parks. A comprehensive lattice-stability limit surface for graphene. *Journal of the Mechanics and Physics of Solids*, 86:19–41, Jan 2016.

[7] Claas Hter, Martin Friák, Marc Weikamp, Jrg Neugebauer, Nigel Goldenfeld, Bob Svendsen, and Robert Spatschek. Nonlinear elastic effects in phase field crystal and amplitude equations: Comparison to ab initio simulations of bcc metals and graphene. *Physical Review B*, 93(21), Jun 2016.

[8] Y. C. Cheng, Z. Y. Zhu, G. S. Huang, and U. Schwingenschlgl. Grneisen parameter of theGmode of strained monolayer graphene. *Physical Review B*, 83(11), Mar 2011.

[9] Simon Gelin, Hajime Tanaka, and Anal Lemaître. Anomalous phonon scattering and elastic correlations in amorphous solids. *Nature Materials*, 15(11):1177–1181, Aug 2016.

[10] A. Glensk, B. Grabowski, T. Hickel, and J. Neugebauer. Understanding Anharmonicity in fcc Materials: From its Origin toab initioStrategies beyond the Quasiharmonic Approximation. *Physical Review Letters*, 114(19), May 2015.

[11] Lorenzo Paulatto, Ion Errea, Matteo Calandra, and Francesco Mauri. First-principles calculations of phonon frequencies, lifetimes, and spectral functions from weak to strong anharmonicity: The example of palladium hydrides. *Physical Review B*, 91(5), Feb 2015.

[12] Ion Errea, Bruno Rousseau, and Aitor Bergara. Anharmonic Stabilization of the High-Pressure Simple Cubic Phase of Calcium. *Physical Review Letters*, 106(16), Apr 2011.

[13] Nicola Bonini, Michele Lazzeri, Nicola Marzari, and Francesco Mauri. Phonon Anharmonicities in Graphite and Graphene. *Physical Review Letters*, 99(17), Oct 2007.

[14] Nicola Bonini, Rahul Rao, Apparao M. Rao, Nicola Marzari, and José Menéndez. Lattice anharmonicity in low-dimensional carbon systems. *physica status solidi (b)*, 245(10):2149–2154, Sep 2008.

[15] Nicola Bonini, Jivtesh Garg, and Nicola Marzari. Acoustic Phonon Lifetimes and Thermal Transport in Free-Standing and Strained Graphene. *Nano Letters*, 12(6):2673–2678, Jun 2012.

[16] Shrikant Kshirsagar, Kranthi K. Mandadapu, and Panayiotis Papadopoulos. Classical molecular dynamics simulations of crystal lattices with truncated Taylor series-based interatomic potentials. *Computational Materials Science*, 120:127–134, Jul 2016.

[17] Jacek C Wojdeł, Patrick Hermet, Mathias P Ljungberg, Philippe Ghosez, and Jorge Íñiguez. First-principles model potentials for lattice-dynamical studies: general methodology and example of application to ferroic perovskite oxides. *Journal of Physics: Condensed Matter*, 25(30):305401, Jul 2013.

[18] John C. Thomas and Anton Van der Ven. Finite-temperature properties of strongly anharmonic and mechanically unstable crystal phases from first principles. *Physical Review B*, 88(21), Dec 2013.

[19] So Hirata, Murat Keçeli, and Kiyoshi Yagi. First-principles theories for anharmonic lattice vibrations. *The Journal of Chemical Physics*, 133(3):034109, Jul 2010.

[20] Yue Chen, Xinyuan Ai, and C. A. Marianetti. First-Principles Approach to Nonlinear Lattice Dynamics: Anomalous Spectra in PbTe. *Physical Review Letters*, 113(10), Sep 2014.

[21] S. Piscanec, M. Lazzeri, Francesco Mauri, A. C. Ferrari, and J. Robertson. Kohn Anomalies and Electron-Phonon Interactions in Graphite. *Physical Review Letters*, 93(18), Oct 2004.

[22] Y Wang, J J Wang, W Y Wang, Z G Mei, S L Shang, L Q Chen, and Z K Liu. A mixed-space approach to first-principles calculations of phonon frequencies for polar materials. *Journal of Physics: Condensed Matter*, 22(20):202201, Apr 2010.

[23] K. H. Ahn, T. Lookman, A. Saxena, and A. R. Bishop. Atomic scale lattice distortions and domain wall profiles. *Physical Review B*, 68(9), Sep 2003.

[24] Tsezar F. Seman, Jichan Moon, and Keun Hyuk Ahn. Symmetry-mode-based atomic scale formalism of lattice dynamics. *Emerging Materials Research*, 2(1):5–16, Feb 2013.

[25] Keivan Esfarjani and Harold T. Stokes. Method to extract anharmonic force constants from first principles calculations. *Physical Review B*, 77(14), Apr 2008.

[26] Keivan Esfarjani, Gang Chen, and Harold T. Stokes. Heat transport in silicon from first-principles calculations. *Physical Review B*, 84(8), Aug 2011.

[27] Junichiro Shiomi, Keivan Esfarjani, and Gang Chen. Thermal conductivity of half-Heusler compounds from first-principles calculations. *Physical Review B*, 84(10), Sep 2011.

[28] Takuma Shiga, Junichiro Shiomi, Jie Ma, Olivier Delaire, Tomasz Radzynski, Andrzej Lusakowski, Keivan Esfarjani, and Gang Chen. Microscopic mechanism of low thermal conductivity in lead telluride. *Physical Review B*, 85(15), Apr 2012.

[29] Xinyuan Ai, Yue Chen, and Chris A. Marianetti. Slave mode expansion for obtaining ab initio interatomic potentials. *Physical Review B*, 90(1), Jul 2014.

[30] Latham Boyle, Jun Yong Khoo, and Kendrick Smith. Symmetric Satellite Swarms and Choreographic Crystals. *Physical Review Letters*, 116(1), Jan 2016.

[31] Boris Kozinsky, Sneha A. Akhade, Pierre Hirel, Adham Hashibon, Christian Elssser, Prateek Mehta, Alan Logeat, and Ulrich Eisele. Effects of Sublattice Symmetry and Frustration on Ionic Transport in Garnet Solid Electrolytes. *Physical Review Letters*, 116(5), Feb 2016.

[32] Yuji Ikeda, Abel Carreras, Atsuto Seko, Atsushi Togo, and Isao Tanaka. Mode decomposition based on crystallographic symmetry in the band-unfolding method. *Physical Review B*, 95(2), Jan 2017.

[33] Eduardo B. Barros, Ado Jorio, Georgii G. Samsonidze, Rodrigo B. Capaz, Antônio G. Souza Filho, Josué Mendes Filho, Gene Dresselhaus, and Mildred S. Dresselhaus. Review on the symmetry-related properties of carbon nanotubes. *Physics Reports*, 431(6):261–302, Sep 2006.

[34] L.A. Falkovsky. Symmetry constraints on phonon dispersion in graphene. *Physics Letters A*, 372(31):5189–5192, Jul 2008.

[35] Donald W. Brenner. Empirical potential for hydrocarbons for use in simulating the chemical vapor deposition of diamond films. *Physical Review B*, 42(15):9458–9471, Nov 1990.

[36] J. Tersoff. Empirical Interatomic Potential for Carbon, with Applications to Amorphous Carbon. *Physical Review Letters*, 61(25):2879–2882, Dec 1988.

[37] Donald W Brenner, Olga A Shenderova, Judith A Harrison, Steven J Stuart, Boris Ni, and Susan B Sinnott. A second-generation reactive empirical bond order (REBO) potential energy expression for hydrocarbons. *Journal of Physics: Condensed Matter*, 14(4):783–802, Jan 2002.

[38] L. Lindsay and D. A. Broido. Optimized Tersoff and Brenner empirical potential parameters for lattice dynamics and phonon thermal transport in carbon nanotubes and graphene. *Physical Review B*, 81(20), May 2010.

[39] Mounzer Dagher, Mounif Kobersi, and Hafez Kobeissi. The true diatomic potential as a perturbed Morse function. *Journal of Computational Chemistry*, 16(6):723–728, Jun 1995.

[40] Aibing Liu and Steven J. Stuart. Empirical bond-order potential for hydrocarbons: Adaptive treatment of van der Waals interactions. *Journal of Computational Chemistry*, 29(4):601–611, Sep 2007.

[41] V. K. Tewary and B. Yang. Parametric interatomic potential for graphene. *Physical Review B*, 79(7), Feb 2009.

[42] Jingchao Zhang, Fei Xu, Yang Hong, Qingang Xiong, and Jianming Pan. A comprehensive review on the molecular dynamics simulation of the novel thermal properties of graphene. *RSC Adv.*, 5(109):89415–89426, 2015.

[43] Jan H. Los, Luca M. Ghiringhelli, Evert Jan Meijer, and A. Fasolino. Improved long-range reactive bond-order potential for carbon. I. Construction. *Physical Review B*, 72(21), Dec 2005.

[44] S. Yu. Davydov and O. V. Posrednik. On the theory of elastic properties of two-dimensional hexagonal structures. *Physics of the Solid State*, 57(4):837–843, Apr 2015.

[45] Steven J. Stuart, Alan B. Tutein, and Judith A. Harrison. A reactive potential for hydrocarbons with intermolecular interactions. *The Journal of Chemical Physics*, 112(14):6472–6486, Apr 2000.

[46] Thomas P Senftle, Sungwook Hong, Md Mahbubul Islam, Sudhir B Kylasa, Yuanxia Zheng, Yun Kyung Shin, Chad Junkermeier, Roman Engel-Herbert, Michael J Janik, Hasan Metin Aktulga, Toon Verstraelen, Ananth Grama, and Adri C T van Duin. The ReaxFF reactive force-field: development, applications and future directions. *npj Computational Materials*, 2:15011, Mar 2016.

[47] Michele Lazzeri, Claudio Attaccalite, Ludger Wirtz, and Francesco Mauri. Impact of the electron-electron correlation on phonon dispersion: Failure of LDA and GGA DFT functionals in graphene and graphite. *Physical Review B*, 78(8), Aug 2008.

[48] Ludger Wirtz and Angel Rubio. The phonon dispersion of graphite revisited. *Solid State Communications*, 131(3-4):141–152, Jul 2004.

[49] G. Kotliar, S. Y. Savrasov, K. Haule, V. S. Oudovenko, O. Parcollet, and C. A. Marianetti. Electronic structure calculations with dynamical mean-field theory. *Reviews of Modern Physics*, 78(3):865–951, Aug 2006.

[50] I. Leonov, V. I. Anisimov, and D. Vollhardt. First-Principles Calculation of Atomic Forces and Structural Distortions in Strongly Correlated Materials. *Physical Review Letters*, 112(14), Apr 2014.

[51] Kristjan Haule and Gheorghe L. Pascut. Forces for structural optimizations in correlated materials within a DFT+embedded DMFT functional approach. *Physical Review B*, 94(19), Nov 2016.

[52] Benjamin Ramberger, Tobias Schfer, and Georg Kresse. Analytic Interatomic Forces in the Random Phase Approximation. *Physical Review Letters*, 118(10), Mar 2017.

[53] Stefano Baroni, Stefano de Gironcoli, Andrea Dal Corso, and Paolo Giannozzi. Phonons and related crystal properties from density-functional perturbation theory. *Reviews of Modern Physics*, 73(2):515–562, Jul 2001.

[54] Paolo Giannozzi, Stefano de Gironcoli, Pasquale Pavone, and Stefano Baroni. Ab initio calculation of phonon dispersions in semiconductors. *Physical Review B*, 43(9):7231–7242, Mar 1991.

[55] Xavier Gonze and Changyol Lee. Dynamical matrices, Born effective charges, dielectric permittivity tensors, and interatomic force constants from density-functional perturbation theory. *Physical Review B*, 55(16):10355–10368, Apr 1997.

[56] Stefano Baroni, Paolo Giannozzi, and Andrea Testa. Green's-function approach to linear response in solids. *Physical Review Letters*, 58(18):1861–1864, May 1987.

[57] Dario Alfè. PHON: A program to calculate phonons using the small displacement method. *Computer Physics Communications*, 180(12):2622–2633, Dec 2009.

[58] O. Dubay and G. Kresse. Accurate density functional calculations for the phonon dispersion relations of graphite layer and carbon nanotubes. *Physical Review B*, 67(3), Jan 2003.

[59] K. Parlinski, Z. Q. Li, and Y. Kawazoe. First-Principles Determination of the Soft Mode in CubicZrO2. *Physical Review Letters*, 78(21):4063–4066, May 1997.

[60] Atsushi Togo and Isao Tanaka. First principles phonon calculations in materials science. *Scripta Materialia*, 108:1–5, Nov 2015.

[61] Terumasa Tadano and Shinji Tsuneyuki. Self-consistent phonon calculations of lattice dynamical properties in cubicSrTiO3with first-principles anharmonic force constants. *Physical Review B*, 92(5), Aug 2015.

[62] N. R. Werthamer. Self-Consistent Phonon Formulation of Anharmonic Lattice Dynamics. *Physical Review B*, 1(2):572–581, Jan 1970.

[63] Ion Errea, Matteo Calandra, and Francesco Mauri. First-Principles Theory of Anharmonicity and the Inverse Isotope Effect in Superconducting Palladium-Hydride Compounds. *Physical Review Letters*, 111(17), Oct 2013.

[64] Ion Errea, Matteo Calandra, and Francesco Mauri. Anharmonic free energies and phonon dispersions from the stochastic self-consistent harmonic approximation: Application to platinum and palladium hydrides. *Physical Review B*, 89(6), Feb 2014.

[65] Nina Shulumba, Olle Hellman, and Austin J. Minnich. Intrinsic localized mode and low thermal conductivity of PbSe. *Physical Review B*, 95(1), Jan 2017.

[66] O. Hellman, I. A. Abrikosov, and S. I. Simak. Lattice dynamics of anharmonic solids from first principles. *Physical Review B*, 84(18), Nov 2011.

[67] Olle Hellman, Peter Steneteg, I. A. Abrikosov, and S. I. Simak. Temperature dependent effective potential method for accurate free energy calculations of solids. *Physical Review B*, 87(10), Mar 2013.

[68] Olle Hellman and I. A. Abrikosov. Temperature-dependent effective third-order interatomic force constants from first principles. *Physical Review B*, 88(14), Oct 2013.

[69] Randall LeVeque. *Finite Difference Methods for Ordinary and Partial Differential Equations: Steady-State and Time-Dependent Problems (Classics in Applied Mathematics)*. SIAM, Society for Industrial and Applied Mathematics, 2007.

[70] Bengt Fornberg. Generation of finite difference formulas on arbitrarily spaced grids. *Mathematics of Computation*, 51(184):699–699, 1988.

[71] Bengt Fornberg. Classroom Note:Calculation of Weights in Finite Difference Formulas. *SIAM Review*, 40(3):685–691, Jan 1998.

[72] C. A. Marianetti, D. Morgan, and G. Ceder. First-principles investigation of the cooperative Jahn-Teller effect for octahedrally coordinated transition-metal ions. *Physical Review B*, 63(22), May 2001.

[73] L.J. Sham. Anharmonic effects of phonons with Kohn anomalies. *Solid State Communications*, 20(6):623–625, Nov 1976.

[74] Hagai Eshet, Rustam Z. Khaliullin, Thomas D. Khne, Jrg Behler, and Michele Parrinello. Ab initio quality neural-network potential for sodium. *Physical Review B*, 81(18), May 2010.

[75] Samad Hajinazar, Junping Shao, and Aleksey N. Kolmogorov. Stratified construction of neural network based interatomic models for multicomponent materials. *Physical Review B*, 95(1), Jan 2017.

[76] Jrg Behler and Michele Parrinello. Generalized Neural-Network Representation of High-Dimensional Potential-Energy Surfaces. *Physical Review Letters*, 98(14), Apr 2007.

[77] Atsuto Seko, Atsushi Togo, Hiroyuki Hayashi, Koji Tsuda, Laurent Chaput, and Isao Tanaka. Prediction of Low-Thermal-Conductivity Compounds with First-Principles Anharmonic Lattice-Dynamics Calculations and Bayesian Optimization. *Physical Review Letters*, 115(20), Nov 2015.

[78] Fei Zhou, Weston Nielson, Yi Xia, and Vidvuds Ozoliņš. Lattice Anharmonicity and Thermal Conductivity from Compressive Sensing of First-Principles Calculations. *Physical Review Letters*, 113(18), Oct 2014.

[79] Atsuto Seko, Akira Takahashi, and Isao Tanaka. First-principles interatomic potentials for ten elemental metals via compressed sensing. *Physical Review B*, 92(5), Aug 2015.

[80] Lance J. Nelson, Gus L. W. Hart, Fei Zhou, and Vidvuds Ozoliņš. Compressive sensing as a paradigm for building physics models. *Physical Review B*, 87(3), Jan 2013.

[81] A. K. Geim and K. S. Novoselov. The rise of graphene. *Nature Materials*, 6(3):183–191, Mar 2007.

[82] A. H. Castro Neto, F. Guinea, N. M. R. Peres, K. S. Novoselov, and A. K. Geim. The electronic properties of graphene. *Reviews of Modern Physics*, 81(1):109–162, Jan 2009.

[83] V. Meunier, A. G. Souza Filho, E. B. Barros, and M. S. Dresselhaus. Physical properties of low-dimensionalsp2-based carbon nanostructures. *Reviews of Modern Physics*, 88(2), May 2016.

[84] C. Lee, X. Wei, J. W. Kysar, and J. Hone. Measurement of the Elastic Properties and Intrinsic Strength of Monolayer Graphene. *Science*, 321(5887):385–388, Jul 2008.

[85] Fang Liu, Pingbing Ming, and Ju Li. Ab initio calculation of ideal strength and phonon instability of graphene under tension. *Physical Review B*, 76(6), Aug 2007.

[86] Chen Si, Zhimei Sun, and Feng Liu. Strain engineering of graphene: a review. *Nanoscale*, 8(6):3207–3217, 2016.

[87] Costas Galiotis, Otakar Frank, Emmanuel N. Koukaras, and Dimitris Sfyris. Graphene Mechanics: Current Status and Perspectives. *Annual Review of Chemical and Biomolecular Engineering*, 6(1):121–140, Jul 2015.

[88] A. L. C. da Silva, Ladir Cândido, J. N. Teixeira Rabelo, G.-Q. Hai, and F. M. Peeters. Anharmonic effects on thermodynamic properties of a graphene monolayer. *EPL (Europhysics Letters)*, 107(5):56004, Sep 2014.

[89] Duhee Yoon, Young-Woo Son, and Hyeonsik Cheong. Negative Thermal Expansion Coefficient of Graphene Measured by Raman Spectroscopy. *Nano Letters*, 11(8):3227–3231, Aug 2011.

[90] Monica Pozzo, Dario Alfè, Paolo Lacovig, Philip Hofmann, Silvano Lizzit, and Alessandro Baraldi. Thermal Expansion of Supported and Freestanding Graphene: Lattice Constant versus Interatomic Distance. *Physical Review Letters*, 106(13), Mar 2011.

[91] Xu-Jin Ge, Kai-Lun Yao, and Jing-Tao L. Comparative study of phonon spectrum and thermal expansion of graphene, silicene, germanene, and blue phosphorene. *Physical Review B*, 94(16), Oct 2016.

[92] C. A. Marianetti and H. G. Yevick. Failure Mechanisms of Graphene under Tension. *Physical Review Letters*, 105(24), Dec 2010.

[93] Eric B. Isaacs and Chris A. Marianetti. Ideal strength and phonon instability of strained monolayer materials. *Physical Review B*, 89(18), May 2014.

[94] Jeongwoon Hwang, Jisoon Ihm, Kyung-Suk Kim, and Moon-Hyun Cha. Phonon softening and failure of graphene under tensile strain. *Solid State Communications*, 200:51–55, Dec 2014.

[95] Sandeep Kumar and David M. Parks. Strain Shielding from Mechanically Activated Covalent Bond Formation during Nanoindentation of Graphene Delays the Onset of Failure. *Nano Letters*, 15(3):1503–1510, Mar 2015.

[96] J. H. Los, A. Fasolino, and M. I. Katsnelson. Scaling Behavior and Strain Dependence of In-Plane Elastic Properties of Graphene. *Physical Review Letters*, 116(1), Jan 2016.

[97] Hessam Yazdani and Kianoosh Hatami. Failure criterion for graphene in biaxial loading—a molecular dynamics study. *Modelling and Simulation in Materials Science and Engineering*, 23(6):065004, Jul 2015.

[98] J. Maultzsch, S. Reich, C. Thomsen, H. Requardt, and P. Ordejón. Phonon Dispersion in Graphite. *Physical Review Letters*, 92(7), Feb 2004.

[99] M. Mohr, J. Maultzsch, E. Dobardžić, S. Reich, I. Milošević, M. Damnjanović, A. Bosak, M. Krisch, and C. Thomsen. Phonon dispersion of graphite by inelastic x-ray scattering. *Physical Review B*, 76(3), Jul 2007.

[100] L. Lindsay, Wu Li, Jesús Carrete, Natalio Mingo, D. A. Broido, and T. L. Reinecke. Phonon thermal transport in strained and unstrained graphene from first principles. *Physical Review B*, 89(15), Apr 2014.

[101] Lorenzo Paulatto, Francesco Mauri, and Michele Lazzeri. Anharmonic properties from a generalized third-order ab initio approach: Theory and applications to graphite and graphene. *Physical Review B*, 87(21), Jun 2013.

[102] D. M. Basko. Theory of resonant multiphonon Raman scattering in graphene. *Physical Review B*, 78(12), Sep 2008.

[103] Nicolas Mounet and Nicola Marzari. First-principles determination of the structural, vibrational and thermodynamic properties of diamond, graphite, and derivatives. *Physical Review B*, 71(20), May 2005.

[104] R. Ramírez, E. Chacón, and C. P. Herrero. Anharmonic effects in the optical and acoustic bending modes of graphene. *Physical Review B*, 93(23), Jun 2016.

[105] R. Ramírez and C. P. Herrero. Elastic properties and mechanical tension of graphene. *Physical Review B*, 95(4), Jan 2017.

[106] Yanguang Zhou, Xiaoliang Zhang, and Ming Hu. Quantitatively analyzing phonon spectral contribution of thermal conductivity based on nonequilibrium molecular dynamics simulations. I. From space Fourier transform. *Physical Review B*, 92(19), Nov 2015.

[107] Yanguang Zhou and Ming Hu. Quantitatively analyzing phonon spectral contribution of thermal conductivity based on nonequilibrium molecular dynamics simulations. II. From time Fourier transform. *Physical Review B*, 92(19), Nov 2015.

[108] M. K. Gupta, Baltej Singh, R. Mittal, S. Rols, and S. L. Chaplot. Lattice dynamics and thermal expansion behavior in the metal cyanidesMCN(M=Cu, Ag, Au): Neutron inelastic scattering and first-principles calculations. *Physical Review B*, 93(13), Apr 2016.

[109] T Tadano, Y Gohda, and S Tsuneyuki. Anharmonic force constants extracted from first-principles molecular dynamics: applications to heat transfer simulations. *Journal of Physics: Condensed Matter*, 26(22):225402, May 2014.

[110] John F. Cornwell. *Group Theory in Physics: An Introduction (Techniques of Physics)*. Academic Press, 1997.

[111] G. Kresse and J. Hafner. Ab initio molecular dynamics for liquid metals. *Physical Review B*, 47(1):558–561, Jan 1993.

[112] G. Kresse and J. Hafner. Ab initio molecular-dynamics simulation of the liquid-metal–amorphous-semiconductor transition in germanium. *Physical Review B*, 49(20):14251–14269, May 1994.

[113] G. Kresse and J. Furthmller. Efficiency of ab-initio total energy calculations for metals and semiconductors using a plane-wave basis set. *Computational Materials Science*, 6(1):15–50, Jul 1996.

[114] G. Kresse and J. Furthmller. Efficient iterative schemes for ab initio total-energy calculations using a plane-wave basis set. *Physical Review B*, 54(16):11169–11186, Oct 1996.

[115] G. Kresse and D. Joubert. From ultrasoft pseudopotentials to the projector augmented-wave method. *Physical Review B*, 59(3):1758–1775, Jan 1999.

[116] Cheol-Hwan Park, Nicola Bonini, Thibault Sohier, Georgy Samsonidze, Boris Kozinsky, Matteo Calandra, Francesco Mauri, and Nicola Marzari. Electron–Phonon Interactions and the Intrinsic Electrical Resistivity of Graphene. *Nano Letters*, 14(3):1113–1119, Mar 2014.

[117] Cheol-Hwan Park, Feliciano Giustino, Marvin L. Cohen, and Steven G. Louie. Electron-Phonon Interactions in Graphene, Bilayer Graphene, and Graphite. *Nano Letters*, 8(12):4229–4233, Dec 2008.

[118] M. E. Cifuentes-Quintal, O. de la Peña-Seaman, R. Heid, R. de Coss, and K.-P. Bohnen. Uniaxial strain-induced Kohn anomaly and electron-phonon coupling in acoustic phonons of graphene. *Physical Review B*, 94(8), Aug 2016.

[119] David B. Laks, L. G. Ferreira, Sverre Froyen, and Alex Zunger. Efficient cluster expansion for substitutional systems. *Physical Review B*, 46(19):12587–12605, Nov 1992.

[120] A V Ruban and I A Abrikosov. Configurational thermodynamics of alloys from first principles: effective cluster interactions. *Reports on Progress in Physics*, 71(4):046501, Mar 2008.